Politecnico di Milano
School of Industrial and Information Engineering
Department of Aerospace Science and Technology
Master of Science in Space Engineering

Methods for assessing the coverage performance of satellite constellations

Master Thesis

Author:
Marta Padoan
915570

Supervisor:
Prof. Camilla Colombo
Co-Supervisor:
Dr. Arnaud Boutonnet

Academic Year 2019/2020

To my parents, Catia and Luca

Acknowledgements

"If you are curious, you'll find the puzzles around you.
If you are determined, you will solve them."
- Erno Rubik

First, I would like to acknowledge my supervisor Dr. Camilla Colombo, who helped me throughout this thesis work and who always gave me valuable and useful advice.

I want also reserve a special thank to my supervisor at the European Space Agency Dr. Arnaud Boutonnet, who believed in me, who gave me the opportunity to do the Internship at ESA and who has always been available for any of my questions and has always helped me. My thesis is based on what I have done during the six months as Mission Analysis Trainee at ESOC, so without it I would probably have never developed a work like this. I did a great experience and even though times were hard due to the Covid-19 pandemic, I learnt a lot of things and I have grown professionally.
A special thank goes also to the Mission Analysis Team, especially to Lorenzo for his precious help and his lessons and to my "coffee-break" colleagues.

I want to thank my fiends and colleagues, the ones that have been around for a lifetime and those I met on this university path. Thank you because you taught me how to work in a team, sharing your knowledge end expertise. A special thanks to my colleague and friend Max, who has always been available to help me, who has tried to teach me computer magic and has always been patient even when I didn't understand and kept needing him. Thank you all also for the conversations and the experiences we shared together.

I want also like to acknowledge my Erasmus family, they made me live an unforgettable experience that changed my life forever. Thank you for all your advice, for all our lunches and dinners in Liège, all our "bières et frites à la sauce andalouse" and our nights "au Le Carrè".

A big thank-you to Andrea, who came into my life when I did not expect anything and who took me by the hand in this path that is life. Thank you for always supporting me and making me happy everyday.

Finally, I wish to thank my mum and dad, you have always supported me by encouraging me to give my best and not to give up despite the difficulties. Without you, none of this would have been possible and if today I am who I am it is only thank to you. You taught me to live and you are and will always be my point of reference, I love you.

Milan, April 2021

Marta Padoan

Abstract

Satellite constellations are a set of satellites working together as a coordinated system to achieve a unique objective, in general used to fulfill spatial and temporal coverage and observation requirements which can not be met with a single satellite.
The aim of this thesis is to perform an analysis of the geometries and the design methods for satellite constellations, to make a simple and clear comparison among the existing design approaches and to determine the most efficient and optimal ones. Either minimisation of the computational effort or development of graphical representations aimed at clarifying the underlying physics are considered as targets of the optimisation process, and field of applicability as well as accuracy of the results are judged of primary importance.
Among all figures of merit that characterise a constellation, visibility conditions and coverage requirements have been the common thread throughout all the work presented as the methods studied are focused on assessing the coverage performance of satellite constellations.
The novelty proposed in the presented work is directed towards the development of a standardised nomenclature and treatment in order to make a direct, intuitive and simple comparison. The proposed algorithms have been created for the purpose of testing the efficiency and the accuracy of the results, but also to graphically visualise numerical results.
In addition, an innovative approach for the determination of the coverage area is introduced, that relies on an analytical method based on the knowledge of the satellite's position vectors, the relative geographical coordinates of the sub-satellite points and the half-aperture angle of the navigation antenna. The analytical formulations reduce the computational cost and increase the accuracy of the results.
A feasibility analysis of the proposed approaches is also performed, by applying the methods to two missions in which the author was able to contribute during the Internship at the European Space Agency, one dealing with a mega-constellation around the Earth and the other with a small constellation around the Moon.
However, the development of the different design methods and the relative results showed some particular peculiarities and sometimes limit in the methodology treated, hinting some possible fields for future investigations.

Sommario

Le costellazioni sono un gruppo di satelliti che lavorano assieme come un sistema coordinato al fine di raggiungere un unico obiettivo. In generale vengono usate per rispondere a requisiti di copertura spaziale e temporale che non possono essere soddisfatti da un singolo satellite.
Il lavoro svolto in questa tesi è un'analisi delle geometrie di costellazioni esistenti e dei relativi metodi di progettazione, con lo scopo di realizzare un confronto facilmente comprensibile tra i vari approcci e di determinare i più efficienti. Gli obiettivi del processo di ottimizzazione di un metodo sono la minimizzazione del costo computazionale e la presenza di simulazioni grafiche esplicative e rappresentative. In più, sono considerati di primaria importanza anche il numero di casi in cui questi metodi possono essere applicati e l'esattezza dei risultati.
Tra tutte le figure di merito che caratterizzano una costellazione di satelliti, le condizioni e i requisiti di visibilità sono stati il filo conduttore dello studio svolto e quindi i metodi analizzati sono basati sulla valutazione delle prestazioni di copertura delle costellazioni.
L'innovazione del presente lavoro di tesi è rappresentata dal fatto che tutti i metodi sono descritti e trattati attraverso una nomenclatura standardizzata in modo da poter effettuare un confronto diretto, intuitivo e semplice. I corrispondenti algoritmi sono stati realizzati allo scopo di testare l'efficienza e la precisione dei risultati ottenuti, ma anche per visualizzare tali risultati graficamente.
Lo scopo di questa tesi è anche l'introduzione di un approccio innovativo per le determinazione dell'area di copertura, basato su calcoli analitici che partono dalla conoscenza del vettore di posizione dei satelliti, dalle relative coordinate geografiche e dall'angolo di semiapertura dell'antenna di navigazione. I calcoli analitici permettono di ridurre il costo computazionale e di aumentare la precisione dei risultati.
Come casi studio, i metodi presentati sono stati applicati a due missioni cui l'autore ha avuto possibilità di contribuire durante l'Internship presso l'Agenzia Spaziale Europea, la prima relativa a una mega-costellazione attorno alla Terra e l'altra a una piccola costellazione attorno alla Luna.
L'implementazione dei diversi metodi di progettazione ha evidenziato alcuni limiti nei vari approcci e possibili campi di sviluppo per investigazioni future.

Contents

List of figures

List of tables

Nomenclature

Symbol	Units	Description
μ	km^3/s^2	Standard gravitational parameter
ε	deg, rad	Elevation angle
h	km	Height of the satellite
R_{Earth}	km	Radius of the Earth
$r_{s/c}$	km	Spacecraft's radius
$\mathbf{r}_{s/c}$	km	Spacecraft's position vector
θ	deg, rad	Half-cone central angle radius of coverage
$\hat{\mathbf{v}}$, $\hat{\mathbf{w}}$	km	Unit vectors
T	-	Total number of satellites
P	-	Number of orbital planes
S	-	Number of satellites per plane
F	$\frac{2\pi}{T}$, $\frac{360}{T}$	Relative phase parameter
W	-	Scaling parameter
m	$\frac{[0,(T-1)]}{S}$	Geometric harmonic factor
Ω	deg, rad	Right ascension angle
a	km	Semi-major axis
e	-	Eccentricity
i	deg, rad	Inclination
$\mathbf{v}$	km/s	Satellite's velocity vector
ω	deg, rad	Argument of pericenter
M	deg, rad	Mean anomaly
TA	deg, rad	True anomaly
h_p	km	Perigee altitude
T_{period}	s	Orbital Period
X	deg, rad	Time-varying phasing angle
n	rad/s	Satellite's mean motion
d	km	Distance
Φ	deg, rad	Angular half-width of the ground swath
α	deg, rad	Inter-plane angular separation between adjacent planes
ΔM	deg, rad	Variation in mean anomaly
$\Delta\Omega$	deg, rad	Variation in right ascension, longitude range
J_2	-	Harmonic coefficient of Earth oblateness
N_p	-	Number of orbit revolutions to complete one period of repetition

Symbol	Units	Description
N_d	-	Number of sidereal days te repeat the relative trajectory
F_n	-	Relative phasing parameter
F_d	-	Relative phasing parameter
ω_{Earth}	rad/s	Earth's rotation rate
λ	deg, rad	Latitude
φ	deg, rad	Longitude
$T_{Beste-nfold,\lambda}$	-	Total N^o of satellites for n-fold coverage beyond λ, Beste
j, k, n	-	Multiple level of coverage
$T_{A\&R}$	-	Total N^o of satellites for global n-fold coverage, Adams and Rider
θ_{MAX}	deg, rad	Largest value of circumcircle radii over the entire propagation
θ_{max}	deg, rad	Largest value of circumcircle radii at an instant of time
r_{ij}	deg, rad	Intersatellite great circle range between a pair of satellites i, j
θ_{ijk}	deg, rad	Equidistance range arc of any three sub-satellite points
u	deg, rad	Argument of latitude
$\Delta\phi_1$	deg, rad	Groundtrack shift between two consecutive ascending nodes
$\Delta\varphi$	deg, rad	Longitude range for non-rotating Earth
β	deg, rad	Inclination angle of the coverage belt
Δt_{REV}	hr	Revisit Time
Δt_B	hr	Revisit Time between straight-line envelopes of coverage belts
δt	hr	Relative shift of each teeth of the coverage belt
$_N$, $_S$	deg, rad	Boundary points of the longitude range
$_A$, $_D$	deg, rad	Ascending and descending passes
$\Delta\Omega_{REV}$	deg, rad	Longitude gap range, for non-visibility
$\delta\Omega^*$	deg, rad	Longitude shift between boundary points in the coverage belt
$\Delta\lambda$	deg, rad	In-plane phase shift of satellites in a constellation with $F \neq 0$
(x_o, y_o)	deg, rad	Corner point coordinates of the parallelogram
Γ	deg, rad	Solid angle corresponding to the circle θ

Acronyms

Acronym	Description
3G	Third Generation
ART	Average Revisit Time
CDF	Concurrent Design Facility
CPU	Central Processing Unit
DOP	Dilution Of Precision
ECEF	Earth Centered Earth Fixed
ECI	Earth Centered Inertial
ELCANO	European LEO Constellation for Augmentation of Navigation and Other services
ELO	Elliptical Lunar Orbit
EL3	European Large Logistic Lander
EME2000	Earth's Mean Equator and Equinox
ESA	European Space Agency
FOW	Field Of View
GEO	Geosynchronous/Geostationary Earth Orbit
GLONASS	Global Navigation Satellite System
GNSS	Global Navigation Satellite System
GPS	Global Positioning System
HDOP	Horizontal Dilution Of Precision
HEO	Highly Elliptical Orbit
ICO	Intermediate Circular Orbit
IGSO	Inclined Geosynchronous Orbit
JD	Julian Days
J2000	January 2000
LCNS	Lunar Communications and Navigation Services
LEO	Low Earth Orbit
LLO	Low Lunar Orbit
LOI	Lunar Orbit Insertion
LTI	Trans-Lunar Injection
LTO	Lunar Transfer Orbit
LUNATIC	Lunar Sample Return with LCNS
MEO	Medium Earth Orbit
MJD	Modified Julian Days

Acronym	Description
MJD2000	Modified Julian Days 2000
MRT	Maximum Revisit Time
NRHO	Near Rectilinear HALO Orbit
OB	Orbit Determination
O3b	Other 3 Billion
PDOP	Position Dilution Of Precision
PNT	Position, Navigation and Timing
RAAN	Right Ascension Of the Ascending Node
SOC	Street Of Coverage
TCM	Trajectory Correction Manoeuvre
ToF	Time of Flight
VDOP	Vertical Dilution Of Precision
WSBT	Weak Stability Boundary Transfer

1. Introduction

A satellite constellation is a set of satellites working together as a coordinated system to achieve a unique mission objective, in general used to fulfill spatial and temporal coverage and observation requirements which can not be met with a single satellite.
The common mission objectives that lead to select a constellation are: to have global or nearly global coverage of the Earth surface, to improve system performance and data collection capacity, to provide new services (e.g. global positioning and navigation, worldwide telecommunications, new applications in the Earth observation and scientific mission domain) and to take advantage of scale economy for the satellite manufacture (reduction of cost and production times). The concept of satellite constellations can be exploited not only around Earth, but even for missions whose center body is another planet: the aim is to provide navigation services and a planetary communication network to surface and orbiting asset (landers, robots) and to perform observation tasks advantage of a multi-spacecraft system orbiting around the planet.

1.1 Scope of the thesis

The aim of the thesis is to present and analyse the concept of satellite constellations and the relative design methods, throughout a study that allows a clear and simple comparison. An attempt to determine the most efficient and optimal geometries and methods in terms of accuracy of the results and minimisation of computational time is then carried out. Indeed, either minimisation of computational effort and graphical/geometrical representation supporting the understanding of the underlying physics are considered as targets of the optimisation process, as well as the applicability domain and the accuracy of the results.
The design process is based on the user requirements, since they define the figures of merit for mission objectives. For instance, a constellation could be desired for Earth observation, telecommunications rather than navigation and positioning.
Some figures that are considered in this work for the design process and for the selection of the optimal constellation geometry are reported in Table 1.1.

Table 1.1: Constellation's figures of merit.

Earth Observation	**Telecommunications**	**Navigation and Positioning**
- Visibility - Instrument duty cycle - Data timeliness/latency - Response time - Illumination conditions	- Visibility - Signal propagation delay - Doppler effect - Satellite/user antenna - Inter-satellite link - Link availability/reliability - Link Budget - Signal Interference - Space network - Fade analysis	- Visibility - Dilution of precision - Link availability/integrity - Positioning accuracy

For Earth observation constellations, the instrument duty cycle, or power cycle, is defined as the fraction of one period in which a signal or a system is active, while the response time is the time span between the delivery of the data requested by the users and the availability of the ordered data, strictly related to the concept of data latency, that is the time it takes for data packets to be stored or retrieved.
Satellite constellations for telecommunications shall consider the signal propagation delay, the signal fading but also the link established between the satellite and the ground or between satellites; the latter concept deals with inter-satellite link and space network requirements.
Dilution Of Precision (DOP) is a term used in satellite navigation and positioning to specify the error propagation as a mathematical effect of navigation satellites geometry on positional measurement precision. However, for this class of constellations, also the link availability between the satellite and the ground shall be taken into account.
By looking at Table 1.1, among all figures of merit that characterise a constellation, visibility conditions must always be considered and so they have been the common thread throughout all the work presented, as the methods studied are focused on assessing the coverage performance of satellite constellations.
The methods are numerical or analytical and can be applied for different constellation geometries; this thesis aims at developing the mathematical formulations and algorithms behind each method, with an attempt to find out similarities and peculiarities among them, as well as to determine the most performant and cost saving solution.
An innovative methodology to determine the coverage area is also developed and applied to the methods: it relies on analytical formulations based on the knowledge of the satellite's position vectors, the geographical coordinates and the characteristics of the satellite's antenna in terms of aperture angle. The analytical approach reduces the computational cost and increases the accuracy of the results.

1.2 Background

The design of satellite constellations began with the work of Luders in the early 1960s [1]. At that time, all satellites were in Low Earth Orbit (LEO) while there were not satellites in higher orbits, including the special case of Geosynchronous (GEO) 24-hours orbits. In particular, the Geostationary satellite is a special case of the GEO type with zero degree inclination, thus in an orbit where it remains directly over a fixed point on the equator. It has the advantage of remaining stationary in the sky relative to a fixed ground antenna, so that the ground-based user antenna may be fixed relative to the mounting base. The main disadvantage is that the satellite becomes unusable in the higher latitudes and at the poles. Hence, in the Soviet Union, many communications satellites were placed in Molniya orbit, highly elliptic and with a 12-hour period, favoring the Northern Hemisphere, that contains the apogee point of the orbit itself. This orbit overcame the high latitude reception problem, but required movable antennas (i.e. to follow the motion of the satellite in its elliptic orbit). Later, the advent of the Navstar Global Positioning System (GPS) constellation introduced the use of circular inclined 12-hour orbits. Systems for continuous coverage of the globe, zonal regions or discrete geographic areas have also been addressed in numerous studies by government agencies and industry.
A major trend in the evolution of satellite systems is an increase in the number of smaller and lower-cost satellites [2]. This led to a dramatic increase in the number of Earth-orbiting constellations for observations, communications, navigation and science and with the consequent birth of the concept of large and mega-constellations.
The most important result of decades of constellation studies has been that no absolute rules exist for constellation design.

The most relevant constellation designs are hereafter presented [3], [4], [5] while a more detailed list is reported in Table 1.2, Table 1.3 and Table 1.4, where the references and a brief description of the correspondent method are listed.

1. Luders (1961): Satellites are equally divided among, and uniformly distributed around, circular orbits of common altitude; the orbit planes are equally inclined with respect to the equator and symmetrically arranged about the polar axis.

2. Walker (1977): Systems of satellites in multiple equal-radius circular orbits, with an equal number of satellites in each orbit, capable of providing continuous coverage of the whole Earth's surface in orbits from synchronous altitude down to relative low altitude. Three satellites of the constellation (satellite triad) are used to assess the coverage performance.

3. Beste (1977): Analysis for simple and triple coverage of the whole Earth and of the polar regions extending to arbitrary latitude, by placing the satellites in orbital planes which have a common intersection (i.e. polar orbits) and to adjust the plane separation and satellite spacing so as to minimise the total number required. The satellite constellations with these characteristics belong to the Street Of Coverage (SOC) class.

4. Ballard (1980): Rosette (flowerlike) constellations of Earth satellites, characterised by circular, common-period orbits all having the same inclination with respect to an arbitrary plane. The orbits are uniformly distributed in a right ascension angle as they pass through the reference plane and the initial phase position of satellites in each orbit plane is proportional to the right ascension angle for the plane.

5. Broglio (1981): "Sistema Quadrifoglio" (Four-Leaf clover system) [6], an equatorial constellation of four satellites proposed to observe and to guarantee continuous measurement of the upper part of the atmosphere in the equatorial region. The satellites each spend about six hours near apogee and two hours in transition between successive apogees.

6. Draim (1986): Elliptical orbits considered; analysis and study of a common-period four-satellite continuous global coverage constellation organised in a tetrahedron form.

7. Adams and Rider (1987): Optimally phased polar orbit constellations using minimum total number of satellites to achieve continuous single or multiple coverage above a specified latitude assuming that all orbital planes have the same number of satellites with the satellites symmetrically distributed in each orbital plane (SOC class).

8. Lang (1987): Symmetric circular orbit satellite constellations for continuous global coverage by means of a method which involves the computation of revisit times to points on the ground.

9. Draim (1987): Six satellite common period elliptic orbit constellation giving continuous global double coverage of a spherical Earth.

10. Bottkol and Di Domenico (1991): Numerical phase-based approach to the calculation of revisit interval [7]; the satellite groundtrack is mapped to the surface of a torus which is then unwrapped to indicate the intersection with a defined visibility region.

11. Lang (1993): Study of symmetric satellite constellations as large as 100 satellites, for which continuous global coverage for single through four-fold coverage are sought and compared with that of non-symmetric, polar constellations.

12. Lang (2002): Genetic algorithm optimisation process enabling a parametric exploration of the design space.

13. Abdelkhalik and Mortari (2006): Propagated satellite orbits over a short time period and use of a penalty function method to design satellite orbits for maximum resolution or maximum observation time.

14. Ruggieri et al. (2006): Flower constellation Set and possible applications to other existing geometries.

15. Ulybyshev (2014): Geometric analysis method for the calculation of revisit time for symmetric constellations.

Table 1.2: Summary of constellation designs.

Author	Year	Orbit Type	Design Method	Remarks
Luders	1961	Circular, inclined, symmetrical	Street Of Coverage (see Section 2.2.3)	Full single coverage
Ullock, Schoen	1963	Circular, polar, non-symmetrical	Street Of Coverage	Phasing of co-rotational planes
Walker	1970, 1977	Star, Delta patterns (see section 2.2.1)	Satellite triad (see Section 3.3)	Naming $(T/P/F)$ and inclination; 5 satellites for global coverage
Mozahev	1972	Circular	Symmetrical group	Difficult to find translations
Emara, Leondes	1976	Circular, inclined	Point coverage simulation	Optimum 4x2 and 3x4 constellation
Beste	1977	Circular, polar, non-symmetric	Street Of Coverage	Systematic, multiple coverage
Ballard	1980	Rosette (Delta pattern)	Satellite triad	Systematic multiple coverage
Broglio	1981	Elliptic, equatorial	One-third of the Earth rotation rate period	Continuous coverage, orbits compatible with respect to a rotating reference frame
Lang, Hanson	1983	Delta pattern	Point coverage simulation	Minimum revisit time
Rider	1986	Delta pattern	Street Of Coverage	Analytical closed-form, multiple coverage
Draim	1986	Elliptic, high altitude	Tetrahedron (see Section 2.3.1)	4 satellites constellation, continuous coverage
Adams, Rider	1987	Polar, circular, non-symmetric	Street Of Coverage	Systematic computational approach
Lang	1987	Circular, inclined	Point coverage + satellite constellation triad	2-step approach for CPU time

Table 1.3: Summary of constellation designs.

Author	Year	Orbit Type	Design Method	Remarks
Hanson, Linden	1988	Circular, inclined	Street Of Coverage	Below-The-Horizon double, Above-The-Horizon single
Mainguy	1989	Geosynchronous, elliptic, inclined	Zonal coverage	Orbit control analysis
Rondinelli	1989	3 GEO + 2 Tundra	Zonal coverage	Orbit control analysis
Hanson, Higgins	1990	Geosynchronous	Point coverage simulation	Geostationary, Walker, elliptic, composite
Maral	1990	LEO circular	Zonal coverage	Network topology concept
Baranger	1991	GPS-like	Point coverage simulation	Adaptive random search Position DOP (PDOP)
Bottkol, DiDomenico	1991	Circular, symmetric	Numerical, Phase-based approach	Satellite groundtrack mapped to the surface of a torus (for visibility regions)
Hanson	1992	Circular, inclined	Coverage timeline meshing	Time gap, partial coverage, repeating groundtrack
Lang	1993	Circular, polar, non-symmetric	Point coverage simulation	Up to 100 satellite constellation, Fortran PC (486)
Werner	1995	LEO - Intermediate Circular Orbit (ICO)	Analytical approach	Network topology simulation
Radzik, Maral	1995	Walker and Beste types	Street Of Coverage	Minimum revisit time, network
Sabol	1996	Ellipso	Refinement	Orbital perturbations
Ma, Hsu	1997	Repeating groundtrack	Coverage timeline meshing	Partial coverage, oblate Earth, Pentium C++
Kelley, Fischer	1997	GPS orbit type	Simulated annealing	VDOP optimisation
Pablos, Martin	1997	GEO + Inclined Geosynchronous Orbit (IGSO)	Zonal coverage	Availability, integrity
Lansard, Palmade	1997	LEO circular	Design to cost	Cost efficiency, spares, availability
Palmade	1997	LEO circular	Double Walker	GEO interference constraint
Boudier	1997	GEO + MEO	Hybrid constellation	Communication, Station Keeping
Renault	1997	GEO + IGSO	Hybrid constellation	Navigation constraint, Horizontal DOP (HDOP), Vertical DOP (VDOP)
Micheau, Thiebolt	1997	GEO + LEO	Walker constellation	Accuracy, integrity, continuity
Perrota	1997	LEO circular	Walker constellation	Navigation, 75 satellite constellation
Palmerini	1997	Elliptical	Hybrid configuration	Additional coverage on given areas
Draim	1997	Elliptical + circular	Hybrid systems	Station Keeping, collision avoidance
Cornara	1997	GEO, LEO	Selected constellations	Geometry and dynamics satellite constellation interaction
Ulivieri	1997	LEO sunsynchronous circular	Revisit time optimisation	Earth observation constellations

Table 1.4: Summary of constellation designs.

Author	Year	Orbit Type	Design Method	Remarks
Lang, Adams	1997	LEO circular	Point coverage simulation	Comparative table of optimal constellations
Wertz	1999	All geometries	Numerical approach	Coverage evaluation utilizing groundtrack plots
Crossley, Williams	2000	All geometries	Genetic algorithm	Annealing approach to minimisation of Maximum Revisit Time (MRT)
Lang	2002	All geometries	Genetic algorithm	Parametric exploration
Ferringer, Spencer	2006	All geometries	Numerical point-coverage simulation	Generated ephemeris through COVERIT and ASTROLIB/Revisit-C tools
Abdelkhalik, Mortari	2006	All geometries	Penalty function method	Propagation of satellite orbits for maximum resolution or observation time
Ruggieri et al.	2006	All geometries	Flower constellation Set	Generalisation of the Flower concept
Wertz	2011	All geometries	Point coverage simulation	Grid of points to evaluate visibility
Abdelkhalik, Gad	2011	Sunsynchronous orbits	Optimal repeated groundtrack	Multiple site surveillance
Ulybyshev	2014	Circular, symmetric	Geometric analysis	Coverage evaluation
Razoumny	2016	All geometries	Analytical method	Route theory for discontinuous coverage evaluation

The study of satellite constellations is still ongoing, mainly taking as reference all the aforementioned methods and trying to optimise and improve them. Some examples are related to the Walker method or the socalled Flower constellations that take origin from Broglio's "Four-Leaf clover system" concept and that have seen a growing interest in the last years.

As regards the computation of the coverage area associated to a satellite, Escobal [8] derived a closed-form solution to the satellite visibility problem. The closed form solution is a single trascendental equation in the eccentric anomalies corresponding to the rise and set times for a given orbital pass of a satellite under the assumptions of Keplerian motion and knowledge of satellite orbital elements, station coordinates and minimum elevation angle. The elevation angle ε is the angle between a satellite and the observer's horizon plane [9]. Escobal solved also the trascendental equation by using numerical methods once per satellite period, which is faster than determining the value of the elevation angle of the satellite with respect to a ground station for each time instant.
Lawton [10] developed a method to solve for satellite-satellite and satellite-ground station visibility periods considering an oblate Earth defining a new visibility function based on the vertical distance above the plane tangent to a ground station by using a Fourier series. This method works well for low eccentricity orbits, but fails for more elliptical orbits

because the visibility waveform becomes aperiodic.
Wilkinson [11] used spherical trigonometry equations for the determination of coverage regions, in order to assess the total amount of time one or more satellites spend inside it.
Walker [12] derived circular orbital patterns providing continuous whole Earth coverage modeling the Earth as a perfect sphere. This assumption can be considered reasonable if the satellites' altitude is low since the spherical geometry and the ellipsoidal one are not so different.
Ma and Hsu [13] proposed a solution for the exact design of a partial coverage satellite constellation over an oblate Earth, that is, the coverage of certain regions of the Earth with gap times in coverage no longer than some specified maximum time, which is based on a visibility function analogous to the one introduced by Escobal [8]. This method can not be efficient for a Global Navogation Satellite System (GNSS) where the coverage is supposed to be global and there is a significant number of satellites. The problem in using the visibility function is the resolution of the trascendental equation to determine the region visible from each satellite.
The analytical method presented by Nugnes et al. [14] determines the coverage area considering the Earth as an oblate ellipsoid of rotation, starting from the position of a spacecraft on its orbit and derives all the locations on the Earth's surface within its field of view.

1.3 State of the art

LEO satellites are often deployed in satellite constellations, because the coverage area provided by a single LEO satellite only covers a small section that moves as the satellite travels. Hence, many LEO satellites are needed to maintain continuous coverage over a region. Instead, by placing a satellite in a Geostationary orbit, permanent coverage is guaranteed over a large area. However, LEO satellites have the advantage of low cost, low latency and low path losses. Constellations of LEO satellites will be an important part of the next generation of global mobile communication networks [15].
For example, the Walker class of constellations developed by Walker was initially used for Medium Earth Orbit (MEO) constellations but was subsequently applied to LEO satellites. Many LEO Walker satellite constellations were created in the 1980s, such as Iridium [16] and Globalstar [17], while Teledesic [18] is another example that is used for multimedia services and integrated broadband applications. In the 2000s, because of the high costs resulting from sub-optimal configurations and the competition from terrestrial mobile communication networks, several of these well-known satellite constellations were abandoned. To satisfy the coverage demands (coverage performance is an important factor

in determining the competitiveness of a new constellation), there are several types of satellite constellation configurations.
Over the last decade, satellite constellation concepts have been envisioned for a broad range of uses. Initially starting with navigation and positioning constellations such as NAVSTAR/GPS [19], Glonass [20] and GNSS/Galileo [21], satellite constellation concepts have branched out into telecommunications for direct telephony, mobile message system and broadcasting and even into Earth observation. In addition, with increasing on-orbit capability and reduced system cost, development of constellations of a large number of small satellites has recently grown significantly.

Several examples of operational and planned satellite systems [22] are reported in Table 1.5, with their service, main characteristics and starting year of service. Some of them are going to be further analysed in Section 2.4

Table 1.5: Satellite Systems.

System	Service	Coverage	Satellites	Start of service
Immarsat-A	Speech and data transmission	Global	4 GEO	1982
Immarsat-B	Speech and data transmission	Global	4 GEO	1993
GPS	Positioning, Navigation and Timing	World-wide	24 MEO at 20200 km inclined orbits	1994
Orbcomm	Low-rate data communication	World-wide	28 LEO at 825 km inclined orbits	1996 USA, 1998 Global
Iridium	Mobile telephony	World-wide	66 LEO at 780 km polar orbits	1998
Globalstar	Mobile telephony	World-wide	48 LEO at 1414 km inclined orbits	1999/2000
Ellipso	Mobile telephony	World-wide	10 Highly Elliptical Orbit (HEO), inclined + 6 equatorial MEO	-
ICO	Mobile telephony	World-wide	10 MEO at 10390 km inclined orbits	-
SkyBridge	Broadband network	Global	80 LEO at 1457 km	-
Boeing	3G Mobile telecommunications	Global	16 MEO at 20180 km	-
Teledesic	Broadband network	Global	288 LEO	-
Glonass	Positioning, Navigation and Timing	World-wide	24 MEO at 19130 km inclined orbits	2010
Galileo	Positioning, Navigation and Timing	World-wide	24 MEO at 23222 km inclined orbits	2012
O3b	Internet Broadband services	Between 62 deg North and South latitude	20 MEO	2014
OneWeb	Internet Broadband services	World-wide	648 LEO or more	2022
Starlink	Internet Broadband services	World-wide	12000 LEO or more	2022

1.4 Original contribution

The work contributes to the area of satellite constellations design and development; it proposes standardised nomenclature and references, making a direct, intuitive and simple comparison of the presented methods. Hence, starting from the theory hereafter described, the author has developed algorithms for the application of the design methods that accept as inputs the parameters expressed always in the same form. Such algorithms have been written, refined and organised so that the computational time is reduced as much as possible and graphical representations have been created, aimed at clarifying the underlying physics. In this way, it is easier to directly understand the more performant method as well as the more accurate and precise in terms of the produced results.

This thesis also introduces an innovative approach for the determination of the coverage area that is purely analytical and the mathematical formulations have been adapted accordingly to the different geometries in order to enlarge the field of applicability (e.g. satellites can be in circular rather than elliptical orbits, constellations can have a symmetric or non-symmetric arrangement). Hence, this novel method is directed toward the determination of the coverage area that can be applied to different satellites in different orbits and scenarios.
Indeed, a fully-analytical technique can considerably reduce the computational time and at the same time increase the accuracy of the results, both key points in the study of the methods for the design of satellite constellations.
Starting from the knowledge of the satellite's position vectors of the constellation and the direction of the antenna line of sight, the relative sub-satellite points in terms of longitude and latitude angles are determined. The boundaries of the coverage area are computed using spherical trigonometry equations, since it often affords better geometric insight than the vector approach.
The determination of the satellite's coverage area in the previous work of Nugnes et al. [14] was done for an oblate Earth and a single satellite, having as input the line of sight of the satellite itself, the half-cone aperture angle of the conical field of view and the satellite position vector, but then the boundary points were determined with vector approach.
In this thesis, the analytical formulations rely on spherical trigonometry, they relate the elevation angle or the half-aperture angle and model the visibility conditions as a conical field of view; they are used for satellite constellations, where the Earth is considered as a perfect sphere since the satellite's altitude is relatively low and so spherical and ellipsoidal geometry are not so different.

In addition, the novelty of this work is the application of these analytical and numerical approaches to two missions currently under development at the European Space Agency (ESA), in which the author contributed. One mission deals with a mega-constellation around the Earth, while the other with a small constellation around the Moon and the work consisted in determining the optimal coverage performance with the lowest computational time.

1.5 Structure of the thesis

Chapter 1 gives an overview of the existing design methods and their evolution throughout the years, with particular attention to the state of the art and the future trend for satellite constellations concept. This is followed in Chapter 2 by a description of the existing satellite constellation geometries and design methods with their theoretical description and the procedure to compute the coverage area of the satellites is presented; the chapter ends with a presentation of existing satellite constellations as proof of the proposed concepts.
Chapter 3 presents the problem of continuous coverage and the different approaches used to determine the optimal satellite constellation to fulfill such requirements, together with the application of the analytical approach to compute the coverage area when needed, while Chapter 4 computes the revisit time for discontinuous coverage.
The presented methods are then validated in Chapter 5.
Lastly, Chapter 6 is an application to two actual missions currently under study and development at ESA, in which the proposed methods have been applied.

2. Satellite constellation geometries and design

In choosing constellation pattern characteristics for global coverage, the primary objective is to minimise the total number of satellites needed to ensure that not less than a certain number of satellites are everywhere visible at all times above some minimum elevation angle; as a secondary objective, it is assumed that a minimum distance between adjacent satellites should be as large as possible; in fact, if two satellites have only a small separation, one of them is effectively useless.
These are just two of the possible considerations that guide the choice toward a certain constellation geometry and many elements and needs must be borne in mind. In addition, not only the geometry should be considered for the optimisation process and coverage requirements, transmission losses, cost and launcher capabilities are only a few of the constraints that must be taken into account.

2.1 Constellation design

When dealing with constellation design the objectives of the constellation itself and the user requirements are of primary importance. Hence, at the very beginning of the design process, it should be distinguished between continuous and discontinuous coverage. Coverage is said to be continuous when the targeted area is always in view of the satellites, while not continuous if a visibility gap in the coverage is allowed. In this latter case the concept of revisit time is introduced [23]. In addition, it is possible to target a global coverage of the planet, a zonal coverage or a local coverage for well identified users. Zonal coverage objectives can be shaped according to complex and tortuous boundaries (e.g. for a country or a region) but they are more often defined as simple latitude ranges.

In modern satellite communications and navigation systems, as well as for some Earth observation systems, one single satellite and geostationary orbits can not be used due to bad coverage of certain latitudes or link budget constraints for small user terminals. By considering then satellite constellations, the design methods rely on geometrical coverage considerations: for example, any ground point must see at least one satellite at each instant above a specified minimum elevation threshold. However, very important in the formulation and choice of a method is also the optimisation of the method itself (i.e. speed

up the computational time and accuracy).

The methods developed and presented in the following are generally valid only for a certain constellation geometry: the major distinctions are made upon symmetric rather than non-symmetric patterns or between circular and elliptical orbits. In addition, the approaches could be distinguished even based on the way they proceed for the computations: they could be purely analytical or numerical methods.

2.1.1 Coverage area

When the elevation angle ε is equal to 0 deg, the instantaneous coverage area of a satellite is at its maximum. Any point located within this coverage area will be within the geometric visibility to the satellite. However, close to zero elevation angle is not operable due to the high blocking and shadowing effects. This leads to the concept of minimum elevation angle. The minimum elevation angle is defined as the elevation angle required for the instantaneous coverage area to be within the radio-frequency visibility [24]. For a given minimum elevation angle, the only factor affecting the coverage area is the satellite altitude. All the relevant variables are reported and shown in Figure 2.1.

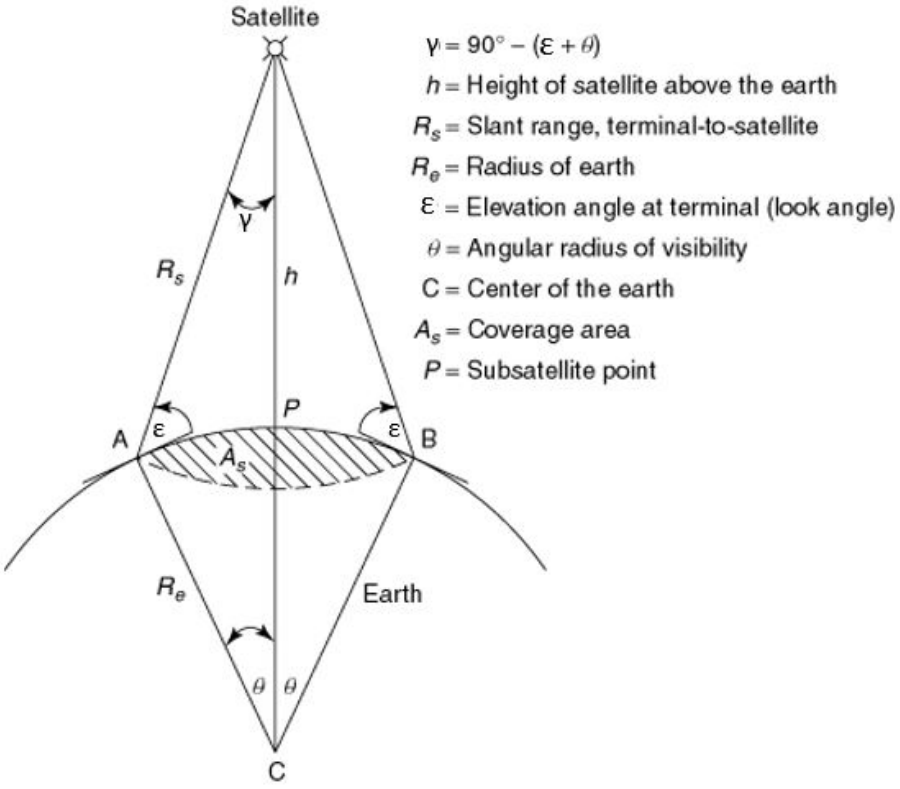

Figure 2.1: Coverage geometry [25].

The coverage equation for circular orbits is:

$$cos(\theta + \varepsilon) = \frac{cos(\varepsilon)}{1 + \frac{h}{R_{Earth}}} \tag{2.1}$$

where h is the satellite's altitude, R_{Earth} the Earth radius and θ the central angle radius of Earth coverage.
The value of θ which is required for the constellation to achieve the desired level of coverage is used as a measure of the efficiency of the constellation configuration; this means it is the performance index that characterises the global system quality and generally the optimisation methods consist of minimising it: the lower the value for fixed number of satellites T, the more efficient the constellation. With minimum elevation angle ε, from the coverage equation, if the altitude h is fixed, ε decreases if θ increases, while if ε is fixed, h increases if θ increases. Thus, an increase in θ always brings about a negative effect, either in terms of altitude or minimum elevation angle. The constellation with the lowest required value of coverage θ will allow the lowest operating altitude for a fixed value of minimum elevation ε. Conversely, if satellite altitude is fixed, the lower operating limits on elevation angle ε will be maximised [24].

While a single geostationary satellite can provide continuous coverage, a constellation of satellites is required for non-geostationary orbits. The choice depends on a number of factors:

- The elevation angle ε used should be as high as possible. This is particularly important for mobile-satellite services. With a high elevation angle, the multipath and shadowing problem can be reduced resulting in better link quality. However, there is a trade-off between the elevation angle used and the dimension of the service area.

- The propagation delay should be as low as possible. This is especially the case for real-time services. This poses a constraint on the satellite altitude h.

- Inter- and intra-orbital interference should be kept within an acceptable limit for the correct propagation and reception of the signal. This poses a requirement on the orbital separation.

- The regulatory issues governing the allocation of orbital slots for different services and different frequency bands.

For an optimal constellation of satellites, the most efficient plan is to have the satellites equally spaced within a given orbital plane and the planes equally spaced around the

equator. The coverage obtained by successive satellites in a given orbital plane is described by ground swath or street of coverage, as shown in Figure 2.2.

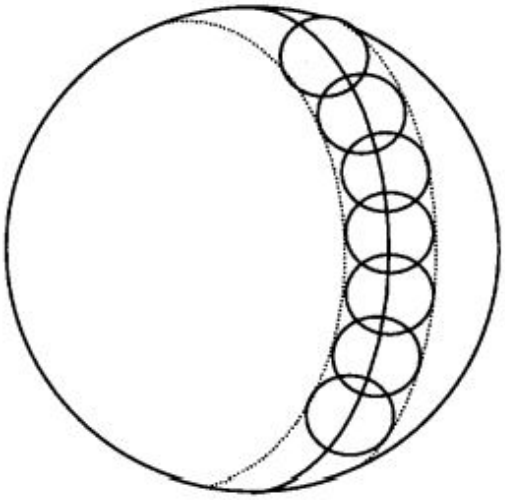

Figure 2.2: Ground swath coverage [24].

Total Earth coverage is achieved by overlapping ground swaths of different orbital planes. The total number of satellites in a constellation is given by $T = P \cdot S$, where P is the number of orbital planes and S is the number of satellites per plane. Another consideration in the design of a satellite constellation is the number of satellites being visible at any one time within a coverage area in order to support certain applications or to provide a guaranteed service. This is referred to as n-fold coverage where n states the number of visible satellites [24].

The provision of continuous whole Earth coverage consists in identifying those orbital patterns which will most economically provide a certain coverage. This standard is considered to be defined in terms of the level of coverage required (i.e. single, double or in general n-fold coverage) and of the minimum acceptable elevation angle to the nearest satellite from any point on the Earth's surface to the nearest sub-satellite point; the problem is to find the pattern, containing the smallest possible number of satellites, which best ensures that this maximum acceptable distance is never exceeded. Moreover, the minimum separation between any two satellites in the pattern should be as large as possible.
The importance of this objective may vary according to the system application. For example, in satellite navigation system accuracy may well increase as the minimum distance between the satellites providing the fix increases, while in a satellite communication system it may only be necessary that the minimum distance should exceed some fixed value to ensure that interference between transmissions in the same frequency band is acceptably

small. However, the larger the minimum distance between satellites, the more uniform the distribution of the satellites over the Earth's surface is and hence more likely the pattern will provide relatively favourable values of the maximum distance to the nearest sub-satellite point for all relevant levels of coverage.

An innovative method for the determination of the coverage area is here reported: it is fully-analytical and it takes as inputs the satellite's position vectors, the direction of the navigation line of sight and the half-aperture angle of the conical field of view for the propagation of the signal γ. The approach takes as reference the previous work of Nugnes et al. [14], but then it introduces some novel considerations that allow the determination of the boundary points of the area.
Unlike the other previous papers where the rise and set times of a satellite are evaluated from a generic ground station, this method starts from the position of a generic spacecraft on its orbit and derives all the locations on the Earth's surface within its field of view.
The Earth is modeled as a perfect sphere, a reasonable assumption since the approach is then applied to satellite constellations and usually the high number of satellites allow for a level of accuracy and precision in the order of kilometers. The geometry of the conical Field of View (FOV) is illustrated in Figure 2.3.

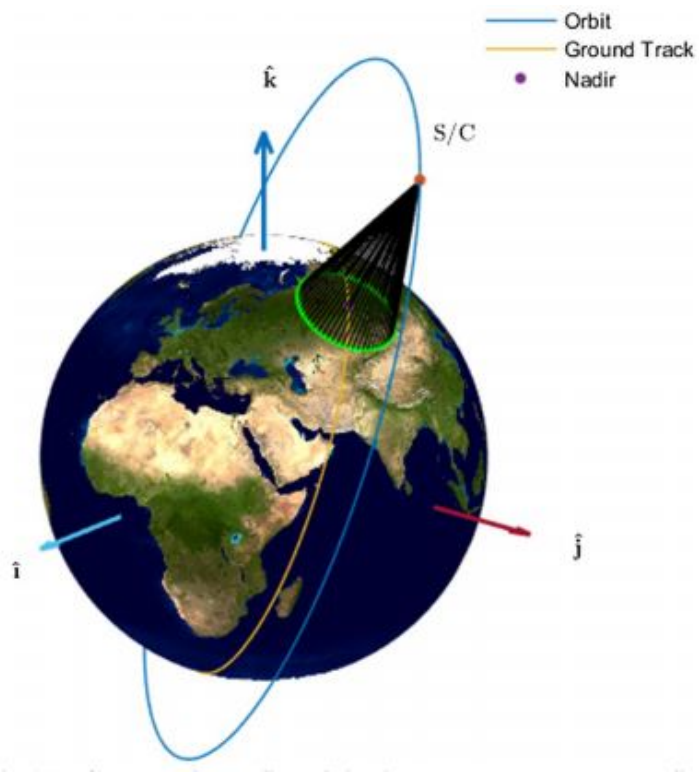

Figure 2.3: Conical Field of View [14].

As previously mentioned, the navigation signal is assumed to be extending as a cone from the center of mass of the satellite with a given half-aperture angle γ; the intersection

of the Earth and the assumed conical field of view is a circle and the points of intersection of the cone with the circle itself, representing the boundaries of the coverage area, can be derived by assuming a proper value of the half-aperture angle γ or the minimum elevation angle ε from which the satellite can be considered visible from the Earth's surface. The first step is to state that the trace of the Earth on a generic plane is a sphere, because in this way it is possible to move from a three dimensional problem to a planar one. The general equation of a plane is:

$$p_1 x + p_2 y + p_3 z = d \tag{2.2}$$

where $\hat{\mathbf{p}} = [p_1, p_2, p_3]$ is a unit vector normal to the plane and d is the distance of the plane from the origin of the coordinate frame. The cutting plane is depicted in Figure 2.4.

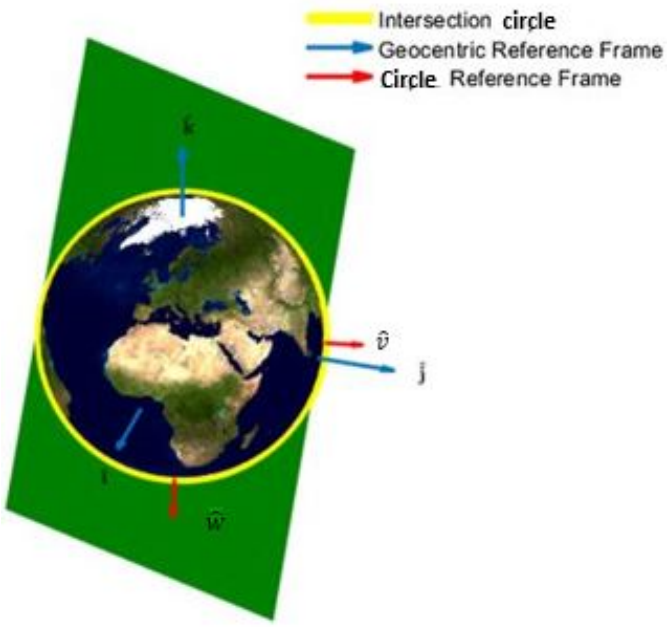

Figure 2.4: Intersection circle with the Earth [14].

In this case $\hat{\mathbf{p}}$ is assumed to be coincident with the line of sight of the navigation signal, while he origin of the coordinate frame is the Earth's center. The equation of the spheroid can be written as:

$$\frac{x^2 + y^2 + z^2}{r^2} = 1 \tag{2.3}$$

where r is the Earth radius R_{Earth}. The trace of the Earth in the generic plane is computed deriving the expression of z in Equation (2.2):

$$z = \frac{d - p_1 x - p_2 y}{p_3} \tag{2.4}$$

By substituting Equation (2.4) into Equation (2.3):

$$(p_1^2 + p_3^2)x^2 + (p_2^2 + p_3^2)y^2 + 2(p_1p_2)xy - 2(dp_2)x - 2(dp_2)y - r^2p_3^2 + d^2 = 0 \tag{2.5}$$

which is the equation of a conic; in particular, this equation represents a circle if its discriminant Δ is less than 0. After some manipulations,

$$\Delta = -r^2p_3^2(p_1^2 + p_2^2 + p_3^2) < 0 \tag{2.6}$$

which is always less than zero. The center of the local circle with respect to the origin of the reference frame is:

$$\mathbf{c} = [p_1d, p_2d, p_3d] \tag{2.7}$$

If the generic plane passes through the center of the Earth, then $d = 0$ and so $\mathbf{c} = [0, 0, 0]$.
Now, if the conic field of view of the navigation signal is divided into different planes having in common the satellite's line of sight, each plane will generate a circle hosting two limiting points for the coverage area. However, a different approach can be used: after the determination of two points of intersection with the aforementioned procedure and consequently of the central angle radius of Earth coverage θ, the other boundary points can be found by means of spherical geometry without the need of changing the orientation of the intersecting plane and to repeat the computations several times. By using longitude and latitude coordinates, the result is the same but the problem is simplified and requires less computations with a consequent reduction of the computational time.

The radius of the local circle is defined by:

$$\tilde{r} = \sqrt{r^2 - d^2} \tag{2.8}$$

which is equal to r if the origin coincides with the center of the Earth. The direction of the generic unit vector $\hat{\mathbf{v}}$ of the two-dimensional space containing the intersection circle is given by:

$$\hat{\mathbf{v}} = \frac{1}{\sqrt{p_1^2 + p_2^2}}[p_2, -p_1, 0] \tag{2.9}$$

and the direction of the generic unit vector $\hat{\mathbf{w}}$ to be perpendicular to $\hat{\mathbf{v}}$ is:

$$\hat{\mathbf{w}} = \frac{1}{\sqrt{p_1^2 + p_2^2}}[p_1 p_3, p_2 p_3, -(p_1^2 + p_2^2)] \tag{2.10}$$

Therefore, it is now possible to define a local reference frame in the plane of the circle obtained by the intersection of the Earth and a generic plane, where $\hat{\mathbf{v}}$ and $\hat{\mathbf{w}}$ are the generic unit vectors. The equation of the circle in this planar reference is:

$$\frac{v^2 + w^2}{\tilde{r}^2} = 1 \tag{2.11}$$

where v and w are coordinates of a generic point in this local frame. The two dimensional geometry is shown in Figure 2.5.

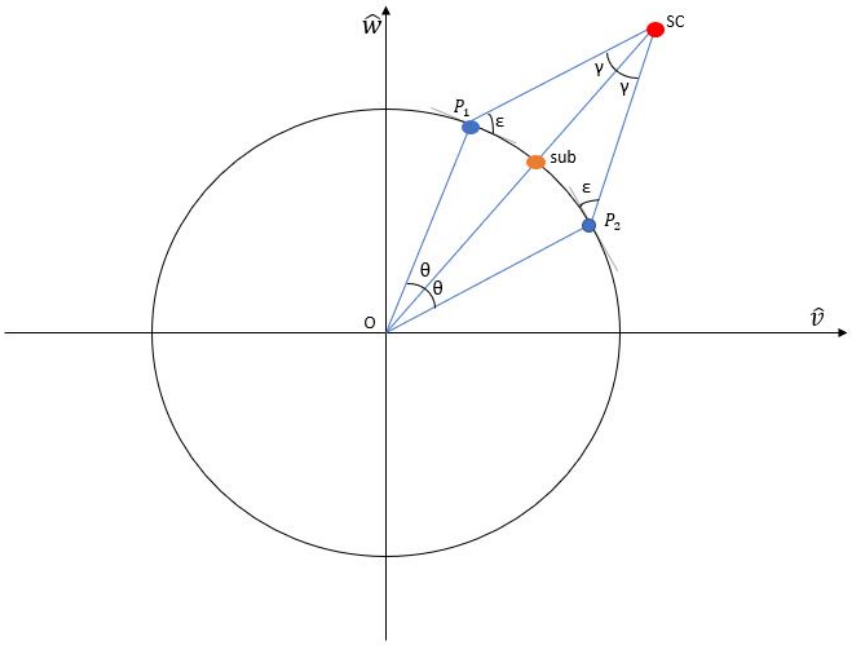

Figure 2.5: 2D Circular geometry.

In order to derive the ground range angle and so the coverage angle θ that is associated to the aperture angle to the instrument on board of the satellite, the equations of the two secants in P_1 and P_2 intersecting the local circle shall be determined. Let m and q be the generic angular coefficient and the vertical intercept of a line in the local reference frame. the equation of a line is:

$$w = mv + q \tag{2.12}$$

During the preliminary mission design according to the mission requirements, the line of sight of the navigation antenna is directed toward the Earth center (i.e. geocentric pointing) and since the Earth is modeled as a sphere, the direction of the vector $\hat{\mathbf{v}}$ can

be assumed coincident with the direction of the line of sight. The simplified geometry is shown in Figure 2.6.

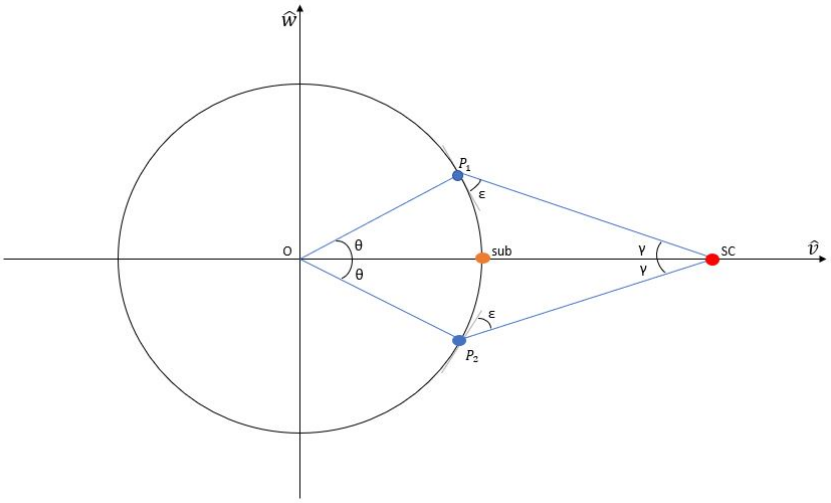

Figure 2.6: 2D Circular geometry used.

Hence, the satellite's coordinates are known if the satellite's position vector in the inertial frame is known and are:

$$\mathbf{r}_{s/c} = [r_{s/c}, 0, 0] \tag{2.13}$$

The angular coefficients of the two secants are:

$$m_{P_1} = \tan(\pi - \gamma) = -\tan(\gamma) \tag{2.14}$$

$$m_{P_2} = \tan(\gamma) \tag{2.15}$$

The following step is to write the generic equation for a line having as angular coefficients m_{P_1} and m_{P_2} and to solve a system with the equation of the local circle. If the discriminant is $\Delta > 0$, there exist two distinct solutions for each angular coefficient and so for each secant.

$$v_{P_1} = \frac{m_{P_1}^2 r_{s/c} \pm r\sqrt{m_{P_1}^2 + 1}}{(1 + m_{P_1}^2)} \tag{2.16}$$

$$v_{P_2} = \frac{m_{P_2}^2 r_{s/c} \pm r\sqrt{m_{P_2}^2 + 1}}{(1 + m_{P_2}^2)} \tag{2.17}$$

Just two of these solutions are correct and these are the ones on the same side and closer to the center of mass of the satellite. Once the values of v_{P_1} and v_{P_2} are obtained, it is possible to compute:

$$w_{P_1} = m_{P_1} v_{P_1} - m_{P_1} r_{s/c} \tag{2.18}$$

$$w_{P_2} = m_{P_2} v_{P_2} - m_{P_2} r_{s/c} \tag{2.19}$$

The position vectors of the two points P_1 and P_2 are defined.

$$\mathbf{r}_{P_1} = [v_{P_1}, w_{P_1}, 0] \tag{2.20}$$

$$\mathbf{r}_{P_2} = [v_{P_2}, w_{P_2}, 0] \tag{2.21}$$

Then, the ground range angle is:

$$\cos(2\theta) = \frac{\mathbf{r}_{P_1} \cdot \mathbf{r}_{P_2}}{r_{P_1} r_{P_2}} \tag{2.22}$$

and the elevation angle is:

$$\varepsilon = \frac{\pi}{2} - \theta - \gamma \tag{2.23}$$

Subsequently, the coverage angle θ is used to determine the other boundary points of the coverage area, but first it is necessary to compute the longitude and latitude of the line of sight, that coincides with the sub-satellite point because of the assumptions made. Since the direction cosines are known from the satellite's position vector and are defined as $\hat{\mathbf{r}}$, the operation can be done considering the same direction but applying the opposite pointing. Indeed, the line of sight is directed from the satellite toward the Earth and it is necessary to introduce the opposite direction $\hat{\mathbf{o}}$.

$$\hat{\mathbf{o}} = -\hat{\mathbf{r}} \tag{2.24}$$

By applying then the conversion from Cartesian to spherical coordinates:

$$\phi_{sub} = \tan\left(\frac{o_2}{o_1}\right)^{-1} \tag{2.25}$$

$$\lambda_{sub} = \sin(o_3)^{-1} \tag{2.26}$$

with ϕ_{sub} and λ_{sub} the longitude and latitude angles associated to the line of sight. Once defined the center point (ϕ_{sub}, λ_{sub}) and the angular radius θ, the geographic coordinates of the boundary of the area are computed from standard equations of spherical trigonometry. The procedure consists in the parameterisation on azimuth Az, by varying it in the range [0, 2π], about the center point. The equations for the geographic latitudes and longitudes are then:

$$\lambda_i = \sin\left(\cos\theta \sin\lambda_{sub} + \sin\theta\cos\lambda_{sub}\cos Az\right)^{-1} \tag{2.27}$$

$$\phi_i = \phi_{sub} + \tan\left(\sin\theta \sin Az, \frac{\cos\theta - \sin\lambda_{sub}\sin\lambda_{sub}}{\cos\lambda_{sub}}\right)^{-1} \tag{2.28}$$

In the work of Nugnes et al. [14], in order to find the intersection points between the cone of view and the Earth, the cutting plane is rotated several times around the line-of-sight direction $\hat{\mathbf{o}}$ and at each time two different points P_1 and P_2 are computed. Instead, the formulations here presented, thanks to the spherical Earth assumption, allow for a faster computation of the boundary points of the coverage area.

2.1.2 Revisit time

The revisit time (also known as coverage gap) is often used as a key performance metric for LEO and MEO systems which do not have continuous coverage of an area of interest and is defined as the duration in time between consecutive viewings of a given location on Earth. For constellations, the revisit time is defined as the interval of time during which no satellite in the constellation can observe a particular ground site. Such intervals are irregular and the longest of these, for a given constellation and ground site, is the maximum revisit time. Usually, based on mission objectives, an upper bound on maximum revisit time for points within region of the Earth's surface is required. Indeed, the Maximum Revisit Time (MRT) and Average Revisit Time (ART) over a given target area and period of analysis are considered during mission design process. For an Earth observation satellite or constellation the evaluation of revisit time therefore forms a critical component of the design and optimisation process. Usually, the analysis of coverage or revisit metrics for satellites and constellations is performed using commercially available orbital propagation and simulation software; however, due to the numerical nature of these programs and potential for long analysis period or large number of satellites, the computational time can become considerable. Furthermore, when many cases are to be considered, for example within a wider framework for system optimisation, a faster, open and stand-alone method would be preferred. Several methods have been developed throughout the years, geometrical or numerical, that allow to speed up the computational time and increase the accuracy of the results; some of them are hereafter going to be presented and developed.

2.1.3 Symmetric and non-symmetric constellations

As stated in Section 1.1, the different design methods are suitable for certain satellite constellation geometries rather than others. Symmetry considerations are of primary im-

portance: indeed, several methods are based on the assumption of symmetric constellation and can be applied in such cases only. Some examples are the Walker's circumcircle method (Section 3.3) and the Lang's method (Section 3.4), but also the Ulybyshev's geometrical methods (Sections 4.2 and 4.3) involving revisit time are based on symmetric patterns. Instead, Beste (Section 3.1) and Adams and Rider (Section 3.2) approaches are valid for non-symmetric constellations. In addition, all the aforementioned methods are applied to circular orbits only.
On the contrary, the classical "brute force" method (Section 4.1) is the only one that can be applied to all kinds of constellation patterns, both elliptical or circular orbits, symmetric or non-symmetric and for continuous or discontinuous coverage.

2.1.4 Analytical and numerical methods

In general, problems can be solved analytically and/or numerically. An analytical solution involves framing the problem in a well-understood form and calculating the exact solution and it does not follow any algorithm to solve the problem; on the other hand, a numerical solution means making guesses at the solution and testing whether the problem is solved well enough to stop, it is concerned with the construction, analysis and use of algorithms to solve the problem and it is sometimes prone to errors.
As examples, the Beste's (Section 3.1) and Adams and Rider's (Section 3.2) methods are analytical, since they make use of mathematical formulations in order to determine the optimal satellite configuration, while the Lang's (Section 3.4) method is numerical, because it is based on an iterative approach.
Also, the methods hereafter described distinguish between analytical and numerical solutions; the classical brute force method is numerical (Section 4.1) and it consists of propagating in time position vectors of satellite(s) and Earth location(s) of interest and determine their relative positions to find out visibility conditions, while the other developed by Ulybyshev (Section 4.2) is analytical and based on geometric considerations about the sub-satellite points on the Earth's surface.

2.2 Constellation geometries for circular orbits

All the existing satellite constellations, both the operational and the proposed ones, rely on a geometrical and mathematical study background, that gives some guidelines for

the design process and the accomplishment of the fixed objectives.

To describe the position of satellites of a constellation, three constant orientation angles plus a time-varying phase angle are needed:

- Right Ascension of the Ascending Node (RAAN) angle or Ω for the i^{th} orbit plane;
- Inclination angle i for the i^{th} orbit plane;
- Initial phase angle of the i^{th} satellite in its orbit plane at $t = 0$, measured from the point of right ascension; [(1)]
- $\frac{2\pi t}{T}$ = time-varying phase angle for all satellites of the constellation or mean anomaly M.

Both circular and elliptic orbits have been studied and the more relevant geometries are hereafter reported and described.

2.2.1 Walker constellations

At MEO and LEO, two types of regular constellation for satellites at the same altitude are generally divided into categories of Walker-Delta and Walker-Star constellations [12], [5].
The main feature of all the Walker patterns (both Delta and Star) consist in circular orbits of equal period and same inclinations for all planes of the constellation; elliptical orbits are advantageous for coverage limited areas, but the more uniform patterns provided by circular orbits appear preferable for whole-Earth coverage [26]. In general, continuous whole-Earth coverage would be provided most effectively by systems in which the distribution of satellites over the Earth's surface was maintained as uniform as possible, subject to the practical limitations imposed on a system necessarily involving multiple interesting orbits. Walker patterns are identified by (T/P/F):

- T = total number of satellites;
- P = total number of planes;
- F = relative phasing parameter, in units of $\frac{2\pi}{T}$ or $\frac{360}{T}$

F may have any value less than P, but for Delta patterns it can take only integer values from zero to $(P-1)$. The relative angular shift between satellites in adjacent orbital planes is equal to $F(\frac{2\pi}{T})$ (or equivalently $F(\frac{360}{T})$).

(1) The phase angle in orbital mechanics is the sum of argument of pericenter ω and true anomaly

The satellite phasing within each plane is determined by the number of satellites in the plane while the relative phasing between orbit planes is determined by F. This phasing between satellites in different orbits has important effects on the coverage properties of the constellation. The phase angle is identified as the geocentric angle traversed by a satellite since passing its ascending node in the reference plane.
Any individual pattern may be identified by the reference $(T/P/F)$ and this is sufficient to determine the general shape. To fix the precise position of the orbital planes it is necessary to specify the common inclination i; hence, inclination may be treated as a parameter to optimise the pattern in accordance with requirements.

Walker-Delta patterns

In the Walker-Delta patterns, T satellites are in equal-period, evenly-spaced circular orbits and all at the same inclination to a reference plane, with a uniform distribution of the satellites among and within the orbital planes [12]. The peculiar characteristic of such geometry is its symmetry.
The pattern contains T satellites: S satellites are evenly spaced in each of the P orbital planes; thus P and S may each equal any factor of T, including 1 and T, provided their relative values are such that $T = P \cdot S$. All orbital planes have the same inclination; the reference plane usually coincides with the equator but this need not necessarily be the case. The ascending nodes of the P distinct orbits are evenly spaced at intervals of $\frac{2\pi}{P}$ (or $\frac{360}{P}$) units. The relative positions of satellites in different orbital planes are such that there are equal intervals between passages of satellites in adjacent orbital planes through their respective ascending nodes [12].

For example, $(T/P/F) = (12/3/1)$ means that there are 12 satellites in 3 orbital planes with 4 satellites in each plane separated symmetrically by 90 deg in mean anomaly and the 3 orbit planes separated symmetrically by 120 deg in longitude of ascending node. The "1" notation indicates that when a satellite in the first orbital plane is at 0 deg mean anomaly (say, over the equator), a satellite in the next orbital plane is at $1 \cdot \frac{360}{12} = 30$ deg mean anomaly. Similarly, a satellite in the third orbital plane is at 60 deg mean anomaly at the same instant.

For each individual satellite in an inclined circular orbit, the Earth-track consists of a series of identical excursions alternatively into the northern and southern hemispheres, each reaching a maximum latitude equal to the orbital inclination to the equator.
It must be noted that when calculating coverage for all Delta patterns having a particular pair of T and P over a range of inclinations, it is only necessary to perform the calculations

for orbital inclinations up to 90 deg; the corresponding values in retrograde orbits are identical to those of the complementary pattern at the inclination which is the supplement of the retrograde inclination under consideration [27].
In general, for most purposes it would be unsatisfactory to choose a satellite pattern in which pairs of satellites passed very close to one another. A number of Delta patterns are such that, independent of the value of the inclination, the ascending node of one satellite coincides with the descending node of another as they pass simultaneously through the reference plane [27].

Walker-Star patterns

In Walker-Star patterns [12] there are two significant differences from the Delta patterns: first, F needs not to have an integer value and the ascending nodes are not evenly distributed over the full 360 deg of the equator but all occur within one 180 deg arc. The latter point is dealt with by introducing an input parameter W, which modifies the spacing of nodes; thus the ascending nodes are separated by $W \cdot \frac{360}{P}$ where W assumes a value equal to 1 for Delta patterns and has a value a little greater than 0.5 (usually in the range 0.525 to 0.625) for a Star pattern. Indeed, the value W=0.5 would perfectly distribute the ascending nodes among 180 deg and in practice this need not necessarily cause any problem, the risk of a physical collision would be extremely small; however, this could in any case be obviated by a small displacement from the optimum phasing which could have an insignificant effect on the coverage, so the [0.525-0.625] range [12].
Generally, Delta patterns are most appropriate for use when medium inclination orbits are required, while Star patterns when near-polar orbits are required.

In the case of Walker patterns, the orbit orientation angles have the symmetrical form:

- RAAN for the j^{th} orbit plane = $W\frac{2\pi j}{P}$ with W=1 for Delta patterns and $j = 1$ to P;
- Inclination i for the j^{th} orbit plane equal for all P;
- Initial phase angle of the k^{th} satellite in its orbit plane $F\frac{2\pi j}{T}$ with $j = 1$ to P;
- $\frac{2\pi k}{S}$ + initial phase = time-varying phase angle M for all satellites of the constellation with $k = 1$ to S.

The algorithm-like logic for the Walker pattern is presented in Appendix B.1.

An example of the Walker geometry for a (12/3/1) constellation with $i = 50$ deg and $h = 25500$ km is reported in Figure 2.7, which represents the satellites' groundtrack, that is the path on the Earth's surface directly below the satellite's trajectory. The yellow stars

are the initial positions of the satellites on their orbits. Figure 2.8 is the constellation in Earth Centered Earth Fixed (ECEF) reference frame (see Appendix A.2), while Figure 2.9 shows the plane containing the initial phase angle and the RAAN.

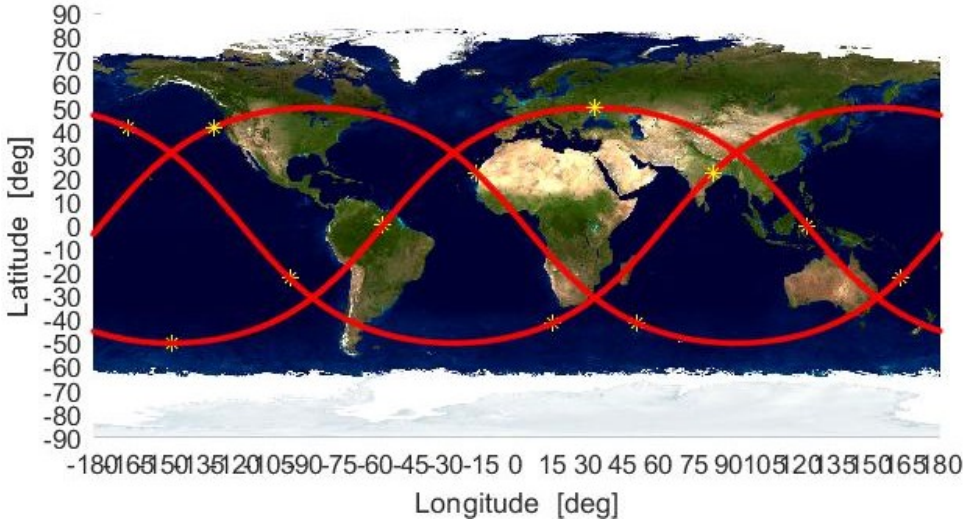

Figure 2.7: Walker (12/3/1) groundtrack.

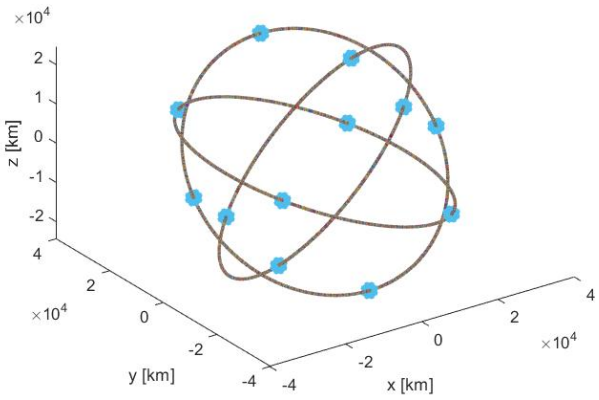

Figure 2.8: Walker (12/3/1) 3D orbits.

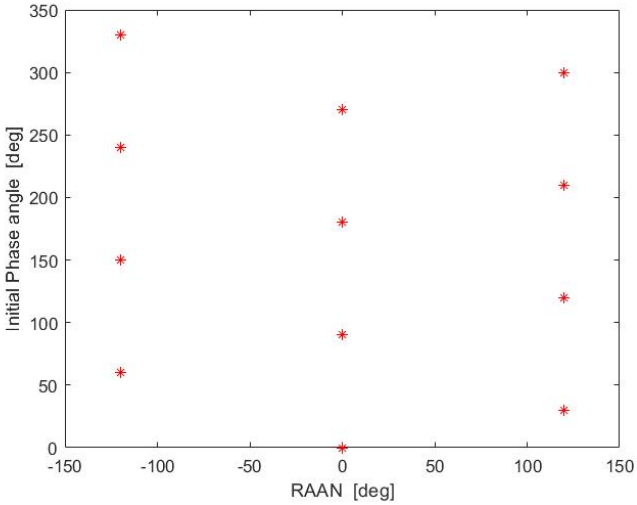

Figure 2.9: Walker (12/3/1) Ω versus Initial phase.

2.2.2 Rosette - Ballard constellations

The Rosette pattern generalises and extends the Walker pattern: methods employed are basically the same but presented in a more unified mathematical framework.
The satellite's orbits are uniformly distributed in a right ascension angle as they pass through the reference plane and the initial phase position of satellites in each orbit plane is proportional to the right ascension angle of that plane.
The name "Rosette" was chosen to designate this class of constellations because the pattern of orbital traces, when drawn on a fixed celestial sphere, resembles a many-petaled flower [26]. Figure 2.10 shows the Rosette-like constellation in the [x,y] ECEF plane.

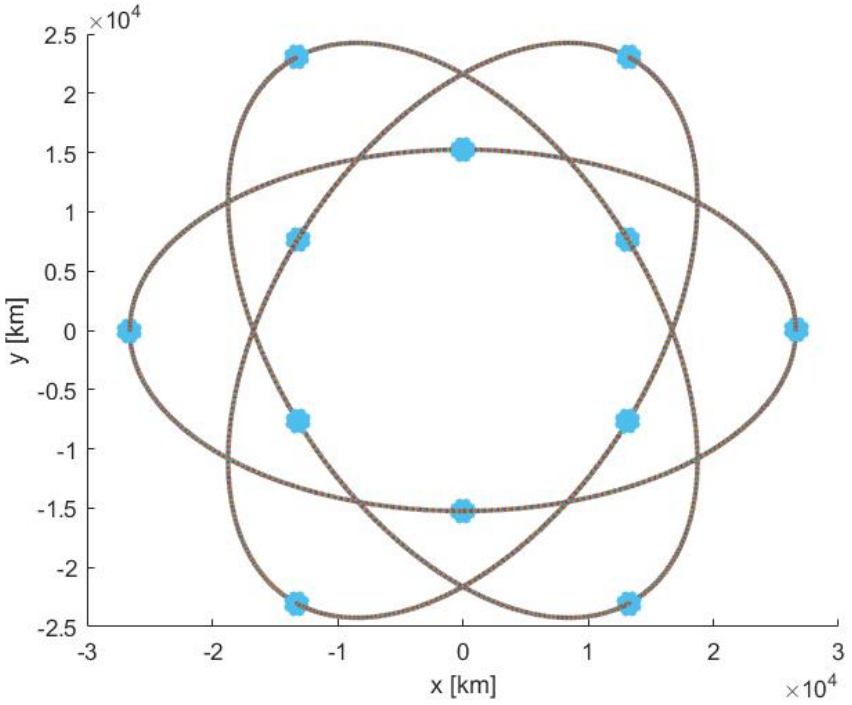

Figure 2.10: Ballard (12/3/2.25) Rosette.

Rosette patterns are identified by $(T/P/m)$:

- T = total number of satellites;
- P = total number of planes;
- m = geometric harmonic factor that plays a role for the initial phase angle determination: initial phase angle = $mS\frac{2\pi j}{T}$, with $j = 1$ to P.

If m is a simple integer, a constellation having one satellite in each of the P planes is being referred to $T = P$; if m is an unreduced ratio of integers equal to $\frac{[0,(T-1)]}{S}$, a constellation having S satellites in each of the P planes is being referred to, where S is the

denominator of m [26]. In addition, it must be noted that as the inclination increases, the flower closes around the pole while as it decreases, the flower opens toward the reference circle.

In the case of Rosette pattern, the orbit orientation angles have the symmetrical form:

- RAAN for the j^{th} orbit plane $= \frac{2\pi j}{P}$ with $j = 1$ to P;
- Inclination angle i for the j^{th} orbit plane equal for all P;
- Initial phase angle of the k^{th} satellite in its orbit plane $mS\frac{2\pi j}{T}$ with $j = 1$ to P and $m = \frac{[0,(T-1)]}{S}$;
- $\frac{2\pi k}{S}$ + initial phase = time-varying phase angle M for all satellites of the constellation with $k = 1$ to S.

The algorithm-like logic for the Ballard pattern is presented in Appendix B.2.

An example of the Ballard geometry is reported in Figure 2.11 for the groundtrack, Figure 2.12 in ECEF reference frame and Figure 2.13 as right ascension versus initial phase angle for a (12/3/2.25) constellation with $m = \frac{9}{S}$, $i = 50$ deg and $h = 25500$ km.

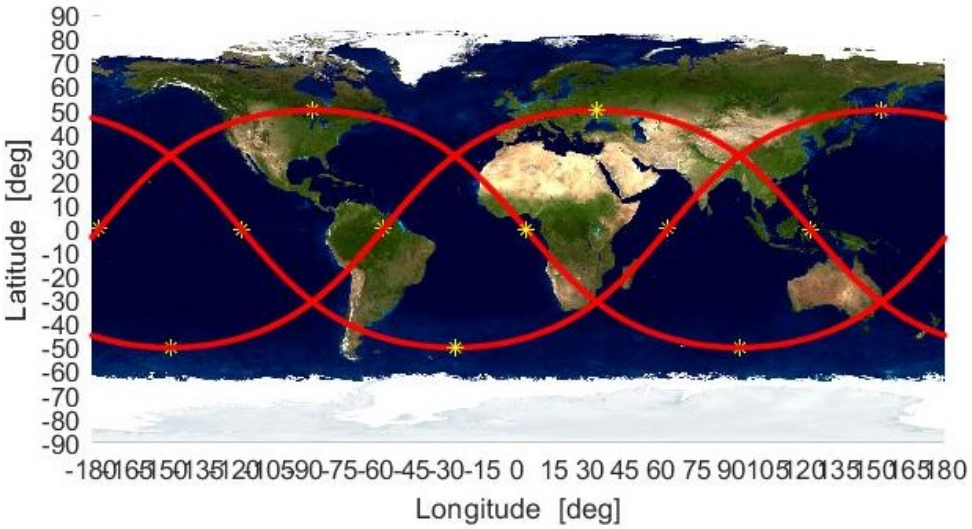

Figure 2.11: Ballard (12/3/2.25) groundtrack.

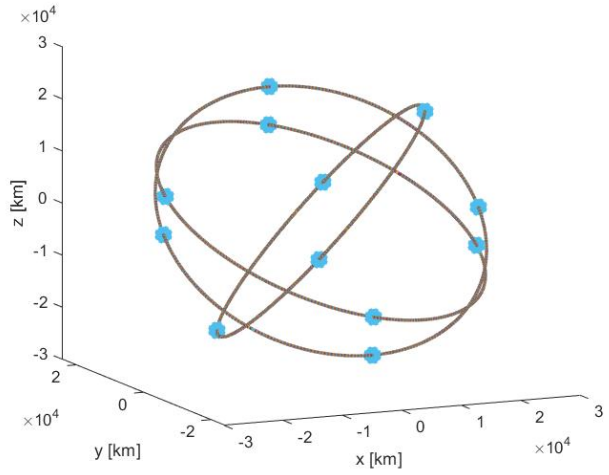

Figure 2.12: Ballard (12/3/2.25) 3D orbits.

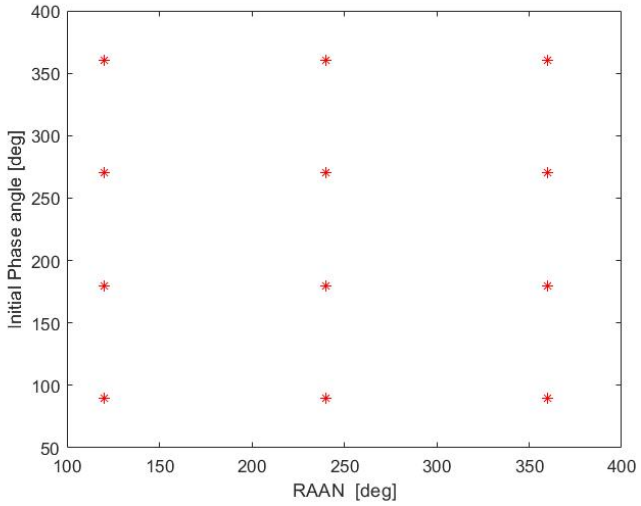

Figure 2.13: Ballard (12/3/2.25) Ω versus initial phase.

2.2.3 Street Of Coverage constellations

The Street Of Coverage (SOC) concept relies on multiple circular orbit satellites at the same altitude placed in a single plane so as to create a Street Of Coverage which is continuously viewed [5]. The objective is then to determine analytically how many such streets (i.e. planes of satellites at the same inclination) are required to cover the zone of interest or the globe. The SOC technique is generally applied to polar constellations and so the resultant optimal configuration is a polar satellite network in which the motion of a spacecraft in one orbital plane is synchronized with that of the spacecraft in the adjacent planes (phased polar constellation) [28].

The relative design methods involving such geometry are analytical (Beste presented in Section 3.1, Adams and Rider described in Section 3.2): they identify families of circular polar orbit constellations using minimal total number of satellites which can provide a desired n-fold of coverage at or above a user-defined latitude.
The basic assumption is that the constellation can be arranged so there are $2(P-1)$ co-rotating interfaces and 2 counter-rotating interfaces. The resultant configuration is defined as non-symmetric because the orbit separation, given in $\Delta\Omega$, between co-rotating planes is different from the orbit separation between the 2 counter-rotating interfaces.

The involved parameters for SOC geometry are:

- Central angle of coverage θ

- Angular half-width of the ground swath Φ [(2)];
- Inter-plane angular separation between adjacent planes $\alpha = \Phi + \theta$
- Inter-plane angular separation between first and last planes 2θ
- Inclination angle of 90 deg equal for all P ;
- Initial phase angle of the k^{th} satellite in its orbit plane $\frac{2\pi j}{T}$ with $j = 1$ to P;
- $\frac{2\pi k}{S}$ + initial phase = time-varying phase angle M for all satellites of the constellation with $k = 1$ to S.

The most important Street Of Coverage parameters involved in the geometry are shown in Figure 2.14 and the algorithm-like logic for the SOC pattern is presented in Appendix B.3.

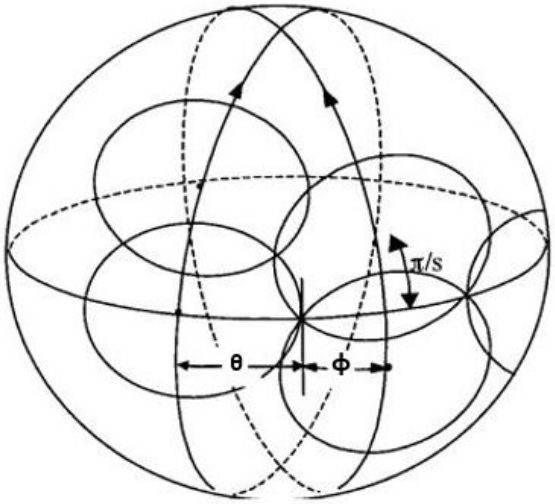

Figure 2.14: Street of Coverage geometry. [24]

An example of the Street Of Coverage geometry is reported in Figure 2.15 for satellite's groundtrack, Figure 2.16 in ECEF reference frame and Figure 2.17 with initial phase angle as a function of the RAAN for a constellation with 28 satellites divided in 4 planes, at an altitude $h = 25500$ km and with inclination $i = 90$ deg.

(2) Swath width: the length along the equator covered by the swath crossing it at a given i

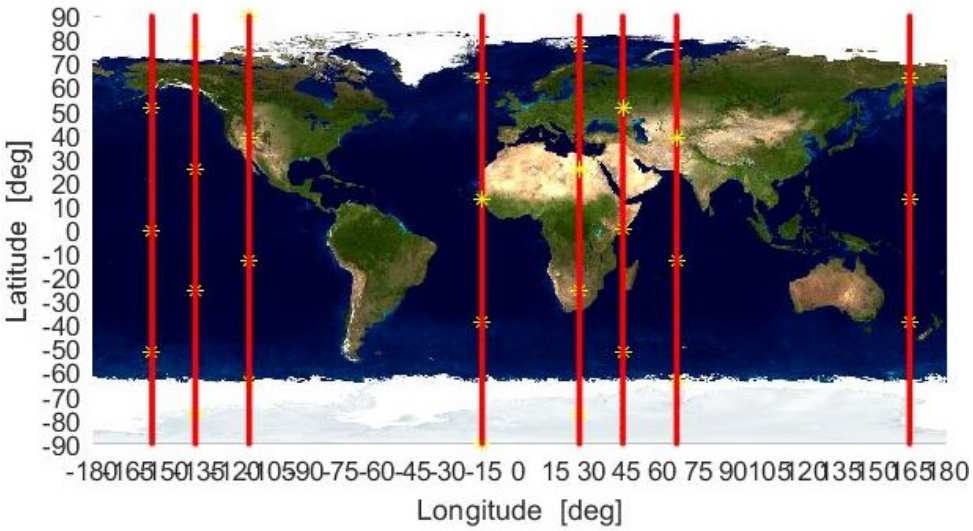

Figure 2.15: Street Of Coverage T=28, P=4 groundtrack.

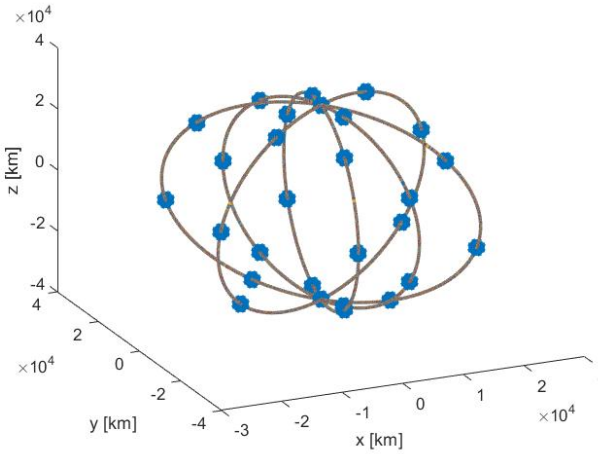

Figure 2.16: Street Of Coverage T=28, P=4 3D orbits.

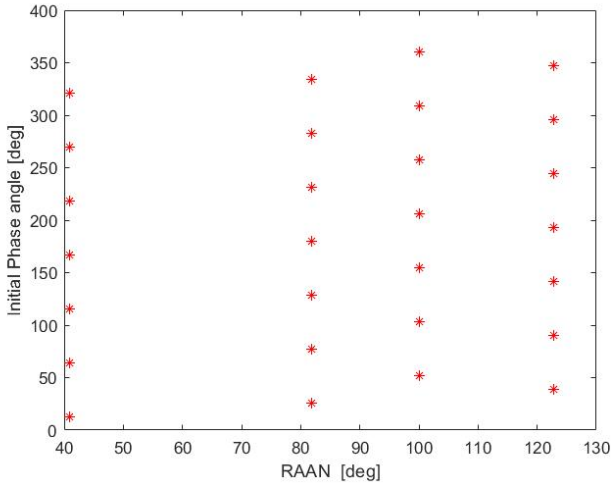

Figure 2.17: Street Of Coverage T=28, P=4 Ω versus initial phase.

2.2.4 Comparison

The two families of methods described, i.e. Walker-type in which also the Rosette geometry is included and SOC-type, are used to generate optimal constellations of large number of satellites in circular orbits for continuous global or zonal coverage. Some general considerations and a comparison about them are here reported.

In general, if the zone (a region between two latitude values on the Earth's surface) is in the low to mid latitudes, then the optimal constellation will consist of inclined orbital planes with nodes spaced evenly through 360 deg. For zonal coverage at high latitudes or any zone including the pole, SOC method using polar orbits with nodes spread over 180 deg were preferable. These polar orbits would require fewer satellites at the same altitude than the inclined orbits.

However, Walker constellations are more efficient than SOC constellations for continuous coverage with inclined orbits or for n-fold coverage. The number of satellites required for continuous global coverage as a function of satellite altitude for both the Walker and SOC methods increases steadily (although not always monotonically) as the satellite altitude decreases (numerical examples are shown in Section 5.1.3).
For single continuous global coverage with 20 or fewer satellites, the symmetric inclined Walker-type constellations are more efficient. For the same number of satellites, Walker constellations offer continuous global coverage at a lower altitude; conversely, at the same altitude, Walker constellations can perform the same job with fewer satellites. The latter case can be well understood in the case presented on numerical examples of Sections 2.2.1 and 2.2.3: at the same altitude h=25500 km, the Walker-type constellation requires 12 satellites, while the SOC needs 28 satellites.
For single continuous global coverage with more than 20 satellites, the optimally phased, non-symmetric polar SOC constellations are more efficient. However, in the region of 30 satellites, the inclined Walker constellations achieve 4-fold coverage at altitudes for which the polar SOC constellations can not even achieve full 3-fold coverage [3].

By summarising:

- Walker
  - Inclined;
  - Symmetrical;
  - Usually few satellites per plane;
  - Best coverage at mid-latitudes;
  - Optimality for 1-fold coverage with $<$ 20 satellites;
  - Optimality even for 2-fold coverage and up.
- Street Of Coverage
  - Polar;
  - Non-symmetrical;
  - Usually many satellites per plane;
  - Best coverage at poles;
  - Optimality for 1-fold coverage with $>$ 20 satellites;
  - No Optimality for 2-fold coverage and up.

2.3 Constellation geometries for elliptical orbits

The studies and researches of satellite constellations do not involve circular orbits only, but several authors (e.g. Draim [1], [29]) investigated the case of elliptical orbits. Anyway, these geometries involve a small number of satellites and they are applied to coverage of specific locations on the planet's surface rather than on the whole Earth. For this reason, it is difficult to determine a general method, but the geometry should be everytime and newly determined depending on the user needs.

2.3.1 Draim method

The Draim method is just an attempt to find out a general method for elliptical orbits that satisfy the request of global coverage, but a lot of different cases exist.
The method involves symmetric, elliptical orbits with a common period and inclination to achieve a single or multiple continuous global coverage using fewer satellites than required with circular orbits. The basic geometry is made of 4 hypersynchronous satellites for world-wide coverage: each satellite is in approximately the same orbit and relative phasing and orientation of the constellation are similar, thereby simplifying some of the maneuvering costs [29].
Draim's analysis of the optimal four-satellite continuous coverage constellation is based on a tetrahedron formed by four planes, each plane contains three of the four satellites in the constellation. The basic requirement is for planes of the tetrahedron to always encompass the Earth, without ever intersecting it, as the tetrahedron changes shape or wraps during the constellation repeat groundtrack period. A repeat groundtrack design is chosen for operational simplicity [30].

The basics geometry for the four satellites is reported in Table 2.1, with values for right ascension, argument of perigee and mean anomaly for each of the four satellites:

Table 2.1: Draim four-satellite constellation characteristics

Satellite	**RAAN Ω**	**Argument of perigee ω**	**Mean anomaly M**
1	0 deg	270 deg	0 deg
2	90 deg	90 deg	270 deg
3	180 deg	270 deg	180 deg
4	270 deg	90 deg	90 deg

All the four satellites share the same set of values for the semi-major axis a, eccentricity e and inclination i. So, for a 27-hour period orbit, Draim used $e = 0.263$ and $i = 31.3$ deg. These numbers make the original Draim configuration. The tetrahedron idea presented by Draim is presented in Figure 2.18 and the correspondent constellation is depicted in Figure 2.19.

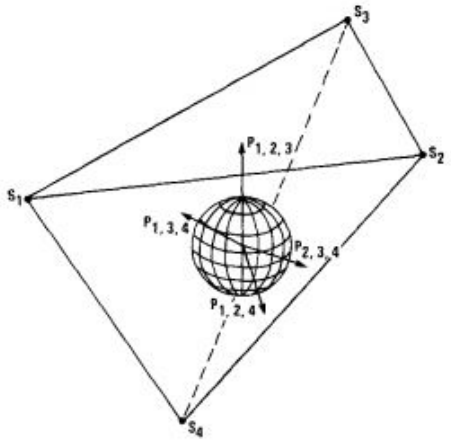

Figure 2.18: Isometric drawing of Draim constellation [29].

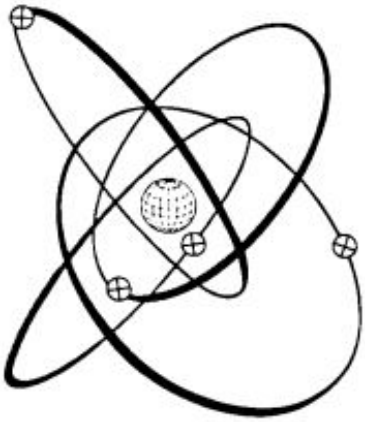

Figure 2.19: 3D Draim tetrahedron [29].

2.3.2 Flower constellations

The Flower constellation pattern comes from the "Sistema Quadrifoglio" conceptualised by Broglio in 1981 as an equatorial constellation of four satellites, whose orbital period is $T_{period} = \frac{T_s}{3}$ (T_s = Sidereal period), $i = 0$ deg, $\Delta M = \frac{\pi}{2}$ (variation in mean anomaly) and $(\Omega + \omega)$ displaced of $\frac{\pi}{2}$ [6], [31]. The general theory of flower constellations has been introduced around 2002 and poses no constraint in the kind of orbits to be used and it can be made using circular or elliptical orbits and equatorial or inclined

orbits. The Flower constellation is a novel methodology to design satellite constellations characterized by compatible orbits with respect to an assigned given rotating reference frame. In this rotating reference frame all the satellites follow the same close-loop relative trajectory (repeated space tracks). A Flower constellation is obtained by means of a suitable phasing mechanism that initially distributes the satellites in a subset of admissible positions. The interplay of the design parameters generates beautiful and intriguing axial-symmetric period dynamics. These dynamics allow to explore a wide range of potential applications which include telecommunications, deep space observations, global positioning system and allow to quickly come up with highly complex satellite formations that no one even knew existed and, consequently, to propose new kind of space missions. Flower constellations open a new frontier in complex satellite constellations, they provide building blocks to enable the creation of arbitrarily complicated ensembles of satellite orbits [31].

Up to now, no general theory of constellations exists that helps the engineers in achieving the desired coverage or to satisfy a different specific mission target. Due to the inherent complexity of the general constellation design, the Walker constellations, which use circular orbits, became so popular and are the most common type encountered in practice, while Highly Elliptical Orbits (HEO) based constellations are rarely used.
It has been proved that many of the existing constellations, including but not limited to the GPS and Galileo (both made of satellites in a Walker constellation), can be easily reproduced as Flower constellations [31].

The theory of Flower constellations is a natural consequence of the theory of compatible (or resonant) orbits. The satellite distribution identifies the edges of rotating figures whose shapes are time invariant. The complex synchronized dynamics of satellites preserve the shape of a space object. The whole Flower constellation is an axial-symmetric rigid object in space that is spinning with prescribed angular velocity. Flower constellations are generally characterized by repeatable groundtracks and a suitable phasing mechanism. The geometries constitute an infinite set of satellite constellations characterized by periodic dynamics. The dynamics of a Flower constellation identify a set of implicit rotating reference frames on which the satellites follow the same closed-loop relative trajectory. In particular, when one of these rotating reference frames is "Planet Centered Planet Fixed", then all the orbits become compatible (resonant) with the planet and consequently the projection of the relative trajectory on the planet becomes a repeating groundtrack.
As a particular case, the Flower constellations can be designed as J_2 compliant, that is with orbit compatibility that takes into account the linear effects of the J_2 perturbation.

In the rotating reference frames the relative trajectories, which depend on five independent integer parameters, constitute a continuous, closed-loop, symmetric pattern of flower petals. Two integer parameters establish the orbit period and the other three distribute the satellites into an upper bounded number of admissible positions. Moreover, all orbits in the constellation have an equal argument of perigee ω, inclination i and perigee altitude h_p. Hence, Flower constellations are identified by eight parameters:

- N_p positive integer = number of petals (number of orbit revolutions required to complete one period of repetition);
- N_d positive integer = number of sidereal days to repeat the relative trajectory (groundtrack);
- T positive integer = number of satellites;
- F_n and F_d integers to rule the phasing;
- ω = argument of perigee;
- i = orbit inclination;
- h_p = perigee altitude.

An orbit is said to be compatible with respect to a reference frame rotating with a certain angular velocity ω_{rot} (e.g. ω_{Earth} if the reference is the Earth) if the orbit period T_period satisfies the relationship:

$$N_p \cdot T_{period} = N_d \cdot \frac{2\pi}{\omega_{rot}} \tag{2.29}$$

Therefore, after N_p orbital periods the rotating reference frame has performed N_d complete rotations and consequently the satellite and the rotating reference frame come back to their initial positions. In the design procedure, once the anomalistic period has been established, the semi-major axis a can be determined. The eccentricity e of the orbit can be calculated from a and a specific perigee altitude h_p. Once a and e have been defined, the shape of the orbit is completely determined and all that remains is to specify its orientation in space. It must be mentioned that the orbit period (equal for all the satellites of the constellation) depends on the ratio $\frac{N_d}{N_p}$. Flower constellations are built with the constraint that all satellites belong to the same relative trajectory:

$$-N_p \cdot \Delta\Omega = N_d \cdot \Delta M \tag{2.30}$$

This is the fundamental equation of the Flower constellation phasing and allows to evaluate the admissible locations where to place the satellites in order they all belong

to the same relative trajectory. The number of admissible locations per orbit in flower constellations is N_d. Figure 2.20 shows a Flower constellation with 5 petals (say N_p).

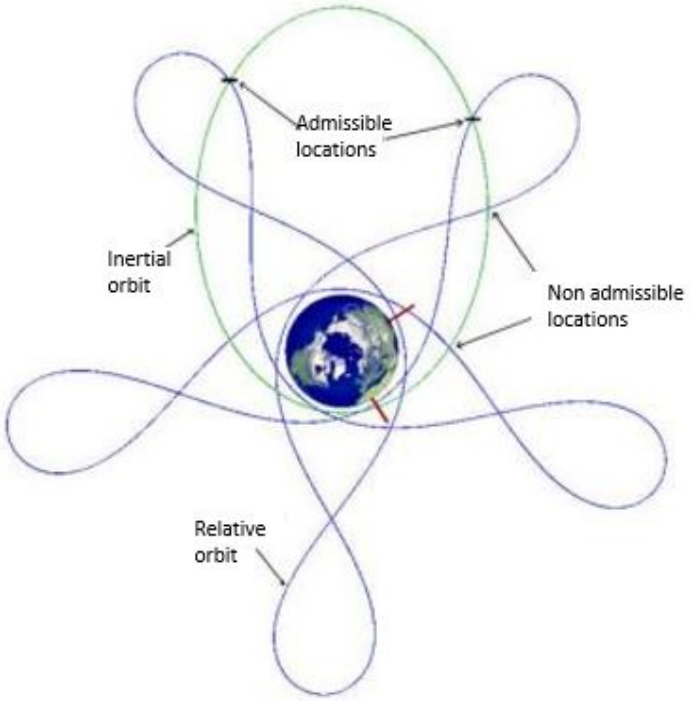

Figure 2.20: 5-2 Flower constellation [31].

The orbiting satellites must belong of the intersection of the two curves representing the relative orbit, as seen from an ECEF frame, and the inertial orbit as observed in the ECI frame. Note that, in the ECI frame the green orbit will appear fixed while the blue orbit will rotate in a counter-clockwise fashion at the Earth's angular spin rate. Looking at this motion in an ECEF frame, then the dynamics will be reversed, with the blue orbit that appears fixed while the green is rotating, at the Earth's angular spin rate, in a clockwise fashion [31]. Two orbits are said to be admissible when the orbital parameters (ω, i, a, e) are identical for both the relative and inertial orbits and only Ω can differ. Hence, the initial position of a satellite in the constellation must be searched among all intersections of the orbits, since it shall belong to both inertial and relative ones. It is possible to demonstrate [31] that, for a one day repeated groundtrack, only one among all the intersecting points has the correct dynamics, that is the angular momentum ($\mathbf{r} \times \mathbf{v}$) is preserved as required by the two-body problem. However, when examining multiple day repeated groundtracks, additional valid intersection points are found. In point of fact, for each day it takes to repeat a groundtrack there is one valid intersection where a satellite could be located. Figure 2.20 shows a constellation where two satellites have been placed in a single orbit; yet, both satellites also belong to the same relative orbit. By extension, if one places a number of satellites that is an integer multiple of the number of days to

repeat, then there will be one orbit for every N_d satellites.
In general, evenly orbits distribution are preferred whenever the symmetry is desired. For the orbit node lines step $\Delta\Omega$ is computed, while two satellites on the same orbit are displaced in function of ΔM; both are function of the eight parameters previously described. The number of satellites per orbit for a chosen distribution sequence is S and the total number of satellites is $T = S \cdot F_d$: S tells how many of the N_d admissible locations are filled in a given satellite distribution.

Summarising, all the orbits in a given Flower constellation:

- Have identical orbit shape: anomalistic period, argument of perigee, height of perigee and inclination;
- Have the orbital period that is evaluated in such a way to yield a perfectly repeated groundtrack (they are said to be compatible);
- Have equally displaced node lines along the equatorial plane for each satellite in a complete flower constellation. Restricted or incomplete flower constellations have orbits whose RAAN are equally displaced within a limited right ascension range $\Delta\Omega$. Therefore, instead of having orbits evenly distributed on the 360 deg around Earth, it is possible to concentrate on a particular region.

As stated before, the orbits in a Flower constellation can be elliptical or circular and, although for a given constellation all the orbits must be identical, multiple flower constellations can be designed to meet particular mission requirements. In Flower constellations there could be more than one satellite that share the same inertial orbit. The only orbital elements that vary from one satellite to another are, in general, the RAAN/Ω and the mean anomaly M. The constraint that is always enforced is that all the satellites share the same relative path, calculated with respect to some relative frame (i.e. ECEF). The relations used to distribute the RAAN and M are:

$$\Omega(k+1) = \Omega(k) - 2\pi \cdot f(F_n, F_d) \tag{2.31}$$

$$M(k+1) = M(k) + 2\pi \cdot f(F_n, F_d) \cdot \left(\frac{n + \dot{M}}{\omega_{Earth} + \dot{\Omega}}\right) \tag{2.32}$$

Where ω_{Earth} is the Earth rotation rate, n represents the satellite mean motion, k = 1, ..., (N_s-1), $\Omega(k)$ is the RAAN of the *k-th* satellite, *M(k)* is the mean anomaly of the *k-th* satellite and $f(F_n, F_d)$ is a term that depends on the phasing parameters. The

algorithm-like logic for the Flower Constellations pattern is presented in Appendix B.4.

An example of the Flower constellation geometry applied to circular orbits is given by the Galileo constellation, reported in Figure 2.21 for the satellite's groundtrack, Figure 2.22 in ECEF regerence frame and Figure 2.23 in right ascension versus initial phase space, with $N_p = 17$, $N_d = 10$, $F_n = 1$, $F_d = 3$, $T = 30$ (both operational and spares considered), $h_p = 23222$ km, $i = 56$ deg and $\omega = 270$ deg.
The Galileo system is a Walker (24/3/1), with satellites lying on three orthogonal orbit planes and 6 in-orbit spares.

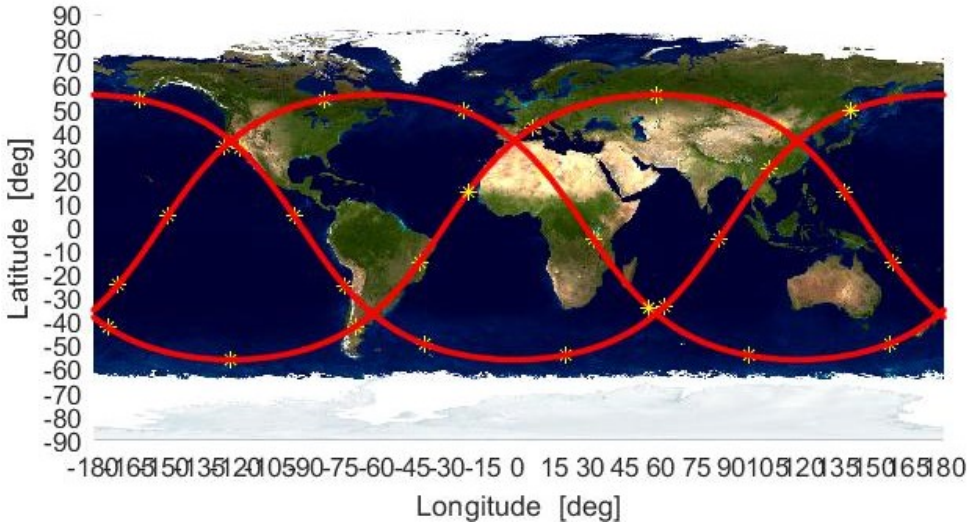

Figure 2.21: Galileo groundtrack with Flower constellation concept.

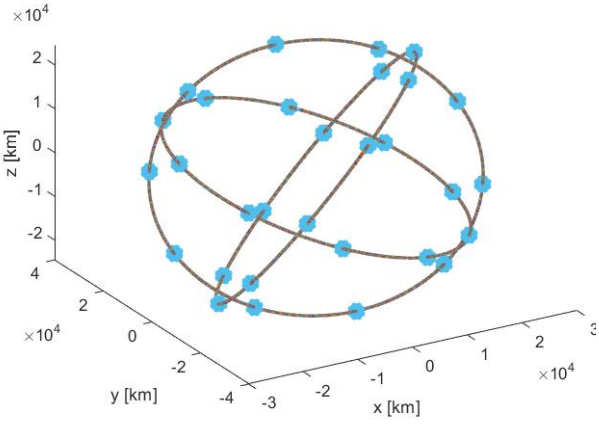

Figure 2.22: Galileo 3D orbits with Flower constellation concept.

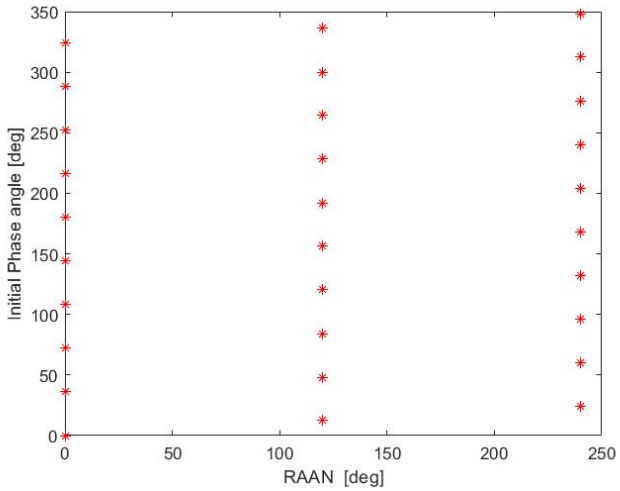

Figure 2.23: Galileo Ω versus M with Flower constellation concept

2.4 Existing and proposed constellations

All the existing constellations, meaning the operative, non operative or just designed but never realised, are based on the presented geometries; some variations could have been done in order to better satisfy the requirements and objectives, but the theory behind is unchanged. This section aims to present some existing constellations as practical example of what stated before at a theoretical level.

2.4.1 Global Positioning System

The Global Positioning System (GPS) is a U.S. owned satellite system that provides users with Positioning, Navigation and Timing (PNT) services. This system consists of three segments: the space segment, the control segment and the user segment. The GPS space segment is a constellation of satellites transmitting radio signals to users and flown by the U.S. Air Force [19]. The GPS is a satellite-based radionavigation system and it is one of the Global Navigation Satellite Systems (GNSS) that provides geolocation and time information to a GPS receiver anywhere on or near the Earth where there is an unobstructed line of sight to 4 or more satellites.
The first constellation of the Global Positioning System (GPS) was designed with a Walker pattern (24/3/2) inclined at 63 deg with 20000 km altitude (12 h orbital period). It successively evolved into an 18 satellite, 6 plane (18/6/2) Walker constellation at 55 deg, then a 21 satellite, 6 plane and finally evolved to the current 24 satellite, 6 plane constellation at an altitude of approximately 20200 km with each satellite that circles the Earth twice per day [32]. In fact, initial Walker patterns guaranteed a world-wide continuous coverage by at least four or five satellites, but proved to be too much sensitive to satellite failures. Extensive computations with one, two or three satellite failures led mission analysts to the current constellation definition where a pair of satellites appears in each of the six orbital planes. Figure 2.24 shows a representation of the GPS constellation.

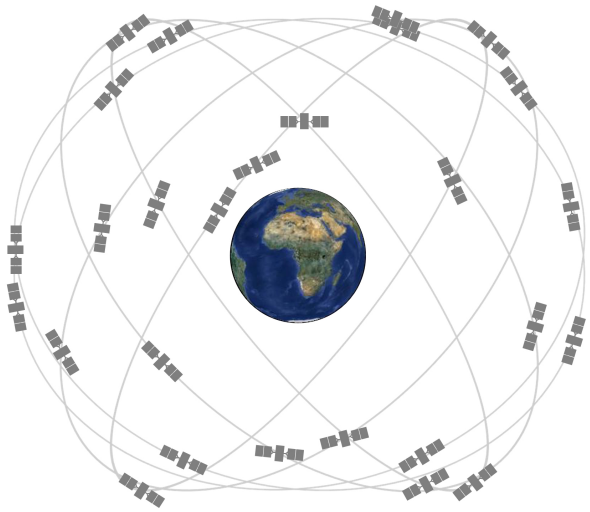

Figure 2.24: GPS: $(T/P/F) = (24/6/2)$, MEO i=55 deg [19].

2.4.2 Galileo

Galileo is Europe's own global navigation satellite system, created by ESA, providing a highly accurate and guaranteed global positioning service under civilian control. Currently providing initial services, Galileo is interoperable with GPS and Glonass; it takes a minimum of 4 satellites to be visible in the local sky to fix a receiver's position. By offering dual frequencies as standard, Galileo is set to deliver real-time positioning accuracy down to the metre range [21]. The fully deployed Galileo system is a Walker constellation that consists of 24 operational satellites plus 6 in-orbit spares, positioned in 3 circular MEO planes at 23222 km altitude above Earth and at an inclination of the orbital planes of 56 deg to the equator. The fully-operational Galileo constellation is capable to provide good coverage even at latitudes up to 75 deg north, which corresponds to the Norway's North Cape (the most northerly tip of Europe) and beyond. The large number of satellites together with the carefully-optimised constellation design, plus the availability of the active spare satellites per orbital plane, ensure that the loss of one satellite should have no discernible effect on the user. Figure 2.25 shows a representation of the Galileo constellation.

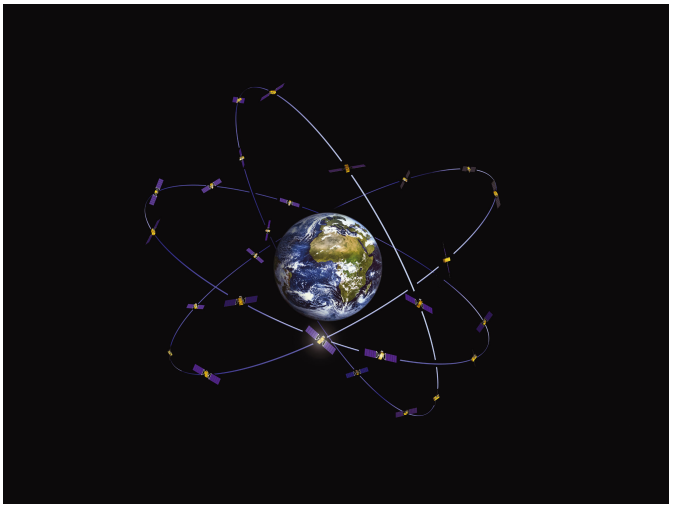

Figure 2.25: Galileo: $(T/P/F) = (24/3/1)$, MEO i=56 deg [33].

2.4.3 Glonass

The GLObal NAvigation Satellite System (GLONASS) is a space-based satellite navigation system operating as part of a radionavigation satellite service and developed by Roscosmos. It provides an alternative to GPS and it is the second navigational system in operation with full global coverage and of comparable precision [20]. The GLONASS supplementum of GPS system improves positioning in high latitudes (both north and south). In 2010, GLONASS had achieved full coverage of Russia's territory and in 2011 the full orbital Walker constellation of 24 satellites was operational enabling full global coverage. Today the constellation counts 24 operational satellites, with 8 of them evenly spaced on each of the 3 orbital planes at an altitude of 19130 km with a 64.8 deg inclination. Figure 2.26 shows a representation of the Glonass constellation.

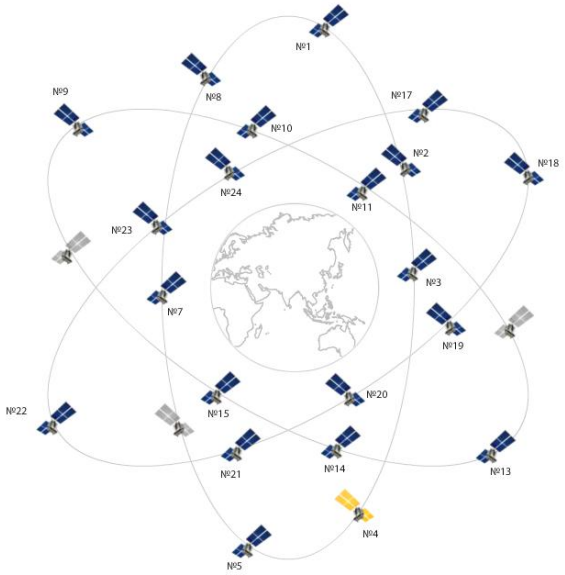

Figure 2.26: Glonass: $(T/P/F) = (24/3/1)$, MEO i=64.8 deg [34].

2.4.4 Globalstar

Globalstar is an American satellite communications company that operates a LEO satellite constellation for satellite phone and low-speed data communications, somewhat similar to the Iridium satellite constellation and Orbcomm satellite systems. The Globalstar second generation constellation consists now of 24 LEO satellites [17].
The first satellites of the original Globalstar mobile telecommunication system were launched in 1998 in a 1410 km altitude and 52 deg inclination orbit. The constellation design relied on a Walker pattern (48/8/1) and was intended to provide continuous coverage between -70 deg and +70 deg latitude [32]. In 2007, Globalstar launched 8 additional first-generation spare satellites into space and between 2010 and 2013 it launched 24 second-generation satellites in an effort to restore their system to full service. The Globalstar constellation of LEO satellites is capable of picking up signals from over 80% of the Earth's surface, everywhere outside the extreme polar regions and some mid-ocean regions. With the fully deployed an operational second-generation constellation, several satellites can pick up a call and this helps assure that the call is not dropped even if a phone moves out of sight of one of the satellites. Globalstar guarantees a coverage over the entire North and South America, Europe, Russia, Australia and part of the Asia (i.e. Africa and some parts of Asia, such India, are excluded) [35]. Figure 2.27 shows a representation of the Globalstar constellation.

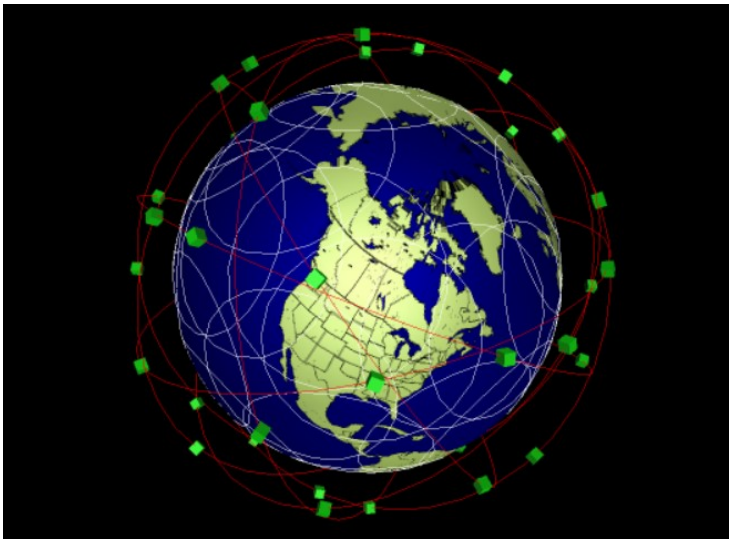

Figure 2.27: Globalstar: $(T/P/F) = (48/8/1)$, LEO i=52 deg [36].

2.4.5 Iridium

The Iridium satellite constellation provides coverage to satellite phones, that means it connects mobile phones by radio through orbiting satellites rather than terrestrial cells.

The major advantage is that such a phone can be used in most or all geographic locations on the Earth's surface since it is not limited to areas covered by cell towers.
The Iridium network is the largest commercial satellite network in the world and the only network that offers true global communications coverage over 100% of the planet. Uniquely, Iridium satellite coverage map spans Earth's polar regions and every land, sea or sky between [37]. The constellation consists of 66 active satellites in LEO at a height of 781 km and an inclination of 86.4 deg divided in 6 planes [16]. The equatorial separation between co-rotating orbits is 31.6 deg, the equatorial separation between counter-rotating orbits is 22.0 deg. In addition, 6 spare satellites are placed in a parking orbit below the operational orbits [22]. All these features mean that Iridium could be considered as a Street Of Coverage constellation. The Iridium satellite constellation initially should have been made of 77 satellites (hence the name, because of the metal with atomic number 77). Anyway, it turned out that just 66 were required to complete the coverage of the planet with communication services [30]. Figure 2.28 shows a representation of the Iridium constellation.

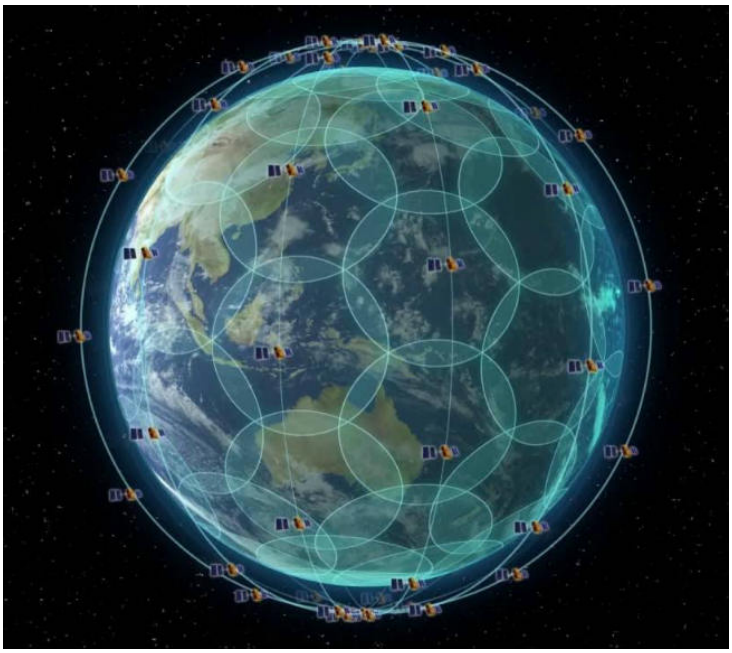

Figure 2.28: Iridium: T=66, P=6, LEO i=86.4 deg [38].

2.4.6 O3b

The O3b satellite constellation (named "the Other 3 Billion" referring to the population of the world that has no access to broadband data services without help), provides telecommunications and data backhaul from remote locations, offering low-latency internet backhaul to emerging markets and developing countries through a series of satellites in equatorial orbits at 8000 km altitude [39].

Since 2016, O3b is wholly-owned by SES S.A., but the first four satellites were launched in 2013, when they were property of O3b Networks Ltd. The second set of four satellites were launched in 2014 and O3b started delivering operational services once their checkout phase was complete. A third set of first-generation satellites lifted off on 2014 too, to add further capacity to the constellation which, by that time, had begun providing services to a number of African countries and remote sensing island states as well as the U.S. Government and cruise ships. With 12 satellites in orbit, O3b switched three from the first batch into stand-by mode due to their degraded signal characteristic to serve as viable backups in case any other satellite suffer technical difficulties. However, nowadays there are 20 O3b satellites in orbit. With the constellation orbiting in MEO, data transfer latency is considerably lower when comparing O3b to Geostationary Communication Satellites that feature latencies of $\sim$ 500 milliseconds. Optimal coverage is provided between 45 deg North and South latitude, through services can be extended to latitude of up to 62 deg [39]. The O3b constellation could be considered as a (20/1/0) Walker constellation, but the orbital inclination is equal to 0 deg because the coverage is desired only at low latitudes. Figure 2.29 shows a representation of the O3b constellation.

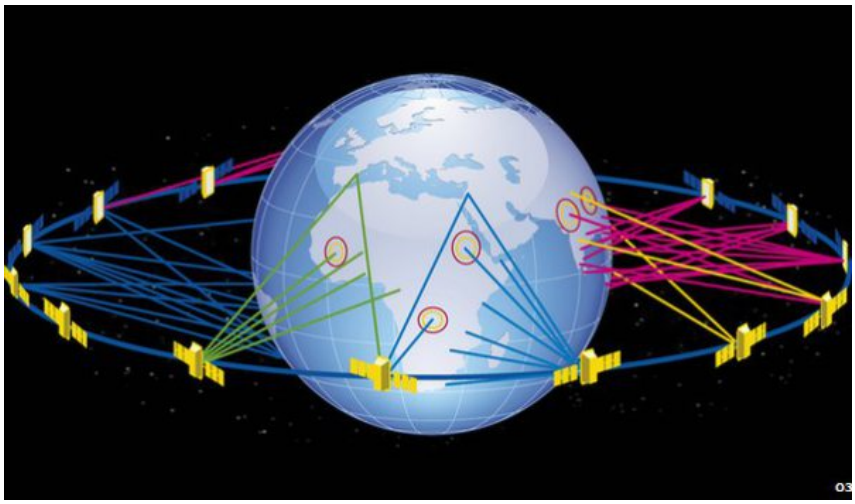

Figure 2.29: O3b: $(T/P/F) = (20/1/0)$ equatorial, MEO i=0 deg [39].

2.4.7 ELLIPSO concept

The ELLIPSO concept was for the first time presented at the beginning of 1990, with the aim to construct and operate satellite mobile cellular telephone systems. The system has been developed to provide affordable personal telephonic and data communications using hand-held (cellular-type) terminals through a unique constellation that includes both elliptical and circular communication satellites [40].

ELLIPSO system employs 18 satellites: 8 circular equatorial satellites are at 8050 km altitude,but in addition there are 2 inclined elliptical, sun-synchronous rings with 5 satellites

each; these rings can provide biased, or tailored coverage over particular latitudes and times of day in which the communications traffic is found to peak. In summary, the different systems engineers have selected widely varying altitudes (and thus periods) for their orbits, all the way from 780 km (Iridium) up to geostationary (35800 km) [30].
The ELLIPSO system, with its patented array of two subconstellations, makes use of elliptical orbits. The BOREALIS subconstellation uses two inclined planes with elliptic orbit satellites, while the CONCORDIA subconstellation has circular orbit satellites. BOREALIS satellites are in two inclined, sun-synchronous, elliptic orbits and are targeted to provide service to customers from 25 deg north latitude up to the North Pole. In and near the equatorial plane, an elliptical and a circular ring are visible, constituting the Gear Array combination. CONCORDIA provides coverage for customers between 55 deg south latitude and 25 deg north latitude (i.e. the tropics and the southern hemisphere) [40].
The design of the ELLIPSO system's constellation was viewed as a major technological advance in the field of non-GEO communications satellite systems and clearly superior to other large-LEO circular orbit systems. Anyway, such a concept has never been realized and the ELLIPSO system merged in the Intermediate Circular Orbit (ICO) constellation concept [41]. Figure 2.30 shows a representation of the ELLIPSO constellation.

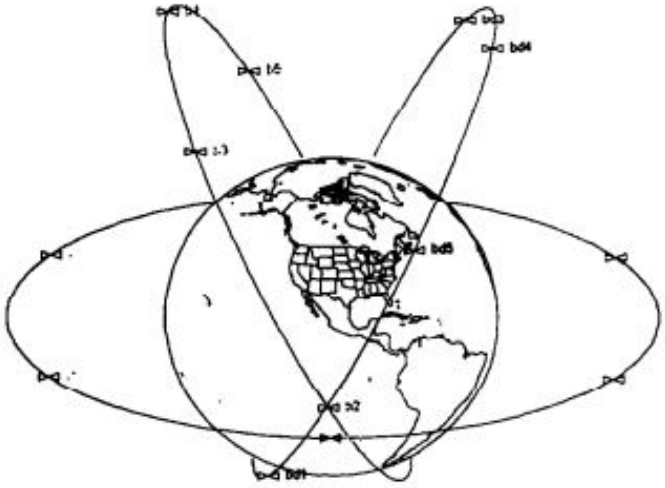

Figure 2.30: ELLIPSO: T=8 MEO equatorial CONCORDIA, T=10, P=2 HEO BOREALIS [40].

2.4.8 Intermediate Circular Orbit concept

The Intermediate Circular Orbit Global Communications is a concept thought by the Boeing Satellite Systems, Inc. and made of satellites that were intended to be used in a global satellite-based mobile communications system capable of offering digital data and

voice services as well as the satellite equivalent third-generation (3G) wireless services, including wireless Internet and other packet-data services [42].
ICO ordered its first 12 satellites in 1995 and 3 more in 2000. However, the first ICO satellite was destroyed in an unsuccessful launch in 2000; the second satellite was launched successfully on 2001. While the original 12 satellites were designed primarily for global mobile voice telephony services, plans were announced in 2000 to modify the 11 remaining original spacecrafts currently in production for the revamped New ICO system. The spacecraft modifications were intended to enhance the new constellation in order to provide high-quality voice and packet-data services.
The New ICO satellite design is one of the most complex ever undertaken and incorporates a number of unique design features. The constellation consists of 10 active satellites operating for 12 years in two orthogonal planes of medium-Earth orbit at an altitude of 10390 km. The orbits are inclined at 45 deg to the equator with each plane having five operational satellites plus one spare. All these features mean that ICO could be considered as a Walker constellation. The orbital pattern is designed for significant coverage overlap, ensuring that usually two (but sometimes three or four) satellites are in view of an user and a Satellite Access Node at any time. Each satellite covers approximately 25% of the Earth's surface at a given time.
However, after a long hiatus, the work on 10 ICO satellites was resumed in 2003. Nevertheless, in 2004 the ICO concept has been abandoned. The only ICO satellite launched was kept operational, albeit without usage, until March 2012, with commercial services purpose [42]. Figure 2.31 shows a representation of the ICO constellation.

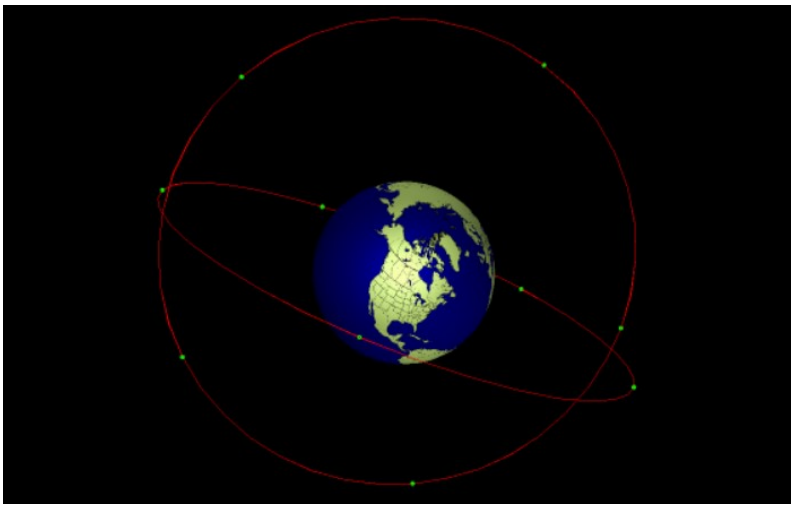

Figure 2.31: ICO: $(T/P/F) = (10/2/0)$, MEO i=45 deg [36].

2.4.9 Teledesic concept

Teledesic is a concept for a global broadband LEO satellite network and the following applications and services are foreseen: computer networking, intranets, virtual private networks, Local Area Network interconnection, high-speed internet access, intranet access, interactive multimedia, video conferencing, high-quality voice, wireless backhaul [22]. The system is capable to provide fiber-optic like links to customers around the world.
The original 1994 proposal was extremely ambitious, planning 840 active satellites with in-orbit spares at an altitude of 700 km. In 1997, the plan was scaled back to 288 active satellites at 1400 km: 24 active satellites are placed in each of 12 polar orbital planes with an inclination of 98.1 deg. Teledesic makes use of an asynchronous polar constellation, which means that the phase shifts between different orbital planes are not controlled. The high number of satellites provides a high system capacity and a high satellite elevation enhancing the link availability and reducing rain fading.
In the light of reducing the number of satellites from initially 840 to 288, the number of satellites may have been further reduced to around 100; in addition, satellite's technical parameters could accordingly have changed during the further development of the system [18]. Teledesic intended to provide global coverage with Earth-fixed cells, served by scanning satellite beams. The minimum satellite elevation of 40 deg mitigates the influence of signal blockage and rain fading. Thus, Teledesic can provide 99.9% availability. Despite the proposal, in 2002 the Teledesic satellite construction work was suspended because the first satellite bubble had burst during the first launch in 1998, but also thanks to the commercial failure of the similar Iridium venture and other systems [18]. Figure 2.32 shows a representation of the Teledesic constellation.

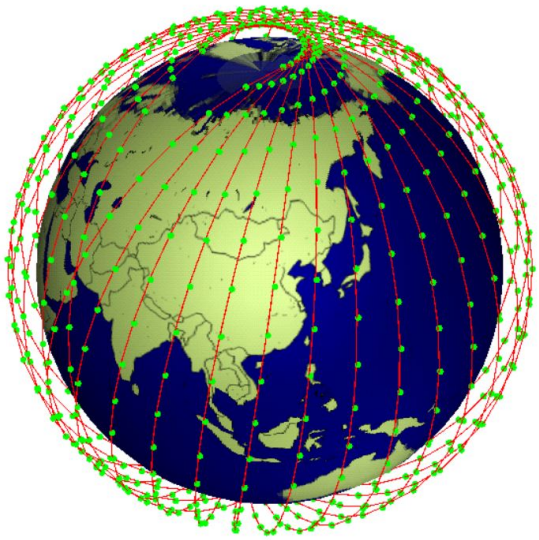

Figure 2.32: Teledesic: T=288, P=12, LEO i=98.1 deg [36].

2.4.10 OneWeb

OneWeb is currently a satellite constellation developed by Airbus and OneWeb made of small satellites in a circular polar LEO (87.9 deg inclination) at approximately 1200 km altitude and is a planned initial 650-satellite constellation [43]. Coverage characteristics include an elevation angle never lower than 50 deg, in order to enhance quality of the signal. The first generation satellites were initially in process of being completed in 2019/2020 with a goal to provide global satellite internet broadband services to people everywhere and initially it was aiming to start global services in 2021. The first 6 test satellites were launched in 2019 and the first, second and third batches of 34, 34 and 36 satellites respectively were launched in 2020. Anyway, at the beginning of 2021, it was announced that this first-generation constellation, of a total of 648 satellites, is going to be fully operational by the end of 2022 and that these satellites will be placed 36 in each of the 18 orbital planes [44]. The second generation of OneWeb satellites is planned to be made of a system with 32 planes of 72 satellites each at an inclination of 40 deg, 32 planes with 72 satellites each at an inclination of 55 deg and 36 planes with 49 satellites each at an inclination of 87.9 deg, for a total of 6372 satellites that would be in addition to the initial first-generation constellation that the company is currently deploying [43]. The whole OneWeb constellation really consists of three different Walker sub-constellations (i.e. three different inclinations are used). Figure 2.33 shows a representation of the Oneweb constellation.

Figure 2.33: Oneweb [45].

2.4.11 Starlink

Starlink is a satellite internet constellation currently under construction by SpaceX providing satellite internet access. The constellation will consist of thousands of small satellites in LEO working in combination with ground transceivers. The aim is to provide satellite internet connectivity to underserved areas of the planet, as well as to provide competitively priced service to urban areas.

Product development began in 2015 and two prototype test-flight satellites were launched in 2018. Additional test satellites and 60 operational satellites were deployed on 2019. The aim is to deploy 1440 spacecrafts to provide near-global service by late 2021 or 2022. At the end of January 2021, Starlink counts 1015 satellites launched (including demo satellites) and other launches are planned to occur as often as every two weeks with 60 satellites each. In total, nearly 12000 satellites are planned to be deployed, with a possible later extension to 42000. The initial 12000 satellites are planned to orbit in 3 orbital shells: first 1440 satellites in a 550 km altitude divided in 72 planes inclined 53 deg with 20 satellites each, second 2825 satellites at 1110 km altitude and third 7500 satellites at 340 km altitude. As for the case of OneWeb, also the Starlink constellation consists of three different Walker sub-constellations.

The lower minimum elevation angle of beams for the first shell is requested to be of 25 deg, while it would be equal to 40 deg for the second and third shells.

The existing plan for a second-generation Starlink constellation expected to include up to 30000 satellites and provide complete global coverage [46]. Figure 2.34 shows a representation of the Starlink constellation.

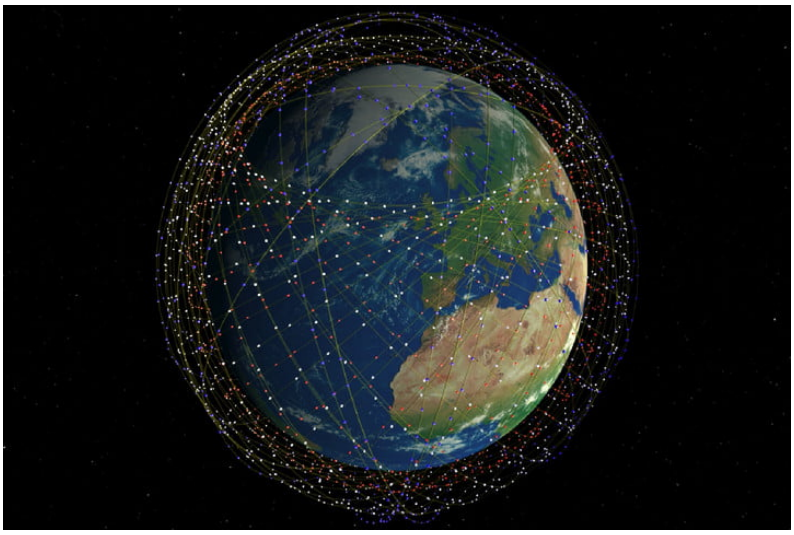

Figure 2.34: Starlink [47].

3. Methods for continuous coverage

Over the years, many methods have been developed to efficiently evaluate the coverage of a constellation pattern. First of all, it is said that a user is seen by a satellite when both are in direct visibility of each other, without any obstruction: this is called geometric visibility (or line of sight visibility) [24]. But in some cases, geometric visibility is not enough, and also the antenna pointing and pattern must be taken into account. This is called radioelectric visibility, but it is a complex problem and the correspondent analysis goes beyond the scope of this thesis [24].
As previously said in Section 2.1, the desired coverage can be continuous or discontinuous and even global, zonal or local. In addition, coverage can also be defined by the minimum number of satellites in user's view at the same time, hence dealing with one-fold, two-fold or n-fold coverage.

Many methods have been developed to evaluate coverage efficiency of a constellation pattern, in terms of continuous and non continuous global or local coverage. The methods are usually suitable for circular orbits, since a general method formulation is much easier than for constellations with elliptical orbits.
This chapter deals with methods applicable for continuous global or zonal coverage, while methods capable of dealing with revisit time are going to be discussed in Chapter 4.

In general, the methods can be grouped in two categories: analytical, usually good at assessing continuous and global coverage properties of a constellation pattern, and numerical, normally more flexible and that can usually deal with more complex objectives. The use of LEO for continuous global coverage requires satellite constellations of from 30 to 100 satellites [48]. Polar orbits have typically been proposed for this application because large polar constellations can be analytically optimised: for example, Adams and Rider (Section 3.2), as well as Beste (Section 3.1), have examined non-symmetric constellations of circular, polar orbit satellites using the Street Of Coverage (Section 2.2.3) approach. Solutions for up to 1000 satellites have been obtained to achieve single through four-fold continuous global coverage. On the other hand, Walker (Section 3.3) and Lang (Section 3.4) developed a method to optimise symmetric, non-polar constellations as large as 100 satellites [48]. Again, results were obtained for single through four-fold continuous

global coverage. In many cases, non-polar constellations outperformed similarly sized polar constellations.

It must be highlighted that these methods do not discuss the problem of orbital perturbations neither their presence. This approach can be accepted because orbital perturbations such the J_2 harmonic effect due to Earth gravity and Earth not perfect spherical shape cause all satellites to face the same drift effects, since they have the same inclination i. In the same way, orbital decay due to drag effects is not considered, because all satellites are assumed to be equal and to have the same area, so the same behaviour [5]. Indeed, orbital perturbations (i.e. non zero eccentricity or long-term drift in orbital constants) can be minimised by deploying the constellation in such a way that all satellites orbits are affected more or less equally.

3.1 Beste coverage method

The method derived by Beste aims at designing optimum satellite configurations for continuous coverage of the entire Earth or of polar regions extending to arbitrary latitude [28]. The method is analytical: it identifies families of circular polar orbit constellations using minimal total number of satellites which can provide a desired n-fold of coverage at or above a user-defined latitude.
Beste considered two approaches to the problem of satellite constellation design. The first approach was to place the satellites in orbital planes which have a common intersection (e.g. polar orbits) and to adjust the plane separation and satellite spacing so as to minimise the total number required. Polar orbits result in higher satellite densities at the poles than at the equator; it seems intuitive that orbital configurations which result in a more uniform distribution of satellites over the Earth would lead to more efficient covering. Therefore, the second approach was to select orbital planes which result in as uniform a distribution of satellites as possible [28]. Hence, Beste found an analytical expression relating latitude λ and Earth-centered half-cone angle of coverage θ with the number T of satellites required for continuous coverage, both for single and triple coverage.

The geometry is shown in Figure 3.1. The angle θ is the Earth-centered half-cone angle corresponding to the coverage of one satellite, or equivalently, the radius of the coverage circle (measured in angular units) on the surface of the Earth. This region will be referred to as the coverage circle of radius θ.

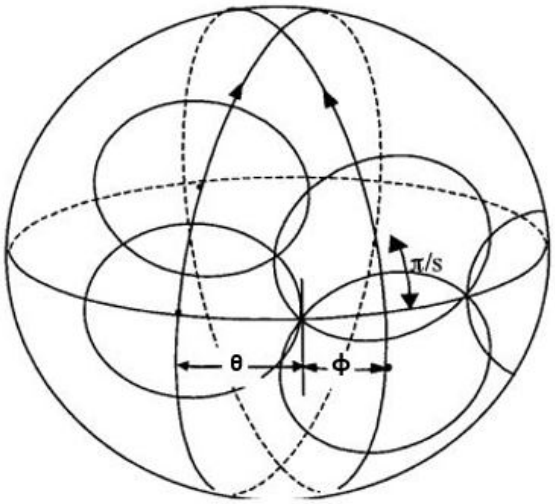

Figure 3.1: Coverage geometry for the Beste method [24].

When optimal phasing of orbital planes is considered for global coverage, the point of intersection of overlapping circles of coverage coincides with the boundary of a circle coverage in the adjacent plane. Since the satellites are uniformly distributed in a given orbital plane, the phase separation between two consecutive satellites within an orbital plane is given by $\frac{2\pi}{S}$ [24].
By applying spherical trigonometry, the angular half-width Φ of the ground swath with single satellite coverage is given by the relation:

$$\cos\theta = \frac{\cos\Phi}{\cos\left(\frac{\pi}{S}\right)} \tag{3.1}$$

Satellites in adjacent orbital planes move in the same direction and the satellites of one plane are shifted relative to those of the adjacent plane by one-half of the intraorbit satellite spacing (i.e. $\frac{\pi}{S}$, where S is the number of satellites per orbit). This configuration clusters the satellites in an optimal manner at the equator. The inter-plane angular separation between adjacent planes α is equal to

$$\alpha = \Phi + \theta \tag{3.2}$$

However, satellites in the first and last planes rotate in opposite directions. Because of this counter-rotation effect, the angular separation between the first and last planes is smaller than that between adjacent planes; hence, at the two boundaries where adjacent orbital chains move in opposite directions, the relative geometry is not constant. At the equator, Φ has to satisfy the condition:

$$(P-1)(\Phi+\theta) + 2\theta = \pi \tag{3.3}$$

where P is the number of orbital planes. It follows that

$$\alpha = \Phi + \theta \geq \frac{\pi}{P} \tag{3.4}$$

and that the angular separation between the first and the last planes is equal to 2θ. From the last two Equations (3.3) and (3.4), Beste computed the values of P and S for single coverage of the entire Earth. Therefore, the proposed formulation to determine the number of satellites required for single-satellite global coverage can be approximated by:

$$T_{Beste-1fold} = P \cdot S \approx \frac{4}{1 - \cos\theta} \tag{3.5}$$

and $1.3P < S < 2.2P$, since the approximated result holds for ratios of S to P in the approximated range of 1.3 to 2.2 [28].

This analysis of entire Earth coverage has been extended to partial coverage for latitudes beyond a specified value λ (i.e. between latitude $+\lambda$ and the north pole and between $-\lambda$ and the south pole), as shown in Figure 3.2. The coverage now is zonal, but the method deals with latitude bands, since all longitudes must be considered and not only a portion of the Earth surface (say a delimited area both in latitude and longitude).

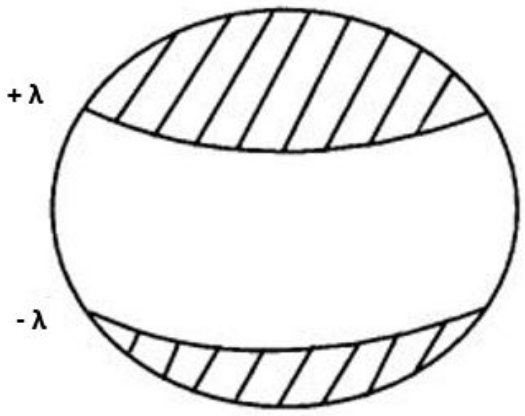

Figure 3.2: Coverage area beyond a specified latitude [24].

Beste has shown that in order to provide coverage beyond a specified value λ the constraint at the equator becomes:

$$(P - 1)(\Phi + \theta) + 2\theta = \pi \cos(\lambda) \tag{3.6}$$

The total number of satellites can be generalised as follow:

$$T_{Beste-1fold,\lambda} = P \cdot S \approx \frac{4\cos\lambda}{1-\cos\theta} \tag{3.7}$$

and $1.3P < S\cos(\lambda) < 2.2P$

Beste [28] continued to extend his analysis for triple coverage by using an iterative method. His approximation for triple coverage is as follows:

$$T_{Beste-3fold,\lambda} = P \cdot S \approx \frac{11\cos\lambda}{1-\cos\theta} \tag{3.8}$$

and $1.3P < S\cos(\lambda) < 2.2P$

3.2 Adams and Rider coverage method

Using a similar geometry to that shown in Figure 3.1 for the Beste method, Adams and Rider arrived at a different expression for the total number of satellites T required for providing multiple satellite coverage by proceeding by optimisation techniques using the method of Lagrange multipliers. The method is analytical as the one developed by Beste [28]. In general, to maximise the number of co-rotating interfaces in a polar network, their ascending nodes should be distributed over $k\pi$ radians (k could be any positive integer value) with an approximate value for the angular spacing between co-rotating orbits of $\frac{k\pi}{P}$.

The exact geometry for the derivation of Adams and Rider approximation [24] is shown in Figure 3.3.

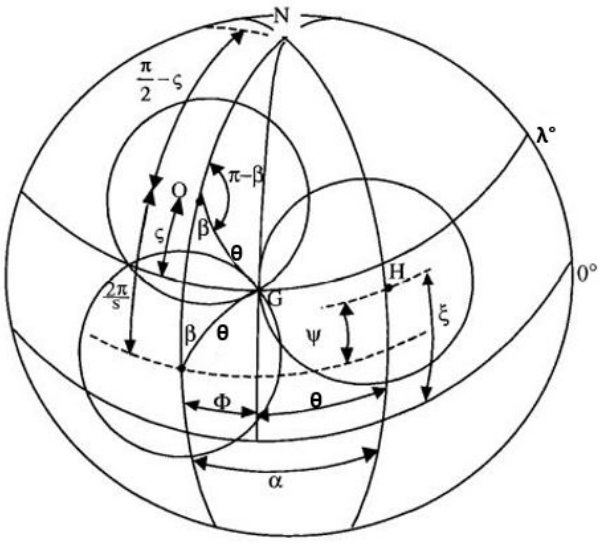

Figure 3.3: Coverage geometry for the Adams and Rider method [24].

In Adams and Rider's approach, polar constellation design for multiple coverage beyond a specified latitude λ is analysed (see Figure 3.2). From Figure 3.3:

$$\varsigma = \lambda + \frac{\pi}{S} \tag{3.9}$$

By applying spherical geometry in spherical triangle $N\hat{G}O$ of Figure 3.3:

$$\cos\lambda = \cos\left(\frac{\pi}{2} - \varsigma\right)cos\left(\frac{\pi}{2} - \lambda\right) + \sin\left(\frac{\pi}{2} - \varsigma\right)\sin\left(\frac{\pi}{2} - \lambda\right)\cos\Phi \tag{3.10}$$

After manipulation, Φ can be obtained as follow:

$$\cos\Phi = \frac{\cos\lambda - \sin\varsigma\sin\lambda}{\cos\varsigma\cos\lambda} \tag{3.11}$$

In the same figure, for a given ψ:

$$\left(\frac{\pi}{2} - \varsigma\right) + \frac{2\pi}{S} = \left(\frac{\pi}{2} - \xi\right) + \psi \tag{3.12}$$

This implies:

$$\xi = \varsigma + \psi - \frac{2\pi}{S} \tag{3.13}$$

For optimum phasing, $\psi = \frac{\varsigma}{2}$. By applying spherical trigonometry to the spherical triangle $N\hat{G}H$ of Figure 3.3:

$$\cos\lambda = \cos\left(\frac{\pi}{2} - \xi\right)cos\left(\frac{\pi}{2} - \lambda\right) + \sin\left(\frac{\pi}{2} - \xi\right)\sin\left(\frac{\pi}{2} - \lambda\right)\cos\theta \tag{3.14}$$

or

$$\cos\theta = \frac{\cos\lambda - \sin\xi\sin\lambda}{\cos\xi\cos\lambda} \tag{3.15}$$

where α has to satisfy the condition:

$$\alpha = \Phi + \theta \geq \frac{\pi}{P} \tag{3.16}$$

Computation can be carried out to obtain the total number of satellites required for single coverage above a latitude λ, for given Φ, θ and S.

The above equations can be generalised for multiple coverage over a given point. Let j be the multiple level of coverage provided by satellites in a single plane and let k be the multiple level of coverage provided by satellites in neighbouring planes. The total multiple level of coverage n can be factorised as $n = jk$. By making use of Lagrange multipliers

technique, it can be shown that:

$$S = \frac{2}{\sqrt{3}} j \frac{\pi}{\theta} \tag{3.17}$$

$$P = \frac{2}{3} k \frac{\pi}{\theta} \tag{3.18}$$

$$T_{A\&R} = P \cdot S = \frac{4\sqrt{3}}{9} n \left(\frac{\pi}{\theta}\right)^2 \tag{3.19}$$

where j denotes the multiple coverage factor in the same orbital plane; k denotes the multiple coverage factor in different orbital planes; $n = jk$ denotes the multiple coverage factor of the constellation. Hence, an expression for optimum triple coverage using Adams and Rider's formula can be made by setting n=3 and k=1.

3.3 Walker coverage method

The Walker's satellite triplets or Walker circumcircle approach is a numerical method developed to evaluate the coverage efficiency of constellation patterns made of circular, common period orbits all having the same inclination with respect to an arbitrary reference plane. The orbits are uniformly distributed in a right ascension angle as they pass through the reference plane and the initial phase position of satellites in each orbit plane is proportional to the right ascension angle for that plane [26].
This method, improved by Ballard [26], is restricted to continuous global coverage analyses: it is a very elegant method, very good at optimising small constellations, but unfortunately it is very slow at evaluating big constellations because of the rapidly exploding number of triplets to check.
Aim of the Walker method is to find a systematic approach to the analysis of coverage by means of circular orbit systems and to show that better coverage is possible with a small number of satellites [12]. Only circular orbits have been considered since, while elliptical orbits have some advantages in the provision of coverage to limited areas mainly confined to either the northern or the southern hemisphere, circular orbits appear to have the advantage for zones extending equally into both hemispheres and even more as regards whole-Earth coverage. In fact, Walker thought that continuous whole-Earth coverage would be provided most effectively by a system in which the distribution of satellites over the Earth's surface was maintained as uniform as possible, subject to the practical limitations imposed on a system necessarily involving multiple intersecting orbits; thus circular orbits of equal period have been chosen as an essential feature of all the patterns considered [27].

For convenience of use, circular orbit patterns having a uniform distribution of satellites within and between orbit planes have been identified by the reference $(T/P/F)$; in general, F may have any value less than P, but for Delta patterns F can take only integer values from 0 to $(P-1)$.
The circumcircle method is based on spherical triangles drawn on the Earth surface by satellites: consider a number of satellites following equal radius circular orbits around the Earth, if a line is drawn connecting each sub-satellite point to adjacent sub-satellite points, such that the Earth's surface is divided into a number of spherical triangles with a sub-satellite point at each vertex, then the point on the Earth's surface most remote from any of the sub-satellite points is the centre of the largest of the circumcircles of these triangles which does not enclose any other sub-satellite point. The point on the Earth's surface at which the minimum satellite elevation angle occurs is the circumcentre of the sub-satellite points of the nearest three satellites, under those conditions which result in the circumcircle being at its largest from any such group of three adjacent satellites. This configuration could be called the critical one, giving critical conditions at the circumcentre, the critical point. So, the radius of the circumcircle in the critical configuration is the maximum sub-satellite distance allowed in order to still achieve continuous global coverage. It often happens that critical conditions occur when one satellite passes through the plane of another three satellites, i.e. its sub-satellite point lies on the circumcircle of their sub-satellite points.
In choosing pattern characteristics, the primary objective should be to minimise the total number of satellites needed to ensure that not less than a certain number of satellites are everywhere visible at all times above some minimum elevation angle; as a secondary objective, it is assumed that the minimum distance between adjacent satellites should be as large as possible. Hence, coverage has been assessed by finding those points on the Earth's surface (namely the centres of the circumcircles of the relevant spherical triangles) which are furthest from appropriate sub-satellite points; each pattern has then been optimised by varying the common inclination of the orbital planes, to reduce the worst-case value of the radius of the largest circumcircle until no further improvement is possible.

The problem consists in providing, in the most efficient manner, an array of satellites which can between them to provide continuous multiple n-fold coverage of the entire surface of the Earth. Since, to provide whole-Earth coverage, the satellites must necessarily be in multiple intersecting orbits, the pattern which the satellites form relative to the Earth is constantly changing, and the coverage requirements must be met by all the configurations which the satellite constellation takes up (basically, it must be ensured that the requirements are still met under worst-case conditions) [49].

Coverage studies have been conducted in terms of the radius from the sub-satellite point to the effective horizon, this radius being measured by the angle it subtends at the centre of the Earth θ. The effective horizon reflects the particular requirements, depending on satellite altitude and on the minimum acceptable elevation angle from a point on the Earth's surface [49]. Coverage properties are thus analysed in terms of the largest possible great circle (namely circumcircle) between an observer anywhere on the Earth's surface and the nearest sub-satellite point. When evaluated in this manner, coverage properties are invariant with deployment altitude. As deployment altitude is reduced, however, higher order constellations must be used to maintain a fixed minimum viewing angle. Coverage properties are also invariant with deployment orientation relative to Earth coordinates, although specific orientations can cause the satellite patterns to appear quasi-stationary [26].

Figure 3.4 represents the instantaneous position of the sub-satellite points of three out of a constellation of satellites in circular orbits. A circle whose radius represents the effective horizon distance has been drawn around each sub-satellite point. These circles divide the area covered by this figure into three types of element: within those marked 1, one satellite is visible; within those marked 2, two satellites are visible, while within the marked 0, no satellite is visible. If the radius of the circles were increased to allow for an increased horizon range (e.g. satellites in higher orbits or lower minimum elevation angle), the area marked 0 would shrink, as shown in Figure 3.5, and full single coverage of this area would eventually be achieved when the three circles all passed through the point + at its centre; this is the centre of the circumcircle of the three sub-satellite points and the radii of the three circles would then be equal to this circumcircle radius. Thus the centre of the circumcircle of three adjacent sub-satellite points represents, for that part of the overall pattern, the worst case for meeting the single coverage requirements and the centre of the largest of such circumcircles is the worst case for the whole pattern. Considering the variation of the pattern during an orbital period, the largest value of the largest such circumcircle radius θ_{MAX} defines the pattern's single coverage capabilities; it is desirable that this value should be as small as possible.
Figure 3.6 illustrates the situation when the circumcircle of any three sub-satellite points passes simultaneously through one or more (in this case two) additional sub-satellite points. In Figure 3.7, as in Figure 3.6, one other sub-satellite point is enclosed within the circumcircle, so that the centre of the circumcircle is again the locally critical point for double coverage. However, under these circumstances it should also be considered a locally critical point for triple and quadruple coverage, since minimal changes in the positions of

one or two of the sub-satellite points lying on the circumcircle could leave two or three sub-satellite points, instead of only one, enclosed within the circumcircle.

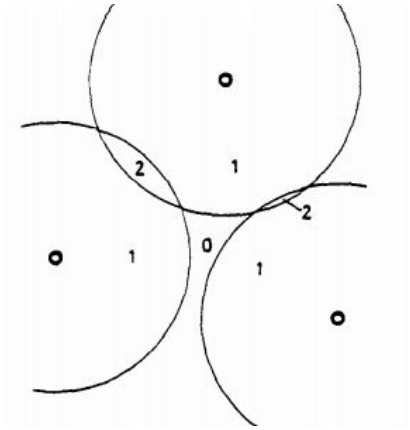

Figure 3.4: Circumcircle centre 1 [49].

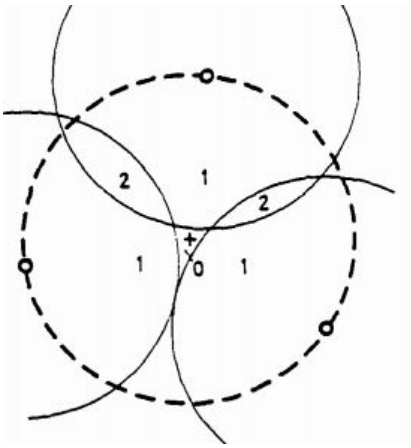

Figure 3.5: Circumcircle centre 2 [49].

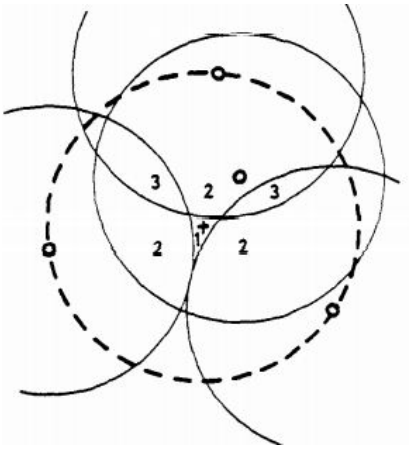

Figure 3.6: Circumcircle centre 3 [49].

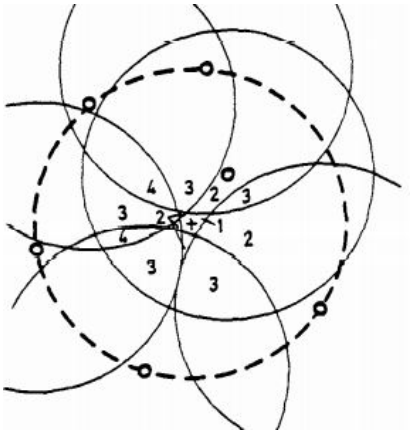

Figure 3.7: Circumcircle centre 4 [49].

Hence, if the circumcircle passes through X sub-satellite points (where X is not less than 3) and encloses Y other sub-satellite points, its centre is locally critical point for degrees of coverage *(n)* from *(Y+1)* to *(X+Y-2)*, though since X will often be equal to 3, these values will often be equal.

The smaller the circumcircle radius θ, the higher is the minimum elevation angle ε at which the required number of satellites (at a given orbital altitude) can be seen from any point within the circumcircle. Likewise, the smaller the circumcircle radius the lower is the orbital altitude necessary for the required number of satellites to be visible (above a given minimum elevation angle) from any point within the circumcircle. Thus in general terms it is desirable that the largest value of circumcircle radius θ_{MAX} should be as small as possible.

However, once the requirements for a particular system have been chosen and the satellite

altitude and minimum elevation angle (determining the maximum circumcircle radius), the required degree of coverage *(n)* and the number of satellites in the system have all been specified, it might be argued that it is only necessary to confirm that all satellite patterns placed on the short-list for selection meet the stated requirements for maximum circumcircle radius and that the choice between them should depend not on which of them has the smallest radius but on some other criterion (e.g. launcher capabilities, cost).

Summing up, the analysis of coverage has been based on the identification of those points at which the elevation angle ε to the nearest satellite (or the n^{th} nearest for n-fold coverage) is locally a minimum. These points are the centres of the circumcircles of the spherical triangles formed by the instantaneous sub-satellite points of neighbouring satellites in the pattern.

In Figure 3.8 , which represents an undefined portion of the Earth's surface, the A to G letters represent the instantaneous positions of 7 out of a total 10 sub-satellite points of some hypothetical 10-satellite pattern. O_1, which is the instantaneous position of the centre of the circumcircle of the spherical triangle $A\hat{B}C$, whose geocentric angular radius is θ_1, is locally the point on Earth's surface furthest from any sub-satellite point; at O_1, an observer's distance d from each of A, B and C is equal to θ_1, but another observer located a short distance from O_1, in any direction, would be at a distance less than θ_1 from at least one of those three sub-satellite points. Considering all the other spherical triangles, such as $B\hat{C}F$ and $C\hat{D}F$, whose circumcircles do not enclose any other sub-satellite point, then the centre of the largest of those circumcircles is the point on the whole Earth's surface which is instantaneously furthest from any sub-satellite point. The radius of that circumcircle is θ_{max}. If the requirement should be for double coverage (i.e. for not less than two satellites to be everywhere visible above the minimum elevation angle) then the problem may be tackled in similar manner, but considering circumcircles which enclose one other sub-satellite point (e.g. $A\hat{B}D$ which encircles C). O_2 is at a distance θ_2 from A, B and D, and at a lesser distance from C; an observer at a little distance from O_2 would be at a lesser distance than θ_2 from at least one of A, B and D, as well as from C. This value of θ_2 would have to be compared with the values of θ_2 for those other circumcircles which each encloses one other sub-satellite point, in order to find the instantaneous value of θ_{max}. Similar considerations apply if the requirement is for simultaneous visibility of any larger number of satellites.

To ensure that every locally least-favoured point has been examined as a possible source of the value of θ_{max}, it is necessary to consider both larger and smaller circumcircle radii of all possible combinations of three sub-satellite points at any instant of time. However, so

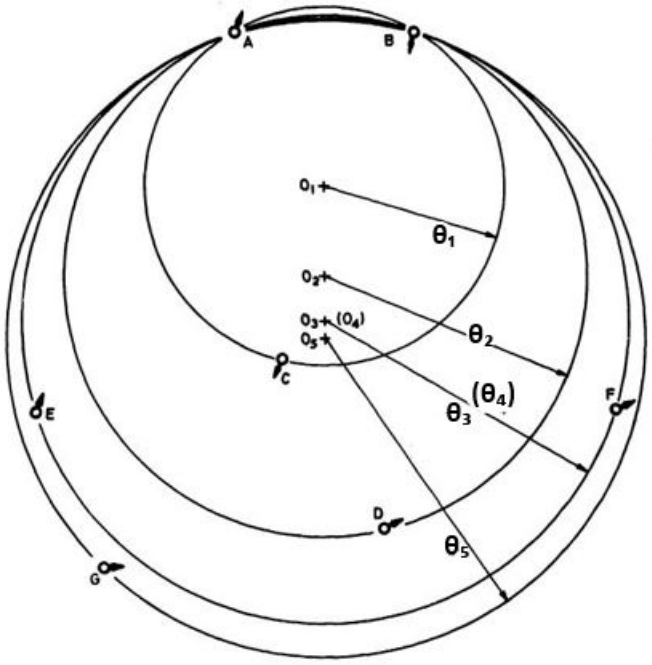

Figure 3.8: Example of determination of θ_n [27].

far only instantaneous configurations of a satellite pattern have been considered, whereas, as stated before, the actual interest is in the maximum value taken over the whole of a pattern repetition interval θ_{MAX}. The list of spherical triangles whose radii are potential candidates for the value of θ_{MAX}, may well change during the course of the propagation of the orbit pattern, as other sub-satellite points move into or out of the circumcircle of any one group of three and all of them must be examined. Values of θ_{MAX}, which represent maximum values of the sub-satellite distance d for a particular pattern with a certain inclination, may be converted to values of the minimum elevation angle ε for any satellite altitude. The value of θ_{MAX} determined for a particular pattern is thus a very suitable criterion for assessing the merits of that pattern; the smaller the value of θ_{MAX}, the larger will be the minimum elevation angle provided by a satellite system using that pattern at a given altitude, or the lower will be the altitude at which it can ensure that a requirement for a given minimum elevation angle is met.

Mathematics formulations to assess coverage make use of the great circle range (or coverage angle as in Section 2.1.1) from an observer anywhere on the Earth's surface to the nearest sub-satellite point. This parameter is a more fundamental measure of good coverage geometry than the direct use of elevation angle ε because it is independent of the altitude at which the satellites are deployed, whereas elevation angle is not and so this would mean less computations to be performed during the analysis and less parameters needed.

Figure 2.1 of coverage geometry in Section 2.1.1 illustrates how elevation angle is related to great circle range and deployment altitude (or period). Notice that for any finite altitude, the great circle range θ must be less than 90 deg for the satellite to be visible at or above the observer's horizon.

In designing a constellation for optimised world-wide coverage, the first step is to choose a set of common-altitude orbits which minimise the maximum value of θ, considering all possible observation points on Earth at all instants of time. The constellation altitude is then chosen to obtain a guaranteed minimum elevation angle sufficiently high (say 10 deg) that atmospheric propagation anomalies or local terrain obstructions are not a significant problem.

As stated before, the optimisation parameter is the coverage angle (the central angle) from an observer anywhere on the Earth's surface to the nearest sub-satellite point and in order to determine it, the worst condition (i.e. correspondent to the greatest circumcircle) shall be determined.
The intersatellite great circle range r_{ij} (angular range) between any arbitrary pair of satellites in a constellation in the i and j planes is illustrated in Figure 3.9. The set of formulas describing r_{ij} for all satellite pairs consists on the use of the law of cosines for sides to the small triangle formed by the two satellites and the intersection point. These formulas completely and uniquely defines the geometry of the constellation as far as its coverage properties are concerned.

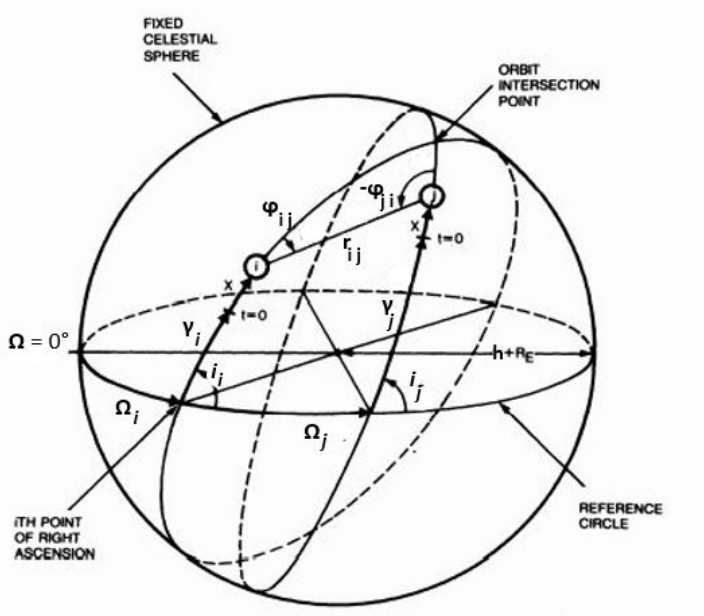

Figure 3.9: Geometry of satellite pair [26].

Using the half-angle formulas for spherical trigonometry and applying the conditions of the orientation angles listed in Section 2.2 describing the position of satellites of a constellation (e.g. Walker and Ballard), the inter-satellite ranges in such a constellation can be expressed in the form:

$$\begin{aligned}\sin\left(\frac{r_{ij}}{2}\right)^2 = &\cos\left(\frac{i}{2}\right)^4 \sin\left((m+1)(j-i)\left(\frac{\pi}{P}\right)\right)^2 \\ &+ 2\sin\left(\frac{i}{2}\right)^2 \cos\left(\frac{i}{2}\right)^2 \sin\left(m(j-i)\left(\frac{\pi}{P}\right)\right)^2 \\ &+ \sin\left(\frac{i}{2}\right)^4 \sin\left((m-1)(j-i)\left(\frac{\pi}{P}\right)\right)^2 \\ &+ 2\sin\left(\frac{i}{2}\right)^2 \cos\left(\frac{i}{2}\right)^2 \sin\left((j-i)\left(\frac{\pi}{P}\right)\right)^2 \\ &\cdot \cos\left(2X + 2m(j+i)\left(\frac{\pi}{P}\right)\right)\end{aligned} \tag{3.20}$$

where i and j are the index representing two generic satellites of the constellation, m is the harmonic factor and X is the time-varying phase angle.

Figure 3.10 illustrates that the worst possible observation point in a spherical triangle formed by joining three sub-satellite points *(i,j,k)* is at the midpoint of the triangle. The range arc from the midpoint of the triangle to any of this three vertices is the equidistance θ_{ijk}. A constellation providing usable coverage only to a range $\theta^* < \theta_{ijk}$ leaves the midpoint of the triangle uncovered and therefore fails the test of worldwide visibility. If θ^* is increased to equal or exceed θ_{ijk}, the number of satellites visible at the midpoint changes from zero to three and at least single visibility coverage is assured everywhere within the triangle.

Knowing the three sides of spherical triangle, its equidistance parameter can be computed directly from the formula:

$$\sin\left(\theta_{ijk}\right)^2 = \frac{4ABC}{[A+B+C]^2} - 2(A^2+B^2+C^2) \tag{3.21}$$

where:

$$A = \sin\left(\frac{r_{ij}}{2}\right)^2 \tag{3.22}$$

$$B = \sin\left(\frac{r_{jk}}{2}\right)^2 \tag{3.23}$$

$$C = \sin\left(\frac{r_{ki}}{2}\right)^2 \tag{3.24}$$

The coverage properties of a constellation can therefore be analysed by examinimg the equidistances $\theta_{ijk}(X)$ of its spherical triangles at all instants of time to find the worst case.

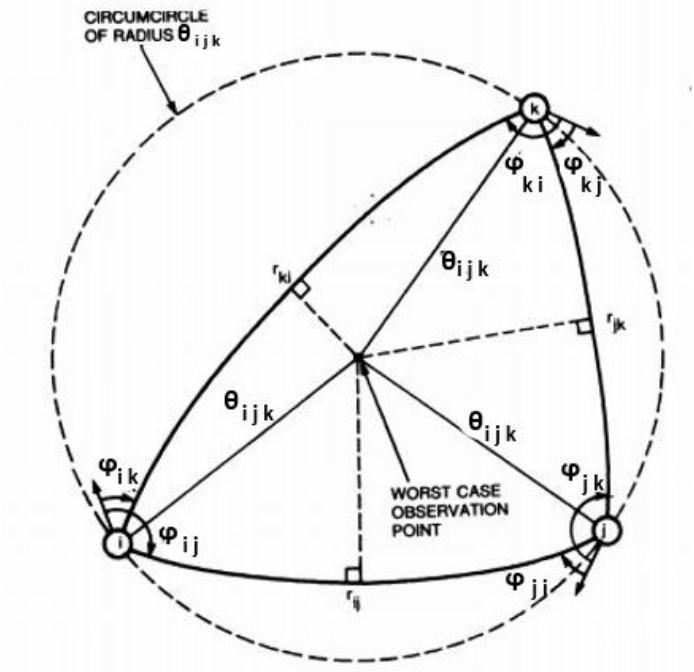

Figure 3.10: Equidistance of satellite triad [26].

With T satellites, a total of $(2T-4)$ non-overlapping triangles are required to cover the sphere and all must be examined for worst-case equidistance. The worst-case observer on the Earth's surface will be one whose position coincides with the midpoint of the spherical triangle having the largest equidistance.

In dividing the sphere into triangles, care must be taken to choose only those triangles whose circumcircles enclose no other satellites. Once another satellite moves inside the circumcircle of a triangle, that triangle is no longer of interest in a single-visibility analysis because a set of smaller triangles can then be chosen whose circumcircles are all empty. In order to verify that the examined satellite triplets and relative triangles do not include other satellites, the so-called "enclosure test" shall be performed: consider Figure 3.11, let r be the range arc from the midpoint of a given triangle *(i,j,k)* with equidistance R<90 deg to a test satellite l and define a test variable to be

$$y \triangleq 1 - \frac{\cos r}{\cos R} \tag{3.25}$$

It can be stated that satellite l is

- inside the circumcircle if $y < 0$
- on the circumcircle if $y = 0$
- outside the circumcircle if $y > 0$

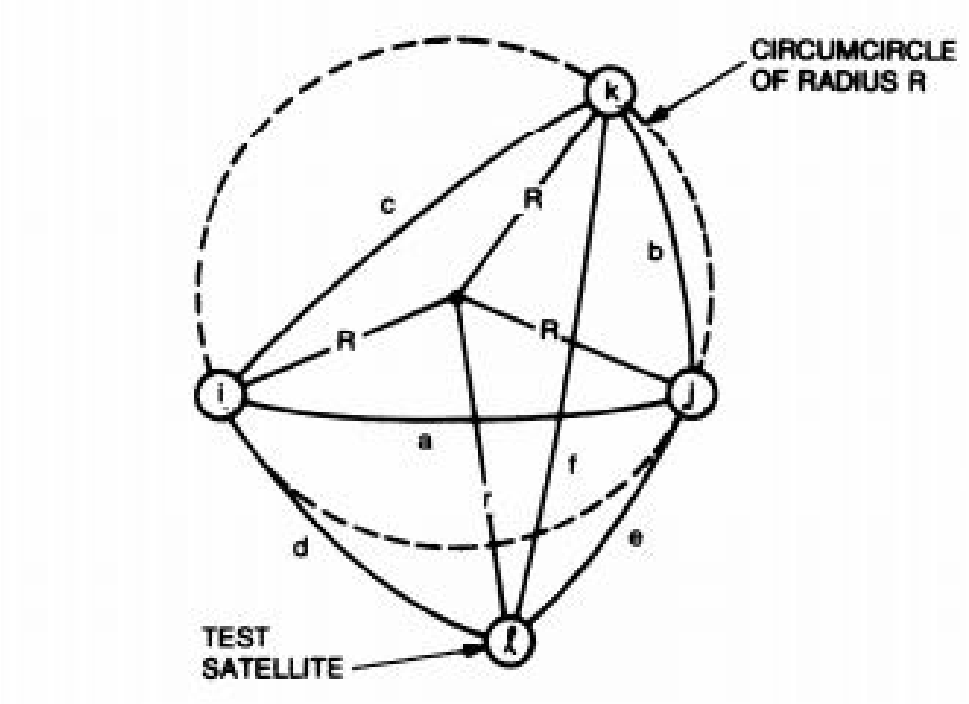

Figure 3.11: Geometry for enclosure test [26].

An analysis of the spherical triangles in Figure 3.11 will show that the test variable y must simultaneously satisfy three equations of the form

$$y^2 + 2Ky + M\tan(R)^2 = 0 \tag{3.26}$$

where:

$$K_1 = \frac{A - D - E}{1 - A} \tag{3.27}$$

$$M_1 = K_1^2\left(\frac{1}{A-1}\right) - \left[\frac{4DE}{1-A}\left(\frac{1}{A} - \frac{1}{\sin(R)^2}\right)\right] \tag{3.28}$$

$$A = \sin\left(\frac{a}{2}\right)^2 \tag{3.29}$$

$$D = \sin\left(\frac{d}{2}\right)^2 \tag{3.30}$$

$$E = \sin\left(\frac{e}{2}\right)^2 \tag{3.31}$$

and the other two equations are obtained by cyclic rotation of *(ABC)* and *(DEF)*. Simultaneous solution of any independent pair of the equations of the second order with the variable y will yield the correct value for y itself. In the degenerate case where all three equations are identical, the sign of y will be opposite to the sign of K.

The algorithm applies the analytical formulas given for the determination of the

worst-case circumcircle radius, but the propagation in time of the constellation is done numerically by selecting a suitable time-step. The diagram here reported summarises the most important steps performed by the algorithm.

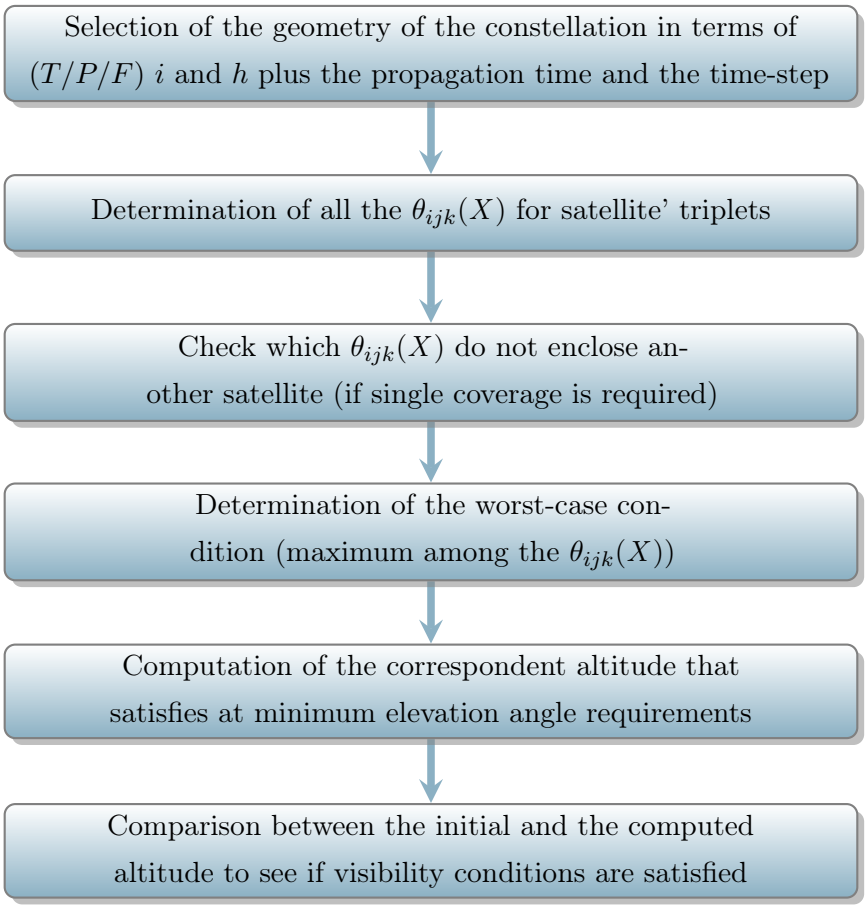

The entire algorithm-like logic for the Walker circumcircle approach is presented in Appendix C.1.

3.4 Lang coverage method

The Lang algorithm allows the optimisation of non-polar, symmetric constellations as large as 100 satellites in circular orbits for continuous global coverage [48].
This method can be uncoupled from altitude and elevation angle considerations, by using the central angle radius of Earth coverage θ as the primary independent variable. For constellations of T circular orbit satellites, the goal is to find the arrangement which requires the smallest value of θ and still achieves continuous global coverage. The constellation with the lowest required θ will allow the lowest operating altitude for a fixed value of elevation angle ε. Conversely, if the satellite altitude is fixed, the lower operating limits on elevation angle ε will be maximised. The value of the central angle radius of Earth coverage θ which is required for the constellation to achieve continuous global coverage is

used as a measure of efficiency of a constellation. The lower the value of θ for a fixed T, the more efficient the constellation.

Lang [48] used the Walker's notation $(T/P/F)$ and inclination i for constellations; in order to have a symmetric arrangement, the $\frac{T}{P} = S$ satellites in a given orbital plane are equally spaced in central angle and the P orbital planes are evenly spaced through 360 deg of right ascension of ascending node. The phasing parameter F relates the satellite positions in one orbital plane to those in another. The parameters $(T/P/F)$ and the orbital inclination i are sufficient definition of a constellation to allow the determination of the central angle of coverage θ which is required for any specified multiplicity of continuous global coverage.

The Lang method takes significant advantage of the properties of symmetry of the constellation. In this approach, T satellites are propagated in time over an Earth containing a set of test points. The smallest value of θ is then determined which ensures that all test points are visible to at least n satellites, where n is the desired multiplicity of coverage, for all times. While this appears to be a straightforward brute force approach, there are several simplifications which have been introduced to make it attractive [48].

If the entire globe or some zone of the globe (between two latitude values) is continuously covered by a constellation of satellites, then it will be continuously covered independent of the rotation rate of the Earth. By choosing to rotate the Earth at the same rate as the motion of the satellites in their orbits, effectively, all satellites are now in Geosynchronous inclined orbits. This assumption leads to two important simplifying features:

- Since orbits repeat each revolution relative to the test points, so does the coverage geometry. Consequently, there is no need to simulate more than one orbital revolution. Additionally, the location of any of the T satellites at any time point can be easily referenced to the time history of the first satellite. Only a single reference satellite needs to be propagated and saved. Consider the groundtracks of the satellites in the geosynchronous (12/3/2) constellation, as shown in Figure 3.12; note that there are only four independent groundtracks, each containing three satellites. Each groundtrack contains a satellite from each of the three orbital planes. If the latitude/longitude history of satellite number 1 is known at appropriate time intervals then the latitude/longitude locations of the other satellites at any time point can be easily found. For instance, the latitude/longitude of satellite 7 at any time point is the same of satellite 1 one-third of a revolution (8 hours) earlier. Satellite 2 occupies the same latitude/longitude location that satellite 1 would in one-fourth

of a revolution (6 hours), except that 90 deg must be added to the longitude. This time and longitude shifts are easily computed for all of the T satellites. The first satellite is then propagated at a time interval which includes all of necessary time shifts so that any satellite position at any time can be found in the precomputed latitude/longitude vectors for satellite 1. By this method the burden of computing satellite locations for T satellites is significantly reduced.

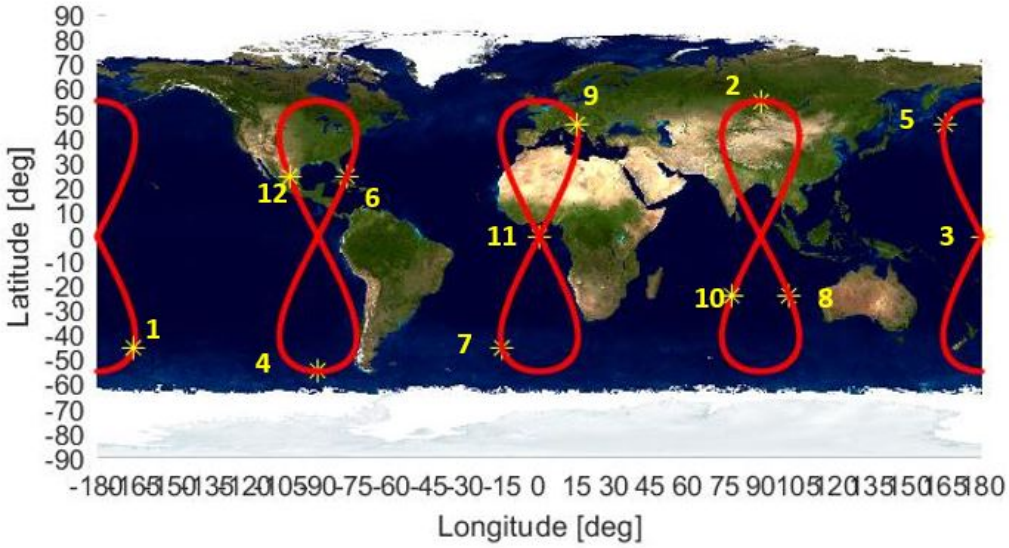

Figure 3.12: Symmetric (12/3/2) constellation.

- Since, over one revolution, the pattern of coverage will be the same between any two of the groundtracks in the constellation, only locate the test points on the ground between any two of the groundtracks is needed. That is, due to the symmetry of the constellation, any coverage gaps are symmetrically located with respect to the groundtracks. Figure 3.13 shows the coverage gaps which occur over one revolution for the (12/3/2) constellation for a central angle radius of Earth coverage $\theta = 46$ deg ($\varepsilon = 37$ deg). Note that the coverage gaps are symmetric about each groundtrack. Test points in the region latitude = 0 deg to 90 deg and longitude = 0 deg to 45 deg (green coloured area in Figure 3.13) would sample all the coverage gaps for continuous global coverage. If this constellation had 12 independent groundtracks instead of just four, then only the longitude range = 0 deg to 15 deg would need to be sampled with test points. In general, as the number of groundtracks increases, the region over which the test points must be placed decreases. This consideration can be used to help decrease computer program run time for large constellations.

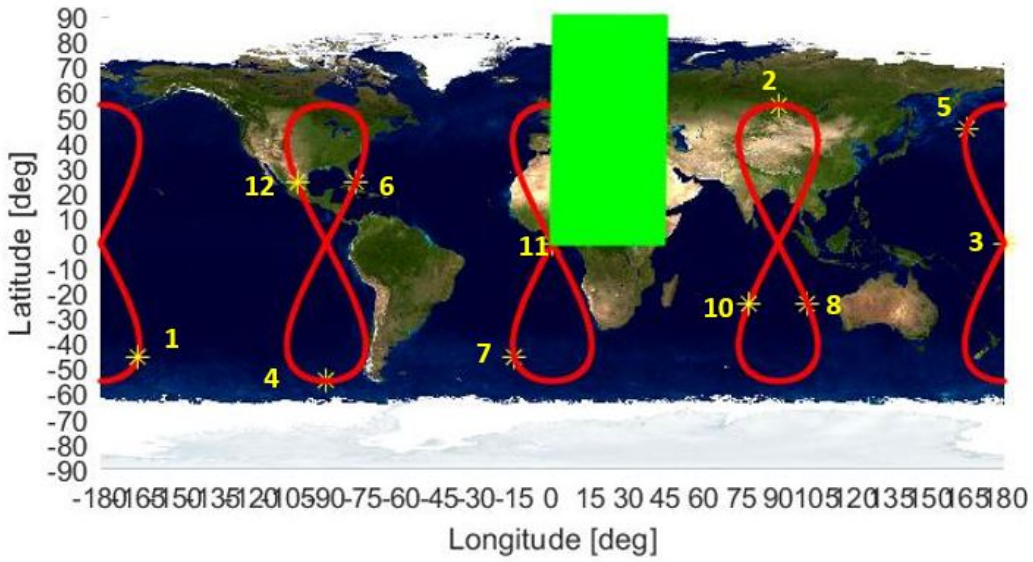

Figure 3.13: Coverage gaps for the (12/3/2) constellation.

The method can be used to optimise symmetric constellations for continuous global or zonal coverage (between two specified latitude bands); coverage multiplicities between any single and quadruple can currently be handled.
In addition, by varying the value of the phasing parameter F, the output of the algorithm would be the value of orbital inclination which requires the smallest θ to achieve the desired fold of continuous global coverage.
Therefore, it is possible to determine the most efficient arrangements for P, F and i and the T correspondent to the lowest θ. These results can be then translated into the minimum altitude at which continuous coverage is achieved for a specified minimum elevation angle (say ε=0 deg).

The novelty proposed in this work for the Lang method consists in the determination of the coverage circles of the satellites of the constellation throughout an analytical formulation, that allows to compute the central angle of Earth coverage θ. Instead of using some visibility function based on Fourier series [10] or by evaluating the rise and set times of each satellite from a generic position on the Earth's surface (e.g. [8], [13]), this approach starts from the position of the reference spacecraft on its orbit projected onto the surface and the position of a point belonging to the grid of tests points. The distance is then directly related to the central angle of coverage and to the conical field of view of the satellite.

By considering the longitude and latitude positions of the sub-satellite point of the reference satellite and of a point on the grid (ϕ_{sub}, λ_{sub}) and (ϕ_G, λ_G) respectively, the central angle of coverage is given by:

$$\Delta\phi = |\phi_{sub} - \phi_G| \tag{3.32}$$

$$\Delta\lambda = |\lambda_{sub} - \lambda_G| \tag{3.33}$$

$$a = \sin\left(\frac{\Delta\lambda}{2}\right)^2 + \cos\left(\lambda_{sub}\right)\cos\left(\lambda_G\right)\sin\left(\frac{\Delta\phi}{2}\right)^2 \tag{3.34}$$

$$\theta = 2\arctan\left(\frac{\sqrt{a}}{\sqrt{1-a}}\right) \tag{3.35}$$

It is also possible to convert the coverage angle to a length by multiplying by the Earth radius:

$$\theta_{km} = \theta R_{Earth} \tag{3.36}$$

The diagram here reported summarises the most important steps performed by the Lang algorithm.

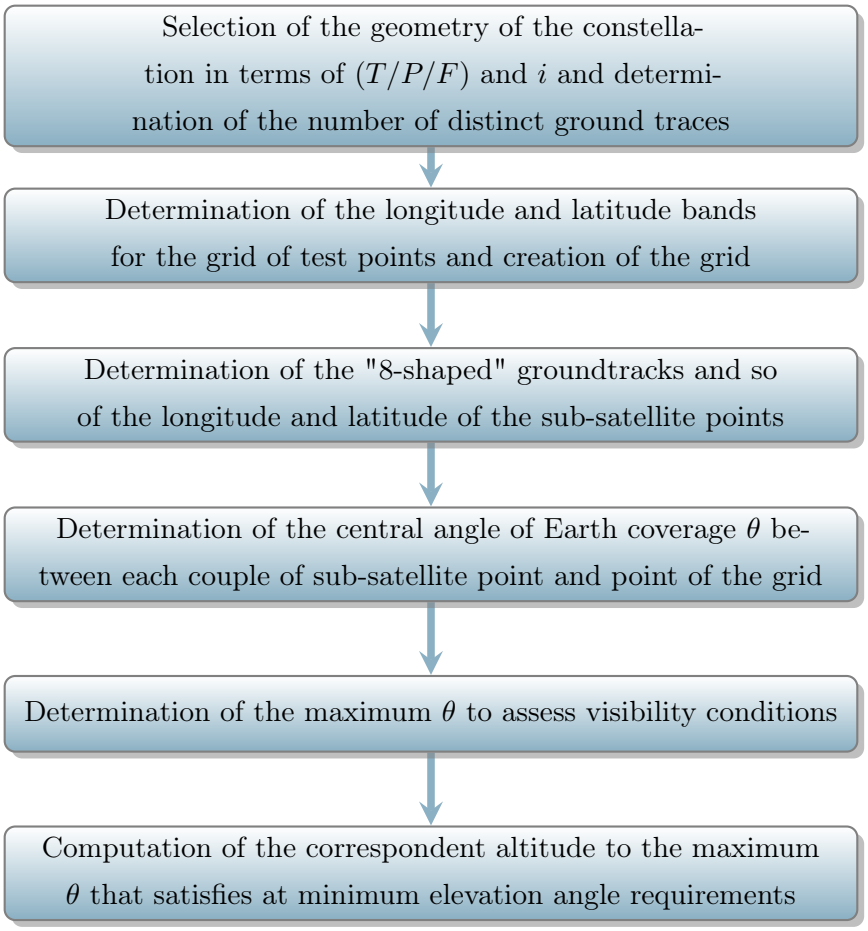

The entire algorithm-like logic for the Lang approach that contains this computation is presented in Appendix C.2 and it follows the theoretical description here above presented.

4. Methods for discontinuous coverage

When performing a constellation selection process, there are certain requirements and constraints that dominate while others have more of a fine tuning effect [3]. The more important requirements are:

1. Service area coverage;
2. Spectrum sharing: as spectrum becomes scarce, multiple systems find that they must develop means to co-exist in the same frequency band;
3. Capacity augmentation: to use the satellite diversity (multi-coverage) characteristics of a constellation to keep the size and cost of each satellite reasonable;
4. Satellite failure mitigation: the constellation itself must provide some measure of immunity to single satellite failures (e.g. double coverage would be one way to mitigate it);
5. Service link maintenance: the system must dynamically maintain service links to Earth-based customers;
6. Altitude considerations: generally altitude is determined from the coverage footprint radius, the service area coverage requirements and coverage levels needed.

However, the most important is the service area coverage. If the requirements demands full Earth coverage, the best suited constellation can be quite different from the solution to regional coverage or coverage within a latitude band.

As far as the orbit design is concerned, researches have focused on the determination of the most suitable configurations to guarantee appropriate performances of coverage by a minimum number of satellites, as in the case of Walker constellations (see Section 2.2.1), which are based on the consideration of regular distribution of satellites and orbital planes, or of Street Of Coverage constellation (see Section 2.2.3), involving polar, optimally phased orbits.

While in Chapter 3 methods valid for continuous coverage only are described, this chapter deals with methods suitable for discontinuous coverage computations.

Indeed, many studies have been conducted about coverage and different methodologies have been developed depending on the requirements and on the geometry of the constellation considered.

4.1 Numerical brute force method

The brute force method is a straightforward purely numerical approach of solving a problem that rely on sheer computer power; in the computation process, the algorithm tries every possibility and does not involve some techniques to improve efficiency and to reduce the computational time. For these reasons, the algorithm is reliable, it gives quite accurate results and it could be used to compare and check the solutions obtained with other, perhaps more complex, methods (e.g. analytical).

The brute force method developed by the author can deal with all kind of geometries and satellite constellations, with non-symmetric or symmetric conditions, with circular or elliptical orbits and even for the case of one single satellite. The central body could be the Earth as well as another planet or Moon; in addition, effects caused by orbital perturbations can be taken into account.

The approach relies on relative vector positions between satellite and location of interest on the planet's surface: the satellite's orbit is propagated for a period of time and its position is investigated at each time-step with respect to the correspondent site. Given all the necessary parameters to describe a satellite constellation, its performance indexes such the area covered on the planet's surface, the level of coverage and the revisit time are determined.
Therefore, the "brute force" is not an optimisation method, but it simply provides the needed information for a given geometry.

The principle of work of the method is to take as inputs the position vectors of each satellite of the constellation at any instant of time of the propagation period. Hence, it must be first selected the time step and the total amount of time the algorithm shall investigate. The time could be given in an absolute way, starting from $t = 0$ and propagating until a selected $t = t_{final}$ or by using existing counts of time (some examples are listed in Appendix A.1).
Moreover, as initial condition for the propagation, a random position on the orbit could be considered. There exist different reference frames that could be used and each of them could be chosen; anyway, it must be paid attention to be consistent throughout all the

propagation and computations performed. Some examples are listed in Appendix A.2. The diagram here reported summarises the most important steps performed by the algorithm.

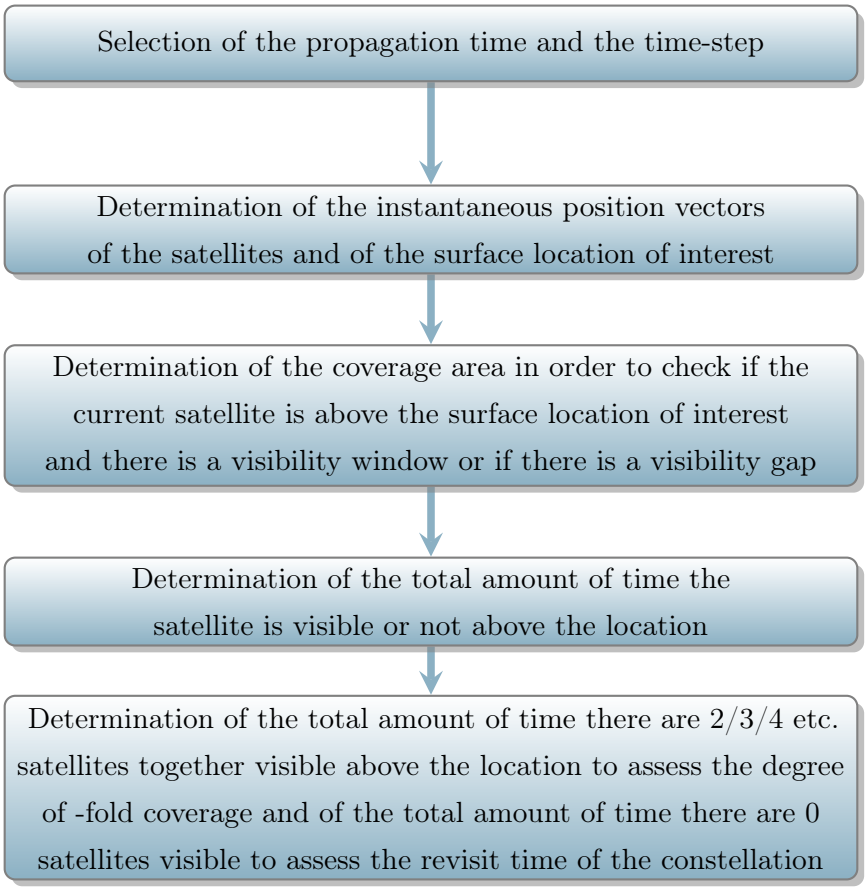

The central angle of Earth coverage, for the more general case, is determined by the equation:

$$\cos(2\theta) = \frac{\mathbf{r}_{s/c} \cdot \mathbf{r}_{surf}}{r_{s/c} r_{surf}} \tag{4.1}$$

where $\mathbf{r}_{s/c}$ is the vector position of the satellite and $\mathbf{r}_{surf}$ is the vector position of the location on the surface. Then the elevation angle ε is determined and compared with the minimum acceptable angle ε_{min} to achieve visibility conditions: if the resulting number is higher or equal to the minimum threshold, then there are visibility conditions. This approach can return the desired results quite fast and the computational time depends on the propagation time and time-step chosen only.
The whole algorithm-like logic for the brute force method is presented in Appendix C.3.

4.2 Geometrical approach for long revisit times

Most traditional satellite constellation design methods are associated with a simple zonal or global, continuous or discontinuous coverage. The geometric approach here presented is valid for discontinuous coverage of satellites in circular orbits; the key assumption and the constraint imposed in order to apply this method is that the revisit time for zonal coverage shall be more than one orbital period. The method is analytical, it is valid for discontinuous coverage satellite constellations and it does not require a numerical simulation for the constellation itself [50]. In addition, the following assumptions are made: Earth is considered a round body, all satellites in a constellation will be at the same altitude with the same number of satellites in each orbital plane and all orbit planes in a constellation will have the same orbit inclination [50].

The method is based on two-dimensional maps of visibility properties for the satellite constellation and coverage requirements, with space dimensions:

- Right ascension of the ascending node Ω (in the ECI frame) on the x axis;
- Time t or argument of latitude u on the y axis.

The boundary points of the region that is presented in such space are the correspondent of the coverage circle of visibility conditions in longitude and latitude dimensions and have been computed throughout the analytical formulation for coverage area determination (see Section 2.1.1). The simplest case is the coverage of a point on the Earth's surface by a satellite. Figure 4.1 shows three examples of such maps for points with different geographical latitudes λ_c of the site of interest on the Earth's surface (65 deg, 0 deg and 30 deg). The longitude and latitude angles of the boundaries of the coverage region that result for a value of the central angle of Earth coverage θ and inclination i of the satellite's orbit are here converted into Ω and u values. From a geometric point of view, they can be convex or non-convex, simple or multiply connected. For computational purposes, the coverage function is presented as a region of boundary points. It should be noted that in contrast to the coverage circle size on Earth's surface that can be appreciated in Figures 4.2, 4.3 and 4.4 for the three cases, the size and shape of the region also depend on the point latitude and orbit inclination.
In particular, the circle on Figure 4.2 is associated to the simple connected convex region of Figure 4.1, the circle on Figure 4.3 with the double connected region and the circle on Figure 4.4 with the simple connected non-convex region.

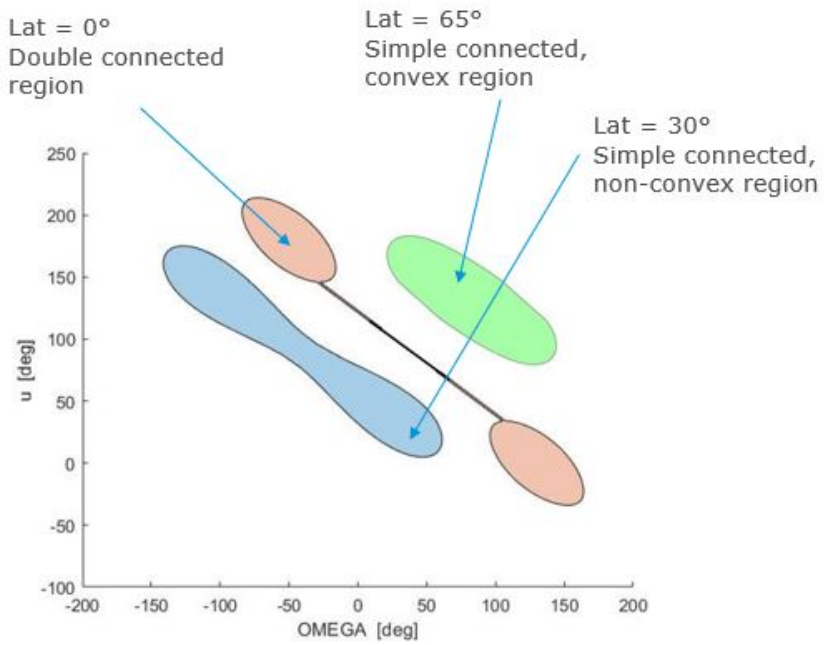

Figure 4.1: Region examples (h=1400 km, i=52 deg, ε=10 deg).

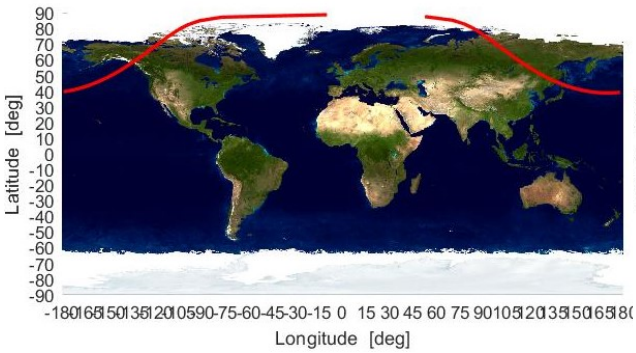

Figure 4.2: Coverage circle (170 deg, 65 deg), simple convex.

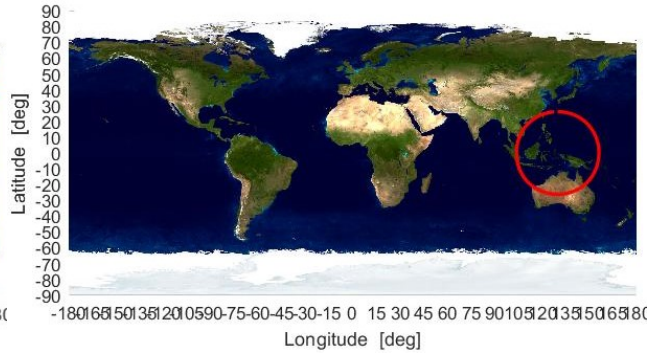

Figure 4.3: Coverage circle (130 deg, 0 deg), double connected.

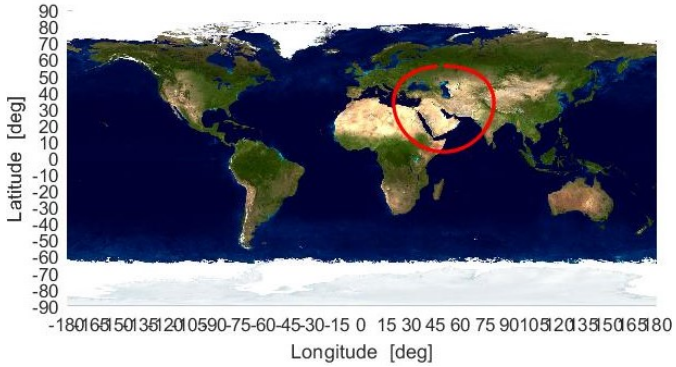

Figure 4.4: Coverage circle (50 deg, 30 deg), simple non-convex.

Let $f(\Omega,u)$ be a coverage function which describes the requirements of the satellite constellation; without loss of of generality, let suppose that all points $f(\Omega,u) \geq 0$ are required values and their map in the space is an area. In the general case, it can be a

multiply connected area. Because, for the following analysis, only shape and size of the maps are important, the choice of Ω is arbitrary and so is the choice of the longitude; in fact, usually the dependence on longitude for the determination of constellation performance is small.

As previously stated, the geometry considered is the one described in Section 2.1.1 and the typical satellite coverage for an observer on the Earth is the one depicted in Figure 2.1: the satellite is located at orbital altitude h and the projection of the footprint onto the Earth's surface defines a circle of coverage of an angle θ; the relation between the coverage angle θ, the orbit altitude h and the elevation angle ε is given by Equation (5.5). Note that the coverage circle size is dependent only on the satellite orbit altitude.

Assuming that the orbit inclination i, altitude h and elevation angle ε are specified, the visibility conditions for the satellite in the (Ω, time) space can be presented by a region of boundary points and the satellite trajectory map in the space is near to a straight line along the y axis. The trajectory is represented by the orange dashed line in Figure 4.5.

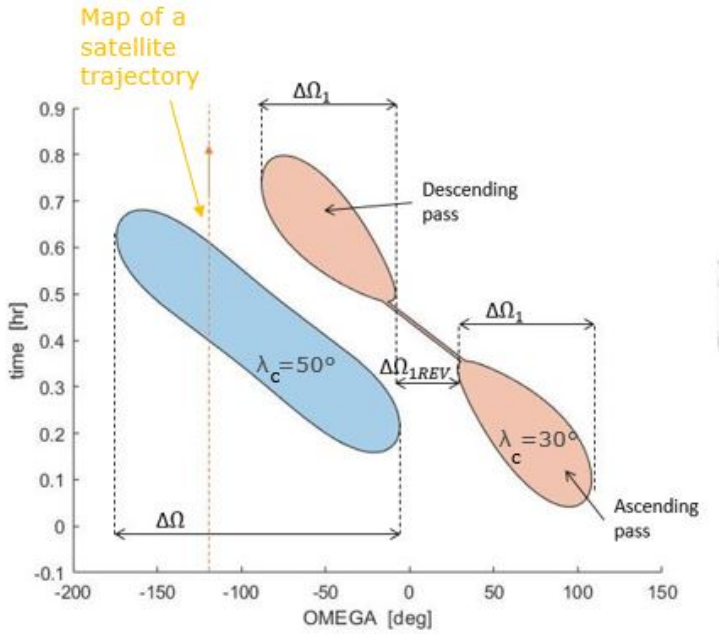

Figure 4.5: Satellite visibility maps (h=800 km, i=55 deg, ε=5 deg).

If the line is intersected by the region, then there is a visibility interval.
It must be highlighted that all the maps presented on Figures 4.1 and 4.5 are shown for one satellite revolution; on the next revolution, the maps would have shifted to the right by $\Delta\phi_1 = \omega_{Earth} T_{period}$ (where ω_{Earth} is the rotation rate of the Earth and T_{period} is the orbital period) and so on for the next revolutions.

For specified values of latitude of the coverage points λ_c, inclination i and coverage angle θ there are two categories of regions. The first correspond to the visibility at ascending and descending passes, for $\lambda_c < i - \theta$ (double region in figure 4.5); the second is a single connected region, for $i - \theta \leq \lambda_c \leq i + \theta$ (single region in Figure 4.5).
For time intervals of the order of several orbital periods, a satellite trajectory in the introduced two-dimensional space is near to a straight line parallel to the y axis. For longer time intervals, a similar map can also be produced, but perhaps the regression of the ascending node due to J_2 effect should be considered. In this case, the straight line is slightly inclined to the y axis, but the current analysis does not consider this latter option. $\Delta\Omega$ presented in Figure 4.5 is the the visibility longitude range and it can be computed analytically using spherical trigonometry equations; the range is function of the point latitude λ_c, orbit inclination angle i and the geocentric coverage angle θ. The boundary ascending nodes of the satellite passes are tangential to the coverage circle θ as shown in Figure 4.6.

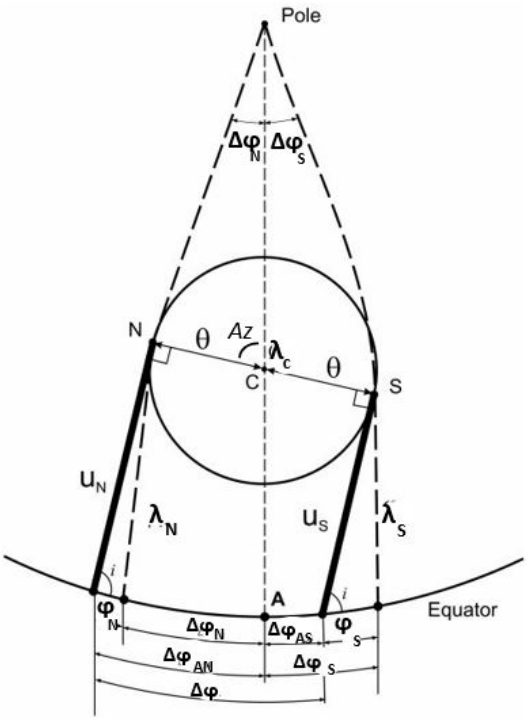

Figure 4.6: Ascending node boundaries.

Moreover, $\Delta\Omega$ is a function of the quantity related to shift due to Earth's rotation and boundary longitudes relative to a non rotating Earth $\Delta\varphi$. The detailed computations involved for the determination of $\Delta\Omega$ are here reported. The formulations that bring to the final $\Delta\Omega$ range value have been developed by Ulybyshev [50], while the calculation of the boundary points of the entire coverage region has been added by the author in order to go deeper in the physical insight of the method and achieve more accurate results.

The boundaries of coverage regions can be computed analytically using spherical trigonometry equations, since it often affords better geometric insight than the more traditional vector approach [11]. This approach allows fast and precise computations, avoiding the rounding errors deriving from the numerical approaches and saving computational cost. The longitude range is function of the point latitude λ_c, orbit inclination angle i and the geocentric coverage angle θ and the boundary ascending nodes of the satellite passes are tangential to the latter.

Geographic coordinates of the coverage region are often needed to graphically display the region on maps. For a given center point (latitude λ_c and longitude ϕ_c) and angular radius θ, the geographic coordinates of the boundary of the region can be computed either from standard equations of spherical trigonometry or by vector equations. A simple spherical trigonometry procedure, illustrated in Figure 4.6, is to parameterise on azimuth Az by varying it in the range [0, 2π], about the center point, being careful to select a triangle that has its apex at the nearest of the North or South Poles. The equations for the geographic latitudes and longitudes, computed from spherical triangle with vertices the *Pole*, C and S of Figure 4.6, are:

$$\lambda_i = \sin\left(\cos\theta \sin\lambda_c + \sin\theta \cos\lambda_c \cos Az\right)^{-1} \tag{4.2}$$

$$\phi_i = \phi_c + \tan\left(\sin\theta \sin Az, \frac{\cos\theta - \sin\lambda_i \sin\lambda_c}{\cos\lambda_c}\right)^{-1} \tag{4.3}$$

The longitudes computed correspond to the satellite traces, which are tangential to the coverage circle at points with a latitude of λ_c (see Figure 4.6).

The equations for 0 deg $\leq \lambda_c <$ 90 deg and $i \leq$ 90 deg are here reported, while for other values of $\lambda_c \leq$ 0 deg and $i >$ 90 deg, it is necessary to replace the signs accordingly. For the latitudes $\lambda_c < i - \theta$, there are two longitude ranges corresponding to the ascending and descending passes (see Figure 4.6):

$$\sin\lambda_N = \frac{(|\sin\lambda_c| + \sin\theta)}{\cos\theta} \tag{4.4}$$

$$\cos\lambda_N = \sqrt{1 - \sin\left(\lambda_N\right)^2} \tag{4.5}$$

$$\sin\lambda_S = \frac{(|\sin\lambda_c| - \sin\theta)}{\cos\theta} \tag{4.6}$$

$$\cos\lambda_S = \sqrt{1 - \sin\left(\lambda_S\right)^2} \tag{4.7}$$

$$\Delta\varphi_N = \cos\left(\frac{\cos\theta - \sin\lambda_c \sin\lambda_N}{\cos\lambda_c \sin\lambda_N}\right)^{-1} \tag{4.8}$$

$$\Delta\varphi_S = \cos\left(\frac{\cos\theta - \sin\lambda_c \sin\lambda_S}{\cos\lambda_c \sin\lambda_S}\right)^{-1} \tag{4.9}$$

$$\varphi_N = \sin\left(\frac{\cos\lambda_c \sin\lambda_N}{\sin\lambda_c \cos\lambda_N}\right)^{-1} \tag{4.10}$$

$$\varphi_S = \sin\left(\frac{\cos\lambda_c \sin\lambda_S}{\sin\lambda_c \cos\lambda_S}\right)^{-1} \tag{4.11}$$

$$\Delta\varphi = \varphi_N + \Delta\varphi_N - \varphi_S + \Delta\varphi_S \tag{4.12}$$

The boundary longitudes for the ascending pass are:

$$\Delta\varphi_{AN} = -(\varphi_N + \Delta\varphi_N) \tag{4.13}$$

$$\Delta\varphi_{AS} = -(\varphi_S + \Delta\varphi_S) \tag{4.14}$$

and for the descending pass:

$$\Delta\varphi_{DN} = -(\pi - \varphi_N - \Delta\varphi_N) \tag{4.15}$$

$$\Delta\varphi_{DS} = -(\pi - \varphi_S + \Delta\varphi_S) \tag{4.16}$$

Arguments of latitude for the boundary points can be determined from the equations:

$$u_{AN} = \sin\left(\frac{\sin\lambda_N}{\sin i}\right)^{-1} \tag{4.17}$$

$$u_{AS} = \sin\left(\frac{\sin\lambda_S}{\sin i}\right)^{-1} \tag{4.18}$$

$$u_{DN} = \pi - u_{AN} \tag{4.19}$$

$$u_{DS} = \pi - u_{AS} \tag{4.20}$$

For the latitudes $i - \theta \leq \lambda_c \leq i + \theta$, both longitude ranges are joined to a longitude range:

$$\Delta\varphi = 2(\Delta\varphi_S - \varphi_S) + \pi \tag{4.21}$$

The bounding longitudes are $\Delta\varphi_{AS}$ and $\Delta\varphi_{DS}$ from Equations (4.14) and (4.16) respectively, and corresponding arguments of latitude u_{AS} and u_{DS} from Equations (4.18) and (4.20).

The procedure to determine other points belonging to the coverage circle and to draw the coverage region in the (Ω,u) space is then nearly the same: once computed the central angle of Earth coverage θ and known the central point (ϕ_C, λ_C) and the inclination angle i, the angles (ϕ_i, λ_i) on the circle can be found through Equations (4.2) and (4.3) and the correspondent Ω and u are:

$$u_i = \sin\left(\frac{\sin\lambda_i}{\sin i}\right)^{-1} \tag{4.22}$$

$$\Omega_i = \phi_i - \tan\left(\cos i \sin u, \cos u\right)^{-1} \tag{4.23}$$

for the ascending pass and

$$u_i^* = \pi - u \tag{4.24}$$

with the correspondent Ω for the descending pass.

After the computation of the boundary longitudes $\Delta\varphi$ relative to a non-rotating Earth throughout the presented equations, additional shifts shall be considered due to Earth's rotation in order to determine the longitude range $\Delta\Omega$:

$$\Delta\Omega = \Delta\varphi - \omega_{Earth} T_{period} \frac{[u_N(\lambda_c, i, \theta) - u_S(\lambda_c, i, \theta)]}{2\pi} \tag{4.25}$$

where u_N and u_S are the argument of latitudes of the boundary points of Figure 4.6.

If the groundtrack shift of a single satellite $\Delta\phi_1 = \omega_{Earth} T_{period}$ is less than the visibility longitude range $\Delta\Omega$, then there are longitude ranges with visibility intervals at consecutive revolutions.
For the satellite, the multirevolution map of the point visibility can be presented as a set of thin regions (near to straight-line segments along the x axis) as presented in Figure 4.7.

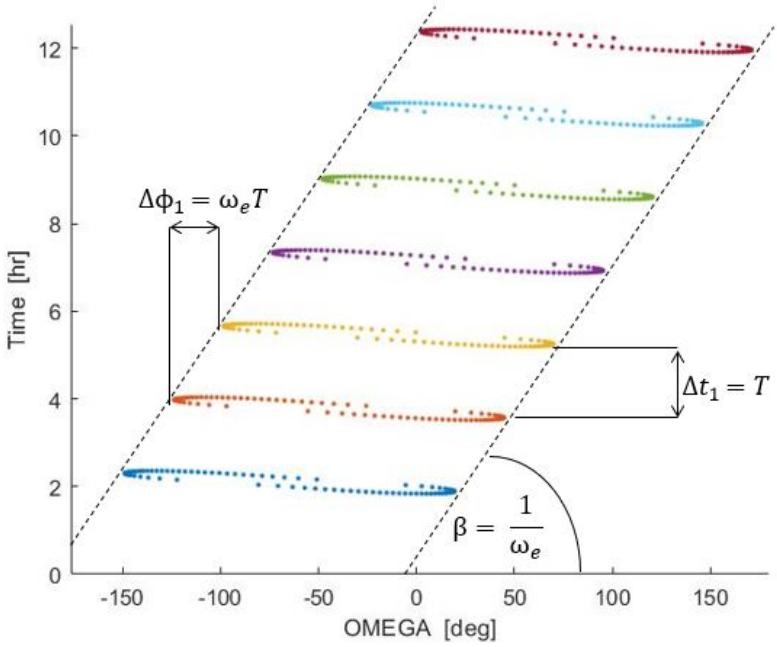

Figure 4.7: Sawtooth coverage belt (h=800 km, i=55 deg, ε=5 deg, λ_c=50 deg).

The regions are bounded by straight lines or envelopes with the same inclination angle β that depends only on Earth's rotation rate.
Suppose that $\Delta\phi_1 = \omega_{Earth} T_{period} < \Delta\Omega$; then, from a geometrical point of view, in the two-dimensional space, the visibility properties can be presented as a coverage belt (see Figure 4.7) with sawtooth boundaries and straight-line envelopes aligned at angle β to the x axis. The angle is defined only by ω_{Earth} as:

$$\tan(\beta) = \frac{1}{\omega_{Earth}} \tag{4.26}$$

The major property is that for all the points inside the coverage belt the revisit times are near to the orbital period.
The representation of the coverage regions in Figure 4.7, as well as all of the following maps in the (Ω, u) and (Ω, t) space, have been created by the author throughout the determination of the boundary points of the region itself and by repetition of the procedure for several orbital periods and a certain period of time (say: one day).

4.2.1 Revisit times for visibility of single satellite

In order to better explain the procedure for revisit time computation, the case of one single satellite is first examined. The coverage belt with sawtooth boundaries is formed by visibility intervals for a satellite at consecutive revolutions and the two-dimensional space is divided into two parts, with the revisit time near to and more than one period, respectively. Figure 4.8 shows the geometric parameters.

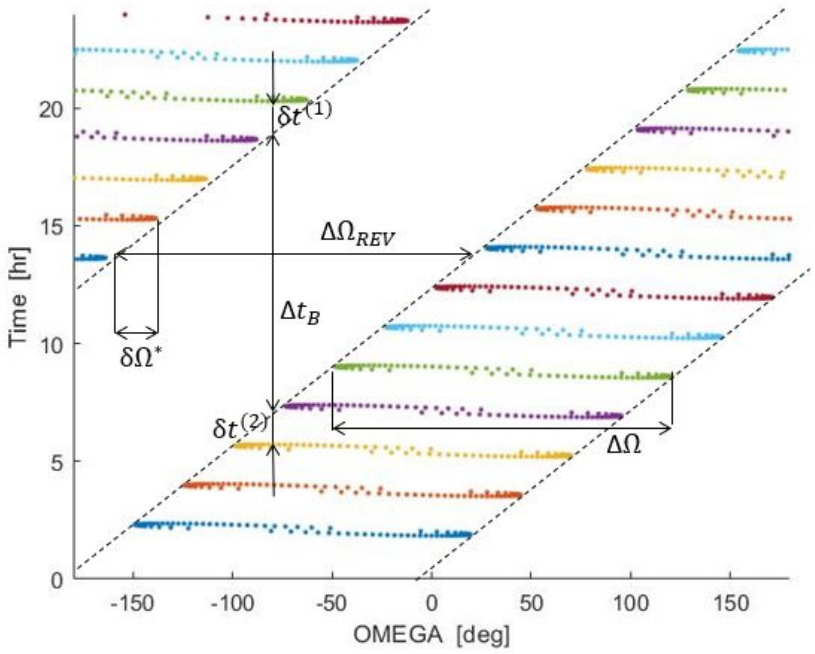

Figure 4.8: Multirevolution map for visibility of single satellite (h=800 km, i=55 deg, ε=5 deg, λ_c=50 deg).

The revisit times Δt_{REV} for the satellite are analytically computed as the sum of two terms [50]:

1. The revisit time between straight-line envelopes of adjacent sawtooth coverage belts Δt_B;
2. The relative shift of the teeth in the belts δt.

As stated before, the coverage belts are very descriptive geometric images for the analysis and computations. Their major property is that, for all of the points inside the coverage belts, the revisit times are near to the period T_{period} [50]. In the following, only the revisit times $\Delta t_{REV} > T_{period}$ will be considered. For latitudes $\lambda_c < i - \theta$, there are double coverage belts, while for $i - \theta \leq \lambda_c \leq i + \theta$ there are single coverage belts.

For the following analysis, only ranges of visibility $\Delta\Omega$ and gap $\Delta\Omega_{REV}$ are important (see Figure 4.8) and a choice of the right ascension of the ascending node is arbitrary.

Single coverage belt

The simplest case of the visibility analysis corresponds to the latitude band of $i - \theta \leq \lambda_c \leq i + \theta$ for which there are single coverage belts, as the case of Figure 4.8. The revisit time can be expressed as the sum of two terms:

$$\Delta t_{REV} \approx \Delta t_B + \delta t \tag{4.27}$$

The first term is defined by a longitude shift of the coverage belt:

$$\Delta t_B = \Delta\Omega_{REV} \tan(\beta) = [2\pi - \Delta\Omega(\lambda_c, i, \theta)] \tan(\beta) \tag{4.28}$$

where $\Delta\Omega_{REV}$ is a longitude gap. The second term depends on a relative phase shift between satellite positions in adjacent coverage belts:

$$T_{period} \leq \delta t \leq 2T_{period} \tag{4.29}$$

Three typical cases for the phase shift are schematically depicted in Figures 4.9, 4.10 and 4.11.

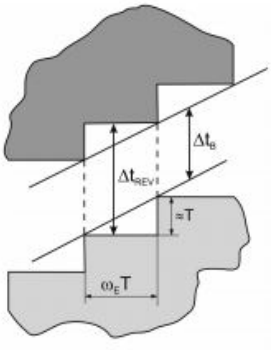

Figure 4.9: $\delta t \approx T$ [50].

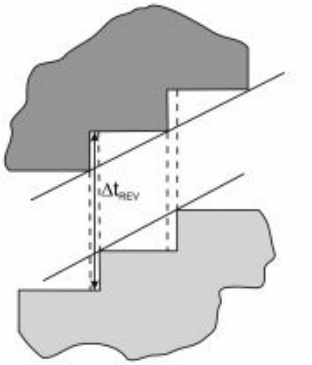

Figure 4.10: $\delta t \approx 2T$ [50].

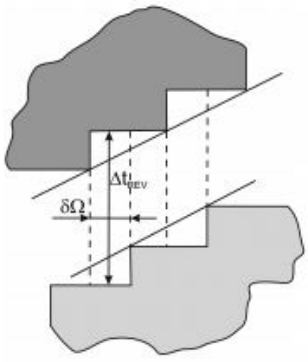

Figure 4.11: $T < \delta t < 2T$ [50].

The boundary arguments of latitude in both coverage belts are the same [50]. Then, the longitude shift between boundary points in the coverage belts is (see Figure 4.8):

$$\delta\Omega^* = \omega_{Earth} T_{period} \frac{[u_{AN}(\lambda_c, i, \theta) - u_{AS}(\lambda_c, i, \theta)]}{2\pi} \tag{4.30}$$

where u_{AN} and u_{AS} are arguments of latitude of the boundary points from Equations (4.17) and (4.18). If $(\Delta\Omega_{REV} - \delta\Omega^*)$ is a multiple of $\Delta\phi_1$, then $\delta t = T_{period}$ (see Figure 4.9). In the opposite case, there is a residue of division:

$$\delta\Omega = (\Delta\Omega_{REV} - \delta\Omega^*) - \Delta\phi_1 \left[\frac{\Delta\Omega_{REV} - \delta\Omega^*}{\Delta\phi_1} \right] \tag{4.31}$$

where $[^o]$ is the integer part function. Then,

$$\delta t \approx 2T_{period} - \left(\frac{\delta\Omega}{\Delta\phi_1} \right) T_{period} \tag{4.32}$$

In this approximate equation [50], the duration of the visibility intervals are neglected because they are usually small values in comparison with Δt_{REV}.

Double coverage belt

A more complex case is double coverage belts for the latitude band of $\lambda_c < i - \theta$. The computation is similar to the preceding case using Equation (4.27) [50], but there are two types of alternate gaps (see Figure 4.12).

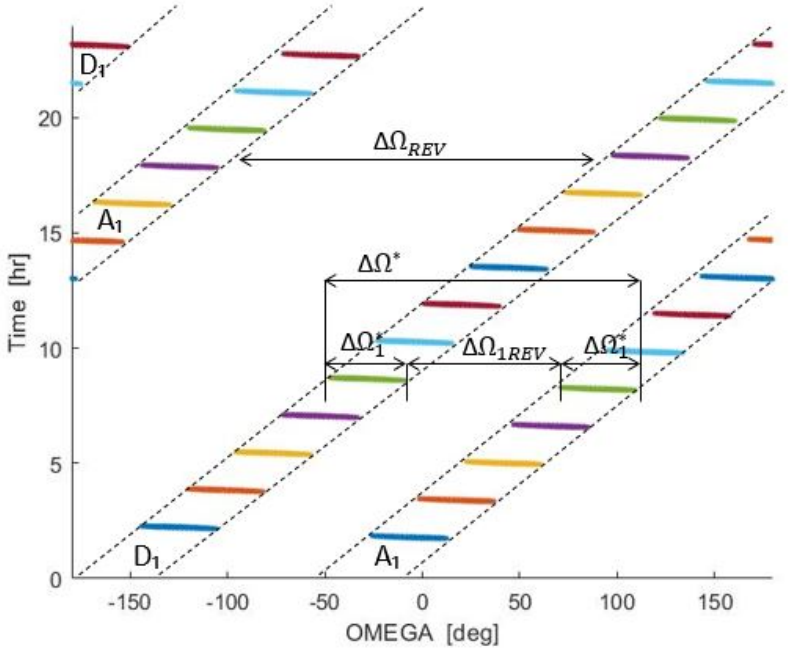

Figure 4.12: Multirevolution map for visibility of single satellite (h=600 km, i=50 deg, ε=20 deg, λ_c=30 deg).

The first is the gap between adjacent coverage belts and the second gap is inside the double coverage belt. The corresponding longitude ranges will be named the external $\Delta\Omega_{REV}$ and the inner $\Delta\Omega_{1REV}$ longitude gaps. For both cases, the first term Δt_B in Equation (4.27) is computed using Equation (4.28) for $\Delta\Omega_{REV}$ or $\Delta\Omega_{1REV}$, respectively. The second term δt is also calculated based on Equations (4.30), (4.31) and (4.32) but, for the inner gap, it is necessary to use the arguments of latitude of u_{DS} and u_{AN} [50].

An example of visibility longitude ranges and inner longitude gap versus latitudes for coverage points along a meridian is presented in Figure 4.13. The picture has been created by the author throughout the determination of the boundary points in order to better understand the behaviour of the longitude range at varying latitudes. The filled area corresponds to the points between straight-line envelopes of the coverage belts.

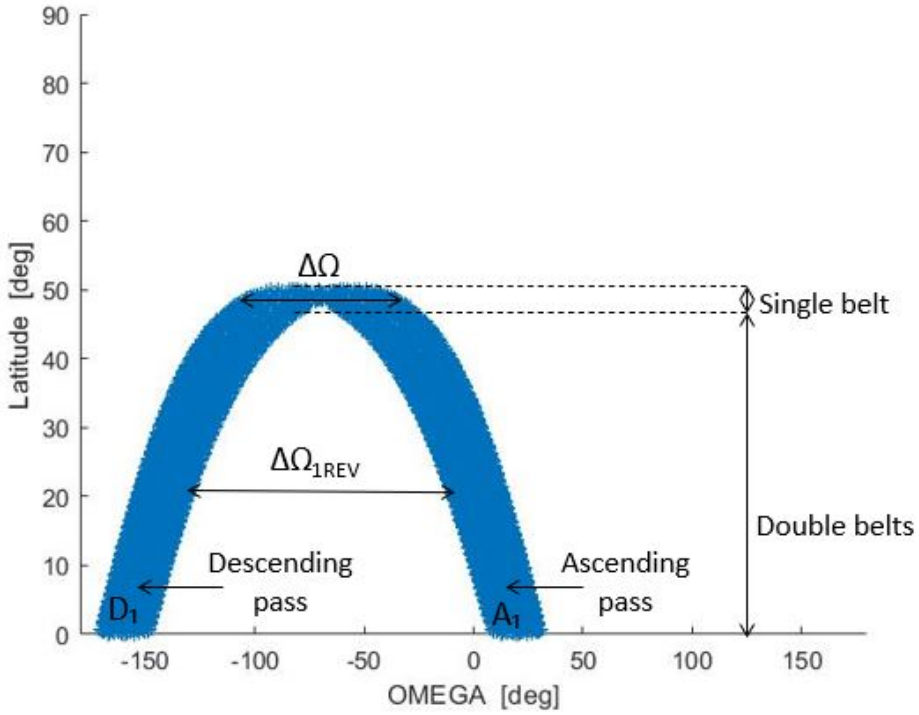

Figure 4.13: Longitude ranges of coverage belts.

4.2.2 Revisit times for visibility of satellite constellations

The analysis is limited to symmetric Walker-type constellations, with symmetric arrangements of similarly inclined circular orbits at a common altitude. The standard notation $(T/P/F)$ is used, with $S = \frac{T}{P}$ satellites evenly distributed in each plane [50].

The proposed coverage belts divide the two-dimensional space (Ω, u) (or equivalently (Ω, t) into two parts with $\Delta t_{REV} \approx T_{period}$ and $\Delta t_{REV} > T_{period}$. For each specified satellite constellation configuration $(T/P/F)$, there is a set of coverage belts. Then, for a satellite constellation, the revisit time computation is a geometric problem for determination of the relative shifts along the y axis for the nearest adjacent coverage belts [50].

Single coverage belts

The simplest case is a satellite constellation with one satellite at each plane for discontinuous coverage for latitudes $i - \theta < \lambda_c < i + \theta$. Suppose that the phase shift between satellites at adjacent planes is zero, that is, $(T/P/F) = (T/T/0)$. An example of two-dimensional space for such constellation is presented in Figure 4.14.

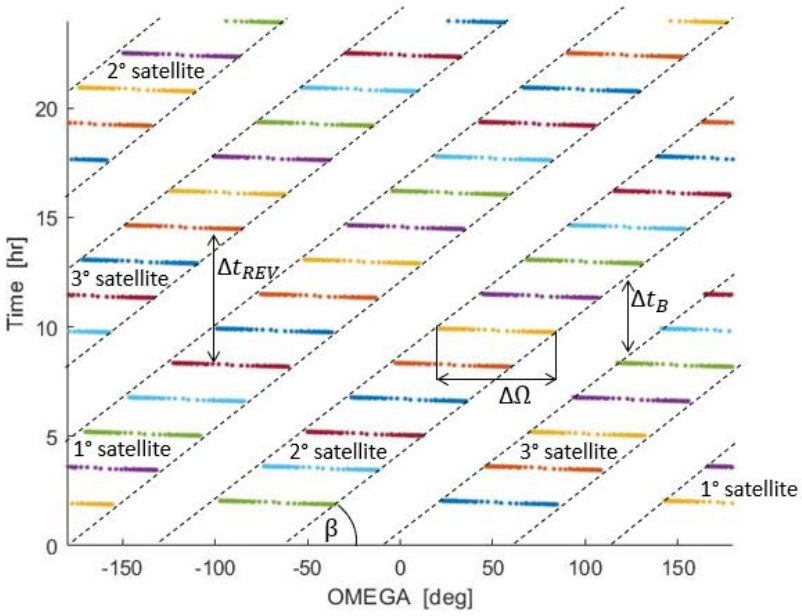

Figure 4.14: Map for visibility of (3/3/0) satellite constellation (h=500 km, i=50 deg, ε=45 deg, λ_c=50 deg).

The maximum revisit time for such constellations can be computed, as for a single satellite, based on Equation (4.27) [50]. The first term is the time between straight-line envelopes of the nearest coverage belts, which are formed by adjacent satellites and it can also be computed using the corresponding longitude gap:

$$\Delta t_B = \Delta\Omega_{REV}\tan(\beta) = \left(\frac{2\pi}{T} - \Delta\Omega(\lambda_c, i, \theta)\right)\tan(\beta) \tag{4.33}$$

It should be noted that the term Δt_B is independent form the phase shift between the satellite positions in the orbital planes and defined only by the total number of satellites T and

$$\Delta\Omega_{REV} = \frac{2\pi}{T} - \Delta\Omega \tag{4.34}$$

If $\Delta\Omega_{REV}$ is a multiple of $\Delta\phi_1$, then the second term in Equation (4.27) is $\delta t = T_{period}$ (see Figure 4.9), in the opposite case, there is a residue of division:

$$\delta\Omega = \Delta\Omega_{REV} - \Delta\phi_1\left[\frac{\Delta\Omega_{REV}}{\Delta\phi_1}\right] \tag{4.35}$$

where $[^o]$ is the integer part function [50]. Then,

$$\delta t = 2T_{period} - \left(\frac{\delta\Omega}{\Delta\phi_1}\right)T_{period} \tag{4.36}$$

For the satellite constellation with a non-zero phase shift $F \neq 0$, the in-plane phase

shift of satellites is defined as:

$$\Delta\lambda = \left(\frac{2\pi}{T}\right) F \tag{4.37}$$

and the value

$$\Delta\Omega^*_{REV} = \Delta\Omega_{REV} + \left(\frac{\Delta\lambda}{2\pi}\right) \Delta\phi_1 \tag{4.38}$$

must be used in Equation (4.35) instead of $\Delta\Omega_{REV}$.

Double non overlapping coverage belts

A more complex case is for the points with the latitudes $\lambda_c < i - \theta$. The maps include double coverage belts for each satellite [50] and an example is presented in Figure 4.15 for double non-overlapping coverage belts.

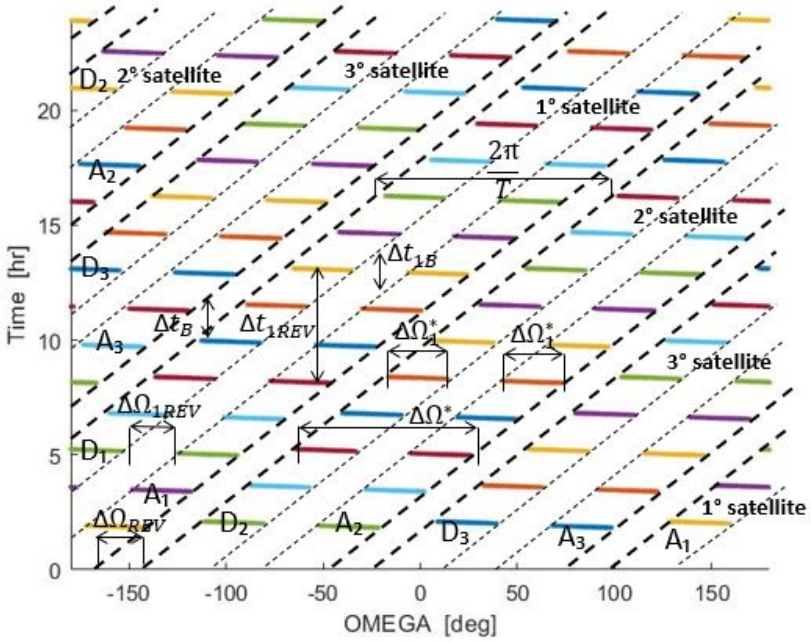

Figure 4.15: Map for visibility of (3/3/0) satellite constellation (h=500 km, i=50 deg, ε=45 deg, λ_c=45 deg).

For the case of:

$$\Delta\Omega^* = 2\Delta\Omega^*_1 + \Delta\Omega_{1REV} < \frac{2\pi}{T} \tag{4.39}$$

there are two gap types [50]:

1. Between double coverage belts with an external longitude gap of $\Delta\Omega_{REV}$,
2. Inside each double coverage belt with an inner longitude gap of $\Delta\Omega_{1REV}$

The revisit times can be computed from Equations (4.27), (4.28), (4.32), (4.37) and (4.38). The inner gap type corresponds to the zero phase shift and the revisit time for the constellation is the maximum from the times [50].

Double overlapping coverage belts

Another case is the constellations with overlapping coverage belts, that is, one coverage belt of a satellite is placed inside the inner longitude range $\Delta\Omega^*$ for another satellite [50]; an example is presented in Figures 4.16 and its zoomed view 4.17.

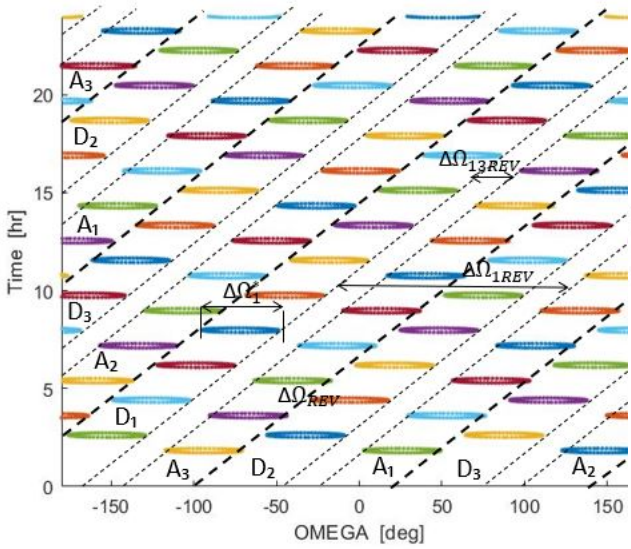

Figure 4.16: Map for visibility of (3/3/0) satellite constellation (h=1100 km, i=86 deg, ε=10 deg, λ_c=10 deg).

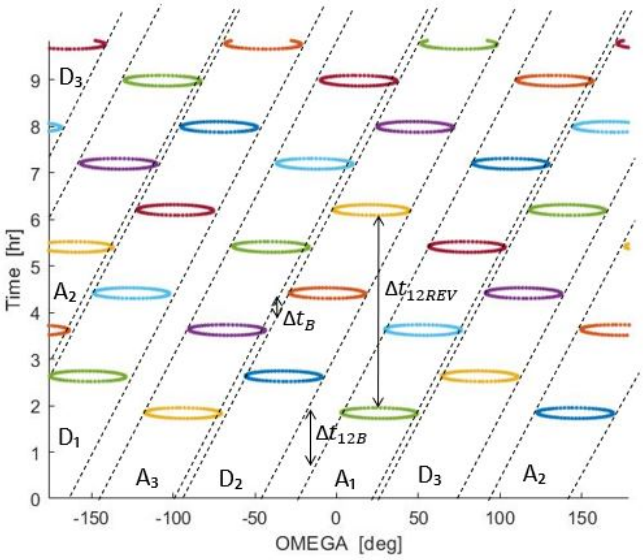

Figure 4.17: Map for visibility of (3/3/0) satellite constellation (h=1100 km, i=86 deg, ε=10 deg, λ_c=10 deg) zoomed.

Here, as shown in the created coverage belts, there are also two gap types between corresponding parts of the double coverage belts; as in the case of non-overlapping double coverage belts, the revisit times can be computed from Equations (4.27), (4.28), (4.32), (4.37) and (4.38); exceptions are related with δt from Equation (4.33). The phase shifts $\Delta\lambda$ depends on the combination of the adjacent coverage belts: for similar passes (i.e. ascending passes A_j - A_k or descending passes D_j - D_k) Equation (4.34) must be used, while for different passes (i.e. ascending and descending passes A_j - D_k or D_j - A_k) it is [50]:

$$\Delta\lambda = \left(\frac{2\pi}{T}\right) F + |u_{DN}(\lambda_c, i, \theta) - u_{AN}(\lambda_c, i, \theta)| \tag{4.40}$$

where u_{DN} and u_{AN} are the arguments of latitude of the boundary points from Equations (4.19) and (4.17) respectively.

In the general case of more than one satellite per orbital plane, it must be used:

$$\Delta\phi_1 = \frac{\omega_{Earth} T_{period}}{S} \tag{4.41}$$

Where $S \geq 2$ is the number of satellites per plane.
The boundaries of the second term of Equation (4.27) are:

$$\frac{T_{period}}{S} \leq \delta t \leq \frac{2T_{period}}{S} \tag{4.42}$$

with T_{period} being the orbital period.

As presented in Figure 4.13 for the case of one single satellite, in Figure 4.18 the diagram created for longitude ranges of the coverage belt envelopes for a constellation made of 3 satellites is shown.

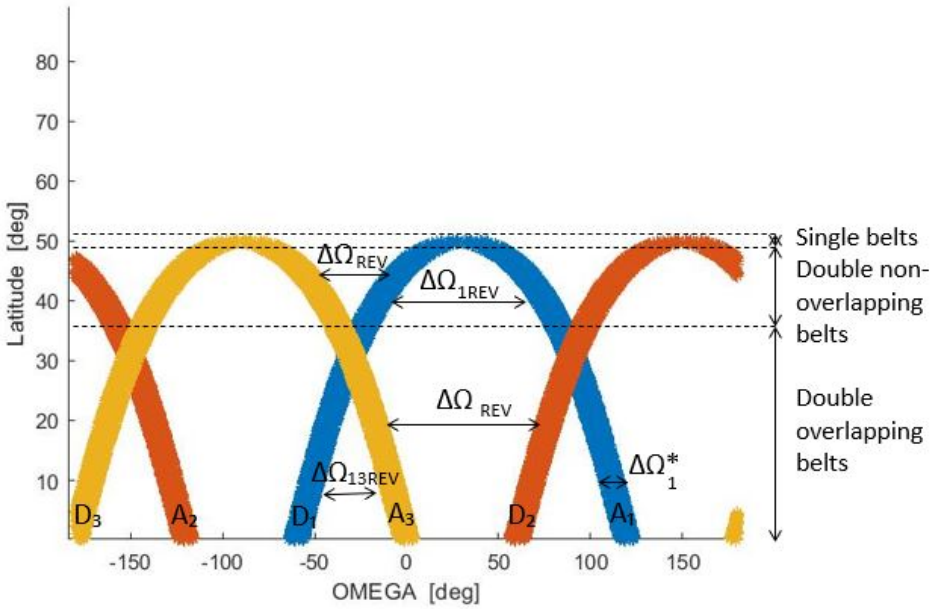

Figure 4.18: Longitude ranges of 3-satellite constellation.

4.3 Geometrical approach for short revisit times

The geometric approach here described considers both full and partial coverage of specific regions of the Earth's surface and is suitable for satellite constellations that allows short revisit times (less than one orbital period). However, this method can also be applied if continuous coverage is desired [51].

The key idea of the method is a two-dimensional space application for maps of the satellite constellation and coverage requirements. As presented in Section 4.2, the space dimensions are Ω and the argument of latitude u. The visibility requirements can be presented as a region (coverage region or coverage area), while any satellite constellation with a number of orbital planes and an equal number of satellites in each plane can be presented as a uniform moving grid, where the satellites are the vertices of the grid. A satellite trajectory in the introduced two-dimensional space for time intervals on the order of several orbital periods is a straight line parallel to the y axis. An example of such grids for Walker-type constellations is shown in Figure 4.19, that represents the Globalstar constellation described in Section 2.4. For time intervals more than several orbital periods, a similar map can also be produced, but the regression of the ascending node due to J_2 effect should perhaps be considered. In this latter case, the lines are slightly inclined to the y axis but as stated before, the current analysis does not take into account such effect.

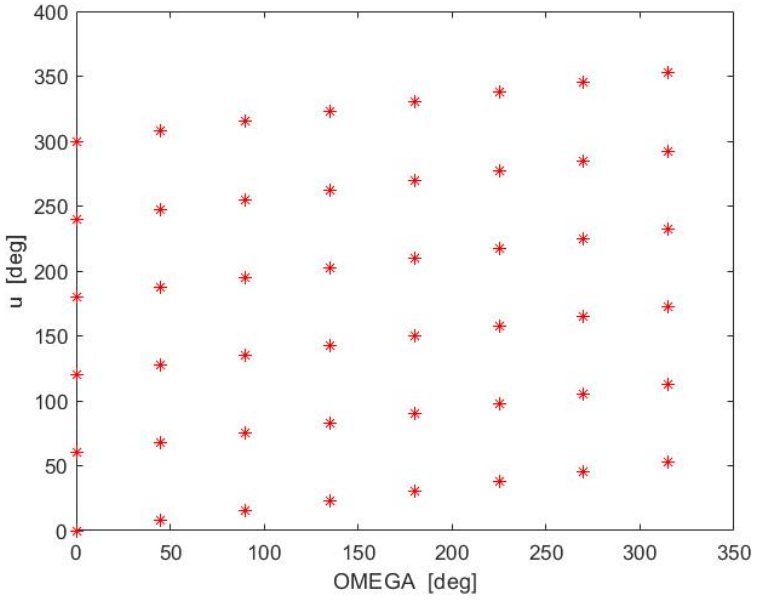

Figure 4.19: Map of the Globalstar (48/8/1) constellation.

As example of local coverage, consider full coverage of a geographical region by a satellite. It implies that the region is completely within the instantaneous access area of the satellite; this area represents the entire surface of the Earth that can be viewed for a minimum elevation angle, at this time. Such cases can be called full region coverage (see Figure 4.20). The next case is the partial region coverage, i.e. only a part of the region is within the access area (see Figure 4.21) [51].

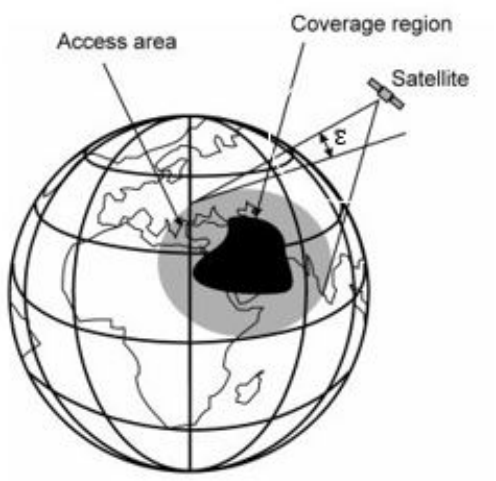

Figure 4.20: Geometry of full coverage [51].

Figure 4.21: Geometry of partial coverage [51].

Each region can be presented as a discrete set of inner and boundary points. For the full region coverage, the coverage function $f(\Omega,u)$ is the intersection of the regions, as in Figure 4.22, and for the partial region coverage, it is the union of the regions, as in Figure 4.23.

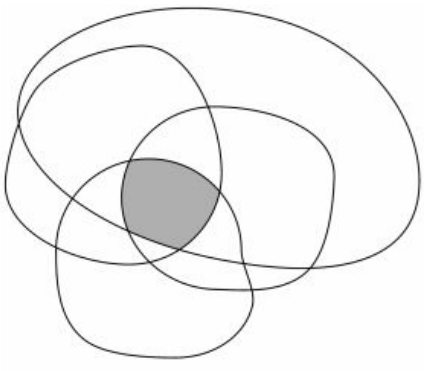

Figure 4.22: Intersection of the regions [51].

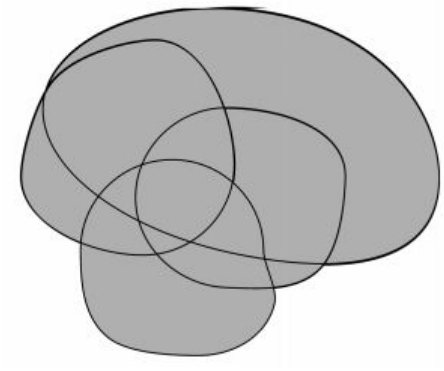

Figure 4.23: Union of the regions [51].

As for the method presented in the previous Section 4.2, the further optimisation process is limited to symmetric Walker-type constellations, with the standard notation $(T/P/F)$. In addition, this approach is based on the assumptions that the Earth is a perfect round body, all satellites in a constellation are at the same altitude, with the same

number of satellites in each orbit plane and all orbit planes in a constellation have the same inclination. Furthermore, it is assumed that the orbit inclination i, altitude h and minimum elevation angle ε are specified [51].

In order to better understand the geometry behind this method, the first case analysed involves continuous coverage of a specific location, then this explanation is going to be extended also to the case of discontinuous coverage.
Since the satellite constellation motion can be presented as a uniform moving grid, in order to achieve continuous coverage, at any time at least one grid vertex must belong to the region in the (Ω, u) space. The grid should also satisfy integer-value constraints for the number of orbit planes and satellites per plane and the optimal configuration of the satellite corresponds to the maximum sparse grid (i.e. minimum number of satellites). In the case of discontinuous coverage, the region should be examined with a revisit time [51]. The values of Ω and u necessary to determine the boundaries of the coverage region are given by the analytical Equations (4.23) and (4.22).

The dimensions that must be respected by the grid of the satellite constellation are reported in Figure 4.24.

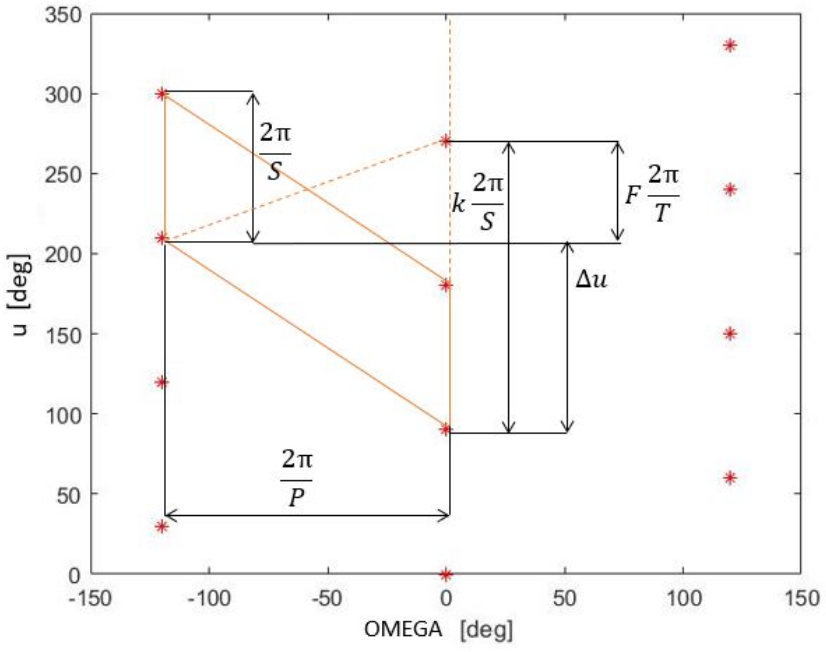

Figure 4.24: (12/3/2) Dimensions of the grid.

It is assumed that $f(\Omega,u)$ map is a convex region; all of the grid cells are the same parallelograms (see Figure 4.24) with the sides equal to:

- $\frac{2\pi}{P}$ along the x axis;
- $2\pi\frac{T}{P} = \frac{2\pi}{S}$ along the y axis.

The slope angle is Δu in units of $\frac{2\pi}{T}$.

It follows that one grid cell only can be considered. The optimal constellation with the minimum number of satellites corresponds to the maximum area parallelogram that can be placed (or inscribed for the limit case) into the region, as shown in Figure 4.25.

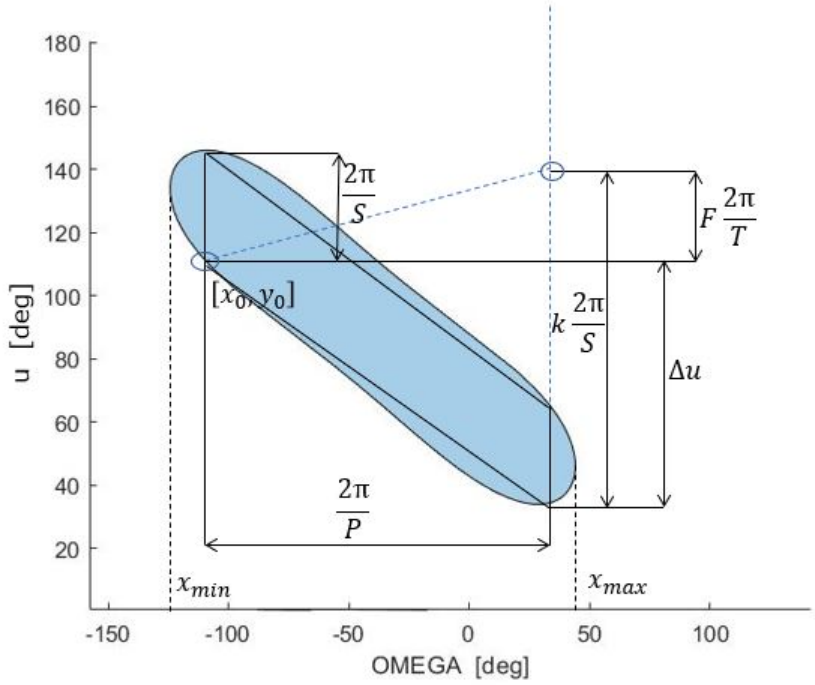

Figure 4.25: Geometry of optimal grid.

For the slope angle, the following inequality must be satisfied [51]:

$$(k-1)\left(\frac{2\pi}{S}\right) \leq \Delta u = m\left(\frac{2\pi}{T}\right) \leq k\left(\frac{2\pi}{S}\right) \tag{4.43}$$

where k and m are integer values. The phasing parameter is:

$$F = \frac{k(\frac{2\pi}{S}) - m(\frac{2\pi}{T})}{\frac{2\pi}{T}} = kP - m \tag{4.44}$$

An enumerative approach then follows: specify the maximum number of orbital planes P_{max} and satellites per plane S_{max} and a current optimal number of satellites

$T = P_{max} \cdot S_{max}$. For each boundary point of the region $[x_o, y_o]$ construct all of the possible parallelograms. Determine the minimum value of P as [51]:

$$P = \left[\frac{2\pi}{(x_{max} - x_{min})} \right] + 1 \tag{4.45}$$

where $[^o]$ rounds toward minus infinity and x_{max}, x_{min} are extreme values of the region in Figure 4.25. The potential values of $P_{max} \geq P \geq P_{min}$ are examined in increasing order. For a selected value of P, all of the possible numbers of satellites per orbital plane $S_{max} \geq S \geq S_{min}$ and Δu are considered. A corner point of the parallelogram coincides with a boundary point of the region. If all other corner points with coordinates

- $[x_o + \frac{2\pi}{P}$, y_o - $\Delta u]$
- $[x_o + \frac{2\pi}{P}$, y_o - $\Delta u + \frac{2\pi}{S}]$
- $[x_o$, $y_o + \frac{2\pi}{S}]$

are inside of the region, then there exists an acceptable constellation because the region is a convex hull. The *Inpolygon* function [52], used by the author, is available on the Mathworks website. If the value of T is determined to be larger than a previous value of T_{min} computed for a previous boundary point, then the constellation can not be optimal and is discarded. On the other hand, if the value of T is smaller than the current value of T_{min}, then the previous optimal constellation can not be minimal and is discarded.
For this solution type, the maximal multiplicity of coverage is quadruple. Allowable solution type is also an inscribed parallelogram with an angle of Δu that is not divisible evenly by $\frac{2\pi}{T}$. In this case, there is a set of constellations with an arbitrary phase parameter F; but for the last solution type, the maximum multiplicity of coverage can be less. As a solution rule, a distinction in the total number of satellites between these solution types is small.

In the case of discontinuous coverage, the polygon should be expanded along the y axis at an angle of ωt_{REV}, as shown in Figure 4.26, where t_{REV} is the maximum revisit time and ω the satellite's mean motion [51].

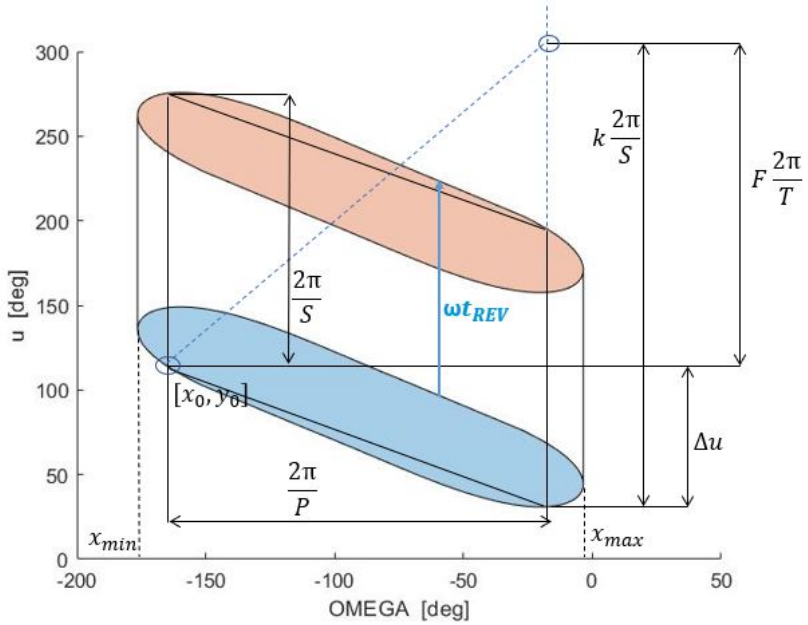

Figure 4.26: Parallelogram for discontinuous coverage.

As stated before, the algorithm is based on the determination of the boundary points of the region, equivalent to the boundary of the coverage circle of visibility, and their investigation in order to determine the optimal satellite configuration (i.e. maximum sparse grid). The detailed algorithm-like logic for the method is presented in Appendix C.4.

5. Numerical results: validation of the proposed methods

Once any method of analysis has been developed, it is necessary to establish how well that method actually performs in practice, which results it is capable to provide and how accurate they are. This process, whereby the performance characteristics of the method are established, is known as method validation.

5.1 Application and comparison of methods for continuous coverage

This section presents an analysis onto all the presented methods in the previous chapters that are suitable for continuous global or zonal coverage.

5.1.1 Beste and Adams and Rider analytical methods

The Beste [28] and Adams and Rider [24] methods, presented in Section 3.1 and 3.2 respectively, are purely analytical: they take as inputs some variables or constraints and give as outputs the optimal constellation configuration. The parameters required are reported in Table 5.1; both approaches are suitable for Street Of Coverage geometries, with a non-symmetric distribution of planes and satellites in polar orbits.

Table 5.1: Beste versus Adams and Rider comparison.

	Inputs	**Outputs**
Beste	h or θ, ε, desired level of coverage, S	T, P
Adams and Rider	h or θ, ε, desired level of coverage	S, T, P

It must be highlighted that, to achieve the desired configuration, the methods must be applied by varying the input values each time, until they are properly tuned and the final result has been reached.

If the requirement is to achieve single coverage of the entire Earth, Street Of Coverage satellite constellations have been determined with different combinations of parameters. By means of the Beste method, some of the results obtained by considering a wide range of combinations of S and h/θ are reported in Table 5.2, with S varying from 3 to 10.

Table 5.2: Beste: requirements for single coverage of the entire Earth (ε=10 deg).

θ [deg]	h [km]	S	P	T	$\frac{PS\Gamma}{4\pi}$
66.7	20925	3	2	6	1.81
57.6	10105	4	2	8	1.86
42.3	3893	5	3	15	1.95
38.7	3139	6	3	18	1.97
30.8	1919	7	4	28	1.97
28.9	1693	8	4	32	1.99
24.2	1216	9	5	45	1.98
23.0	1111	10	5	50	1.99

By defining Γ as the solid angle corresponding to the circle θ given by $\Gamma = 2\pi(1-\cos(\theta))$, the last column of Table 5.2 gives the ratio of the total solid angle covered by all satellites to 4π steradians. Note that in all cases this ratio is nearly equal to 2; the implication is that the coverage averaged over the entire sphere is double. The result, which holds for ratios $\frac{S}{P}$ in the approximate range of 1.3 to 2.2, leads to the formulation presented in Section 3.1 for specifying the relationship between the number of satellites and their orbital configurations and coverage requirements $T_{Beste-1fold}$ of Equation (3.5). The same results have been obtained also with the Adams and Rider method (see Table 5.3), but this time the number of satellites per plane S has become an output.

Table 5.3: Adams and Rider: requirements for single coverage of the entire Earth (ε=10 deg).

θ [deg]	h [km]	S	P	T	$\frac{PS\Gamma}{4\pi}$
66.7	20925	3	2	6	1.81
57.6	10105	4	2	8	1.86
42.3	3893	5	3	15	1.95
38.7	3139	6	3	18	1.97
30.8	1919	7	4	28	1.97
28.9	1693	8	4	32	1.99
24.2	1216	9	5	45	1.98
23.0	1111	10	5	50	1.99

The same approach could be used even for multiple coverage of the whole Earth as well as for coverage beyond a specified latitude.
Several results for coverage of polar regions extending to latitude $\lambda = 30$ deg are here reported by means of the Beste (see Table 5.4) and Adams and Rider (see Table 5.5) methods.

Table 5.4: Beste: requirements for single coverage of polar regions extending to λ=30 deg (ε=10 deg).

θ [deg]	h [km]	S	P	T	$\frac{PST}{4\pi}$
64.1	16549	3	2	6	1.69
53.4	7650	4	2	8	1.62
48.1	5508	5	2	10	1.66
35.8	2632	6	3	18	1.70
33.3	2253	7	3	21	1.72
26.8	1466	8	4	32	1.72
25.3	1318	9	4	36	1.73

Table 5.5: Adams and Rider: requirements for single coverage of polar regions extending to λ=30 deg (ε=10 deg).

θ [deg]	h [km]	S	P	T	$\frac{PST}{4\pi}$
64.1	16549	3	2	6	1.69
53.4	7650	4	2	8	1.62
48.1	5508	5	2	10	1.66
35.8	2632	6	3	18	1.70
33.3	**2253**	**6**	**4**	**24**	**1.97**
26.8	1466	8	4	32	1.72
25.5	**1318**	**8**	**5**	**40**	**1.92**

As it can be noted, the results are nearly the same; some small discrepancies are caused by the choice of approximation to an integer value for the S, P and T in the computations. In fact, the parameter S is given at the beginning as an integer in the Beste approach, then T is determined through the aforementioned Equation (3.5) and $P = \frac{T_{Beste}}{S}$. Once the two values have been found, the second is rounded toward the nearest integer and the final T is determined with the approximated P.
On the other hand, the Adams and Rider method provides as outputs all S, P and T, so common sense and reasoning led to the decision to round both S and P toward the nearest integer and to determine $T = P \cdot S$ consequently. This decision appeared to be the most suitable in order to do not prefer always a higher number of satellites per plane and lower number of planes or vice-versa. However, by looking at the fractional part of the resulting values, a different choice could be made.

Lastly, the case of polar satellite constellations for triple coverage is analysed. A direct comparison can be performed only for this requirement, since Beste studied exclusively such condition for multiple coverage, while the procedure of Adams and Rider is capable to provide results for generic n-fold coverage.
Results achieved by means of the Beste method are reported in Table 5.6.

Table 5.6: Beste: requirements for triple coverage of the entire Earth (ε=10 deg).

θ [deg]	h [km]	S	P	T	$\frac{PST}{4\pi}$
70.3	30901	5	3	15	4.97
63.9	16272	6	3	18	5.04
61.1	13013	7	3	21	5.43
48.3	5575	8	4	32	5.36
41.1	3624	9	5	45	5.54
35.8	2632	10	6	60	5.67

With the requirement of triple coverage, the ratio of the total solid angle of coverage of all satellites to 4π steradians remains close to 5.5; in other words, a point is in view of 5.5 satellites on the average when this average is taken over the entire Earth.

The application of Adams and Rider method, with *j=3*, *k=1* and so *n=3* gives the configurations listed in Table 5.7.

Table 5.7: Adams and Rider: requirements for triple coverage of the entire Earth (ε= 10 deg).

θ [deg]	h [km]	S	P	T	$\frac{PST}{4\pi}$
70.3	**30901**	**8**	**2**	**16**	**5.97**
63.9	**16272**	**9**	**2**	**18**	**5.60**
61.1	**13013**	**10**	**2**	**20**	**5.17**
48.3	**5575**	**13**	**2**	**26**	**4.35**
41.1	**3624**	**15**	**3**	**45**	**5.54**
35.8	**2632**	**17**	**4**	**68**	**4.82**

Again, there exist discrepancies in the results, this time more evident mainly because of the triple coverage requirement: indeed, the choice to have j multiple coverage factor in the same orbital plane equal to 1 and k multiple coverage factor in different orbital planes equal to 3 is the major cause, since it changes the obtained S and P accordingly to the equations:

$$S = \frac{2}{\sqrt{3}} j \frac{\pi}{\theta} \tag{5.1}$$

$$P = \frac{2}{3} k \frac{\pi}{\theta} \tag{5.2}$$

Anyway, this decision has revealed to be the more suitable, since *j=3* and *k=1* would have required to place satellites in a lot of different orbital planes, less convenient considered that launching into polar orbits is quite cost demanding: in fact, since launch vehicle performance is usually dependent upon both orbital altitude and inclination, it may be usually desirable to reduce orbital inclination so as to achieve a higher altitude orbit with a specified launched vehicle and fixed satellite weight [48]. Instead, if only the results for

the total number of satellites T given by equations (5.3) and (5.4) would have been taken into account (by selecting directly n=3), the numbers would have been nearly the same, as reported in Table 5.8.

$$T_{Beste-3fold,\lambda} \approx \frac{11\cos\lambda}{1-\cos\theta} \tag{5.3}$$

$$T_{A\&R} \approx \frac{4\sqrt{3}}{9} n \left(\frac{\pi}{\theta}\right)^2 \tag{5.4}$$

Table 5.8: Beste versus Adams and Rider triple coverage comparison.

θ [deg]	$T_{Beste-3fold,\lambda}$	$T_{A\&R}$
70.3	16.59	15.14
63.9	19.64	18.32
61.1	21.29	20.04
48.3	32.86	32.07
41.1	44.64	44.30
35.8	58.22	58.38

Two interesting applications examples of these two analytical methods are represented by the existing near-polar constellations:

- Iridium (described in Section 2.4): the Adams and Rider method for single world-wide visibility with altitude h=780 km and ε=10 deg gives an optimal configuration made of 66 satellites, 11 in each of the 6 orbital planes, that are exactly the Iridium characteristics;

- Teledesic concept (presented in Section 2.4): the Beste approach applied for single visibility at altitude h=700 km and ε=28 deg gives a total number of satellites T=288, divided in the P=12 orbital planes.

To better understand the general features and the major differences between the two analysed approaches, the total number of satellites T required has been plotted in function of a varying altitude, both for single and triple whole Earth coverage (the trend would have been the same even for coverage beyond a specified latitude).
For h spacing from 500 km until 50000 km and single coverage requirement, Figure 5.1 and its zoomed view on Figure 5.2 show the trend.

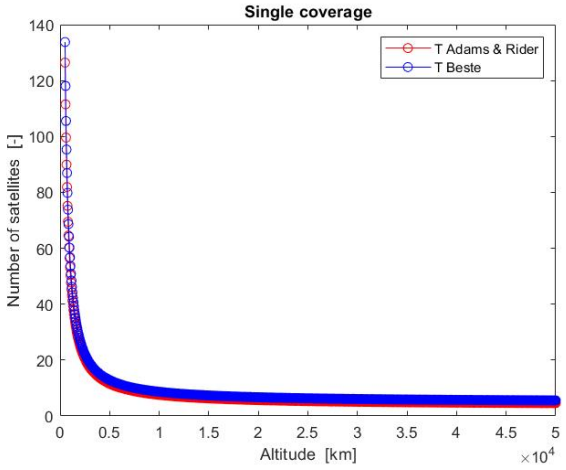

Figure 5.1: T versus h single coverage.

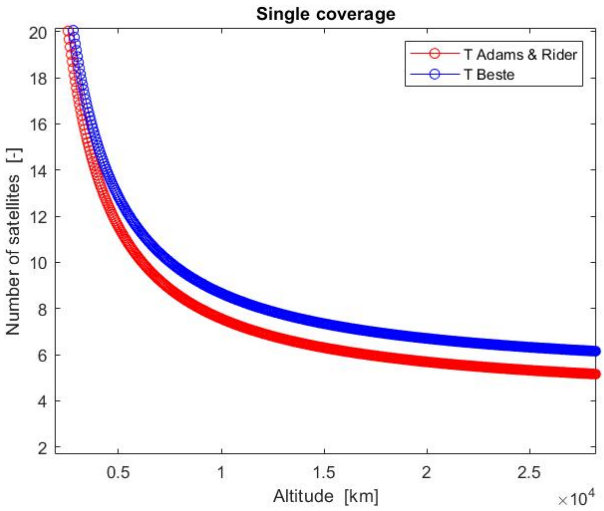

Figure 5.2: T versus h single coverage zoomed.

As it can be noted, the obtained numbers are nearly identical; however, the Adams and Rider method gives a slightly lower number of T satellites required to achieve single coverage of the entire Earth and this difference increases as far as altitude values increase, becoming quite evident starting at h=1000 km yet.
By looking now at triple coverage requirement, Figures 5.3 and 5.4 (zoomed view) show the results.

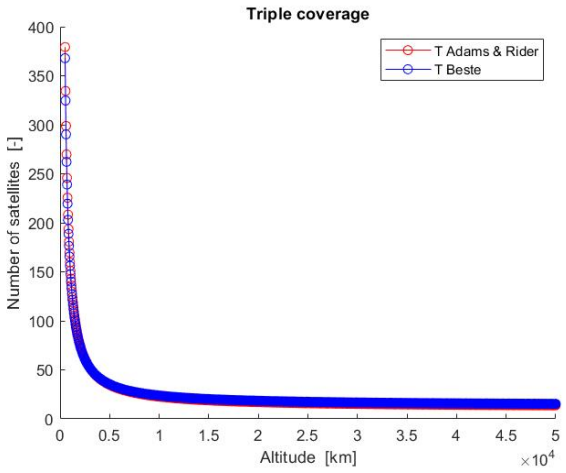

Figure 5.3: T versus h triple coverage.

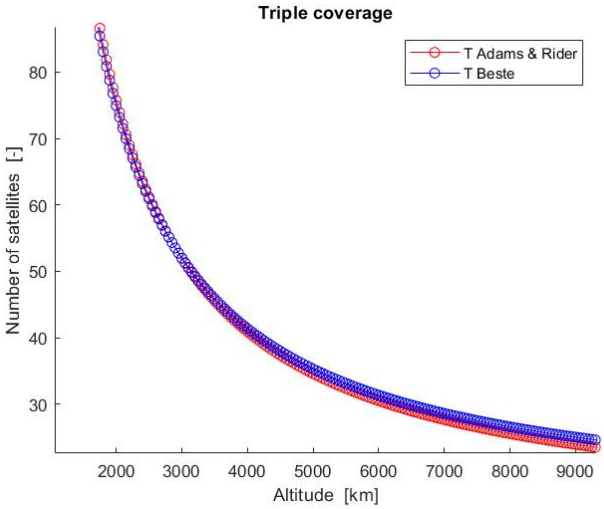

Figure 5.4: T versus h triple coverage zoomed.

Here, on the contrary, Adams and Rider provides a higher number of T for low altitudes, while starting from $h \approx$3000 km, the trend reverses and Adams and Rider requires less satellites than Beste.

Summarising, both the methods can be used for the design of SOC satellite constellations, but it must be kept in mind that the Beste method [28] requires an additional input

parameter (the number of satellites per plane S), that shall be guessed at the beginning of the procedure. In addition, the charts guide toward the decision of adopting the Adams and Rider method if single whole Earth coverage is required (see Figures 5.1 and 5.2) or for triple whole Earth coverage at altitudes higher than 3000 km (see Figures 5.3 and 5.4), and the Beste method if the objective is to achieve triple whole Earth coverage at lower altitudes (see Figures 5.3 and 5.4).

5.1.2 Walker and Lang numerical methods

The Walker circumcircle method, presented in Section 3.3, is validated first, by applying the algorithm to constellations characterised by circular, common-period orbits all having the same inclination and uniformly distributed in a right ascension angle, so with symmetric pattern.

To determine an optimised constellation for world-wide coverage, this approach is based on a trial-and-error process: the algorithm takes as inputs the analysed constellation in terms of $(T/P/F)$ and i, the altitude h and the minimum acceptable elevation angle ε. The value of the largest possible great circle range θ is used as performance index, so, for a selected constellation, once chosen a set of common-altitude orbits that guarantee a minimum elevation angle sufficiently high, the goal is to minimise the maximum value of θ; the best result obtained represents the optimal satellite constellation configuration.

An exhaustive search has been conducted to find the best single-visibility constellation for T from 5 to 15 satellites with the correspondent number of planes P and phasing parameter F. The chosen total period of propagation corresponds to one orbital period, with a time step of 10 seconds. Table 5.9 shows the different combinations of $(T/P/F)$ with orbit inclinations i and altitudes h which produce the smallest θ_{MAX}, compared with the computed θ through Equation (5.5) for a minimum elevation angle ε=10 deg. The CPU time is also reported in the last column [(1)].

[(1)] Intel(R) Core(TM) i7-1065G7 CPU @ 1.30 GHz

Table 5.9: Best single visibility constellations with ε=10 deg.

T	P	F	h [km]	i [deg]	θ [deg]	θ_{MAX} [deg]	CPU time [s]
5	5	1	26992	43.66	69.15	62.22	46.44
6	6	4	20371	53.13	66.42	55.77	100.06
7	7	5	12220	55.69	60.26	49.27	126.17
8	8	6	9388	61.86	56.52	43.85	206.35
9	9	7	8381	70.54	54.81	36.92	321.01
10	10	7	6799	47.93	51.53	43.42	462.53
11	11	4	5345	53.79	47.61	37.23	613.46
12	3	1	5440	50.73	47.90	39.70	687.90
13	13	5	4248	58.44	43.76	33.58	1153.57
14	7	11	3814	53.98	41.96	31.85	1224.60
15	3	1	3852	53.51	42.13	36.00	1830.12

To find the θ_{MAX}, the satellite positions are computed at small time intervals; at each time interval, all combinations of three satellites are examined and the radius of the spherical circle which contains them is determined. The largest circumcircle over all time intervals which does not include another satellite is equal to the size of the central angle of coverage that is necessary to achieve continuous global coverage. To optimise the constellation, satellite parameters such as inclination are varied in order to minimise the required central angle of coverage; once selected altitude and minimum elevation angle, the value of θ is determined and in order to have acceptable conditions must be $\theta_{MAX} < \theta$. The accuracy of this method depends on the size of the time steps; additionally, as the number of satellites T increases, the number of combinations of three satellites at each time step $\frac{T\times(T-1)\times(T-2)}{3!}$ increases dramatically. For example, a (5/5/1) constellation involves a search among 358'092 cases to be investigated and a (15/3/1) constellation requires 2'576'256 cases over the entire period of propagation.
For these reasons, the circumcircle method is computationally demanding in terms of CPU time for constellations containing large numbers of satellites and this must be added to the need of a trial-and-error process in which both altitude h and inclination i must be guessed and varied in order to minimise θ_{MAX}.

For two-fold coverage, the largest circumcircle which includes one satellite is sought, and so on for multiple folds of coverage. What stated for long CPU times is always valid.

By moving now to the Lang method, the algorithm allows the optimisation of non-polar, symmetric constellations of circular orbit satellites for continuous global coverage. Such approach can deal with constellations of as many as 100 or more satellites providing single through four-fold coverage. The Lang method came historically later than the Walker method and, mainly because it relies in some simplifying assumptions described in Section

3.4, it is much faster in terms of computational time.

The constellation optimisation problem is uncoupled from altitude and elevation angle considerations, by using the coverage circle θ as the primary independent variable. For constellations of T circular orbit satellites, the goal is to find the arrangement which requires the smallest value of θ and still achieves continuous global coverage.
T satellites are propagated in time over an Earth containing a set of test points; the smallest value of θ is then determined which ensures that all test points are visible to at least n satellites (where n is the desired multiplicity of coverage) for all times.

In order to determine an optimised constellation for world-wide coverage, this approach is based on a trial-and-error process: the algorithm takes as inputs the analysed constellation in terms of $(T/P/F)$ and i and the minimum acceptable elevation angle ε.
The value of the great circle range θ is used as performance index, so, for a selected constellation and once chosen a certain inclination, the goal is to find the lowest required value of θ that allows the lowest operating altitude (conversely, it would also have been possible to fix a certain altitude and to consequently find the maximum operating limits in terms of ε).

With respect to the Walker method, that requires a search both in terms of optimal inclination i and altitude h, Lang involves a trial-and-error phase in terms of inclination only: the optimised altitude becomes an output of the algorithm.

For a number of cases between 30 and 100 satellites, the computer program was run to find the most efficient arrangements in terms of $(T/P/F)$ and i; for each value of T the best constellations (i.e. lowest θ) are summarized for single coverage in Table 5.10 .

Table 5.10: Best single visibility constellations with ε=0 deg.

T	P	F	i [deg]	θ [deg]	h [km]	CPU time [s]
21	7	3	61.3	36.29	1535	9.22
22	22	6	58.4	35.18	1426	9.58
23	23	14	58.8	34.58	1369	8.77
24	6	1	58.4	35.44	1451	9.05
25	25	7	61.2	34.15	1329	9.44
26	26	16	59.7	33.03	1230	8.52
27	9	5	60.0	32.56	1190	9.26
28	7	2	59.1	32.89	1217	9.27
29	29	25	75.1	32.12	1153	9.41
30	10	6	60.7	31.45	1099	8.46
40	20	15	73.4	27.65	822	9.43
50	25	20	72.9	24.63	638	9.52
60	20	14	68.5	22.28	515	8.46
70	70	64	80.3	20.96	452	43.10
80	40	33	72.5	18.60	352	45.91
90	45	38	74.1	18.14	334	43.44
100	50	43	74.6	16.82	285	43.28

As it can be noted from Table 5.10, in general the larger is the value of θ, the lower is the optimal inclination.
In addition, the computational time does not increase as the number of satellites T increases: this is due to the fact that CPU time directly depends on the dimension of the grid of points built on the planet surface (and so on the number of test points contained), that is strictly related to the number of repeated groundtracks of a particular constellation and on its symmetry properties; two examples can be observed in Figures 5.5 and 5.6.

- Figure 5.5 represents the (60/20/14) constellation with i=68.5 deg; the number of independent Groundtracks is 60 and so the grid scans 3 deg in longitude and 90 deg in latitude for global coverage. As consequence, the number of test points, with a spacing of 1 deg, is equal to 270.

- Figure 5.6 represents the (90/45/38) constellation with i=74.1 deg; this time, the number of independent groundtracks is 18 and so the grid scans 10 deg in longitude and 90 deg in latitude for global coverage. As consequence, the number of test points is equal to 900.

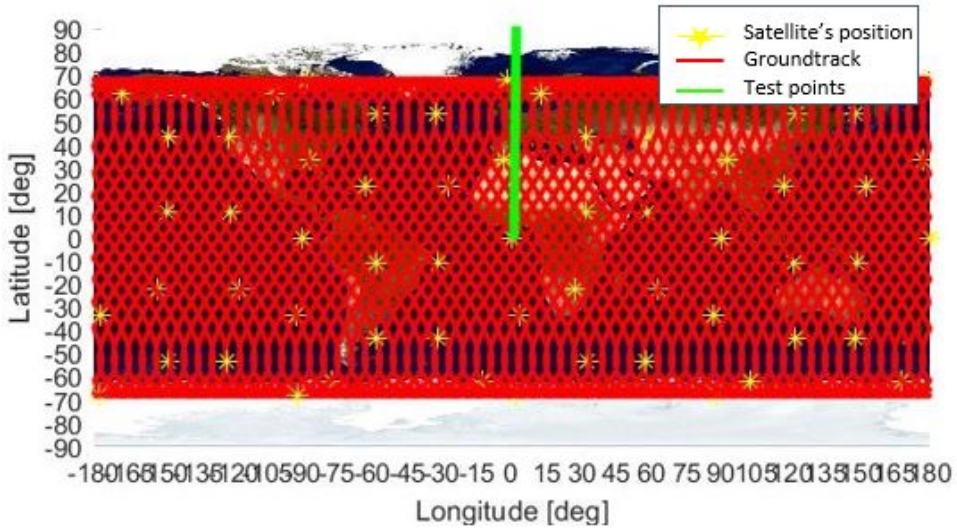

Figure 5.5: "8-shaped" groundtrack for (60/20/14).

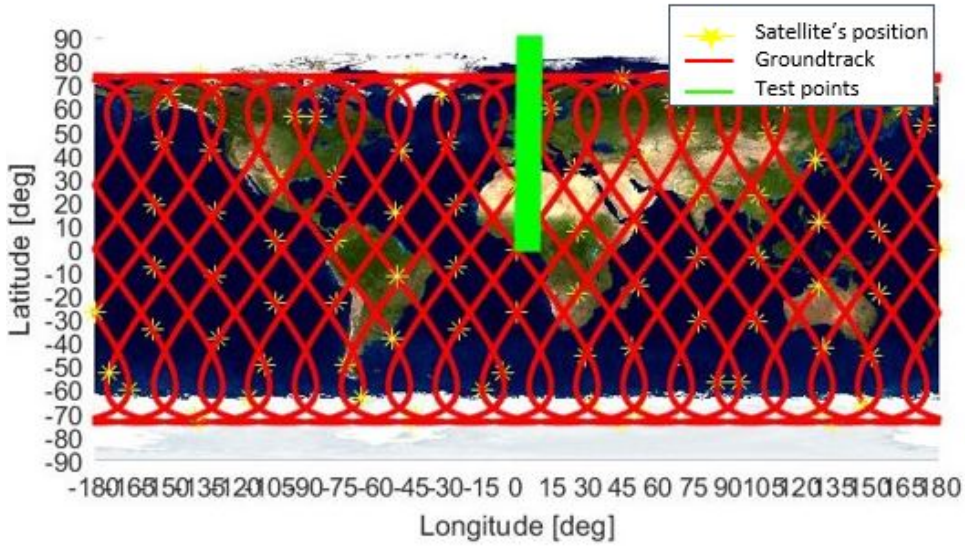

Figure 5.6: "8-shaped" groundtrack for (90/45/38).

Indeed, by looking at the last column of Table 5.10, the computational time increases considerably from the case (60/20/14) to (90/45/38) because of the increasing number of satellites to be investigated, but mainly because of the dimensions of the grid of test points.

Two interesting examples are given by the existing Galileo and Globalstar constellations described in Section 2.4:

- Galileo is a (24/3/1), i=56 deg constellation deployed to achieve continuous global coverage of the Earth; indeed, the application of the Lang method proved that such configuration is optimal at an altitude of 23222 km, where the satellites are really placed; moreover, the number of independent "8-shaped" groundtracks is 8, with 90

deg in latitude and 22.5 deg in longitude as dimensions of the grid of test points. The "8-shaped" groundtrack and the respective grid are shown in Figure 5.7.

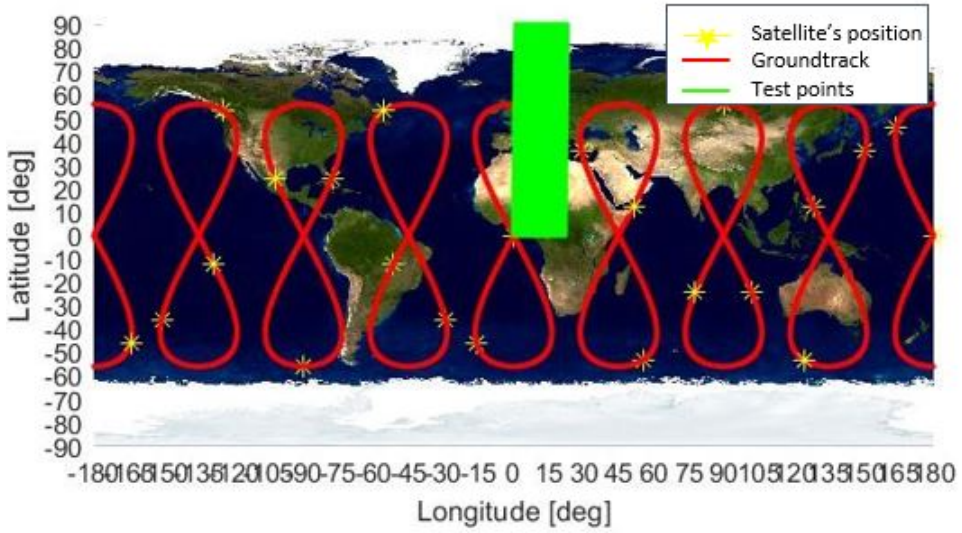

Figure 5.7: Galileo "8-shaped" groundtrack.

- Globalstar is a (48/8/1), i=52 deg constellation intended to provide continuous coverage between -70 deg and +70 deg latitude and not all around the globe: the resulting optimal altitude with Lang approach is 1414 km (as its actual value), but this time the dimensions of the grid of test points are 70 deg in latitude and 3.75 deg in longitude, with 48 independent groundtracks. The "8-shaped" groundtrack and the respective grid are shown in Figure 5.8.

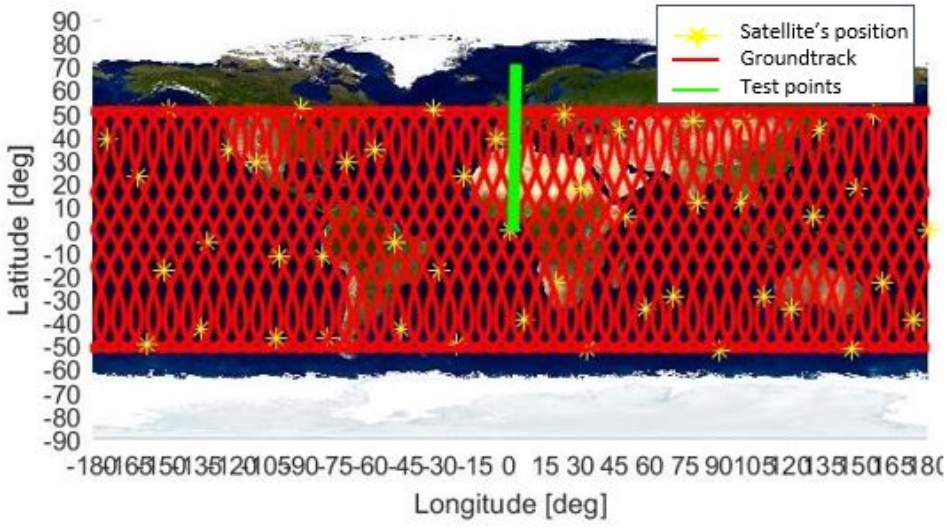

Figure 5.8: Globalstar "8-shaped" groundtrack.

From all the previous considerations, it could be said that the Lang method [48] is more performant and precise than the Walker circulcircle approach [27]: first of all, the computational time is substantially reduced, second, the Lang's method requires as inputs the $(T/P/F)$, i and ε, while Walker circumcircle method needs also the value of altitude h, hence an additional parameter that must be varied and tuned in order to find the optimal configuration. In fact, in Lang theory the altitude is determined as output and it automatically fits the other parameters.

A significant example for direct comparison of the two approaches could be provided by the GPS constellation presented in Section 2.4, with (24/6/2), i=55 deg, h=20200 km. Table 5.11 shows the more relevant results:

Table 5.11: Walker versus Lang comparison for GPS (ε=42 deg).

	θ **[deg] obtained**	h **[km]**	**CPU time [s]**
Lang	37.68	20196	53.40
Walker	35.67	**20200**	50'163.87

It is evident the large difference in computational time between the two methods: the Lang approach spent less than a minute to find the result, while Walker needed more than 13 hours to give the outputs. Indeed, the relatively high number of satellites T is responsible of such CPU time, however an important role is played also by the orbital period: since the altitude h is quite high, the period is long (equal to 11.98 hours) and so the number of instants of time to be investigated during the propagation increases considerably.
It must be highlighted that the value of altitude obtained with the Lang method is an output, that demonstrates how the selected altitude for the GPS constellation is the optimal one; on the other hand, this number is given as input to the Walker algorithm, assuming the optimality of the geometry is known yet.

A three dimensional representation of the GPS constellation is given in Figure 5.9 and the initial values of right ascension and mean anomaly for all satellites are shown in Figure 5.10. Instead, a direct comparison between the actual groundtrack and the "8-shaped" groundtrack used in the Lang method is possible by looking at Figures 5.11 and 5.12.

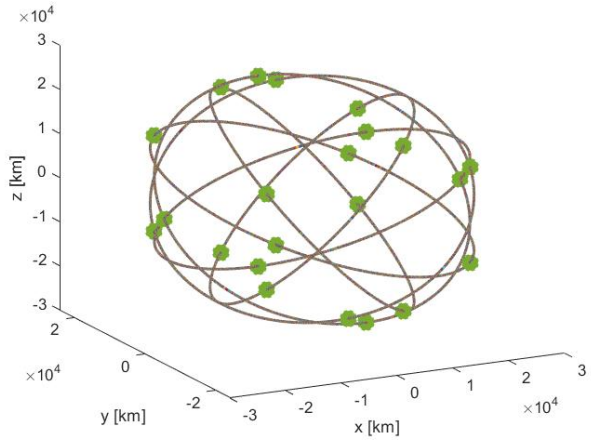

Figure 5.9: GPS 3 dimensional representation.

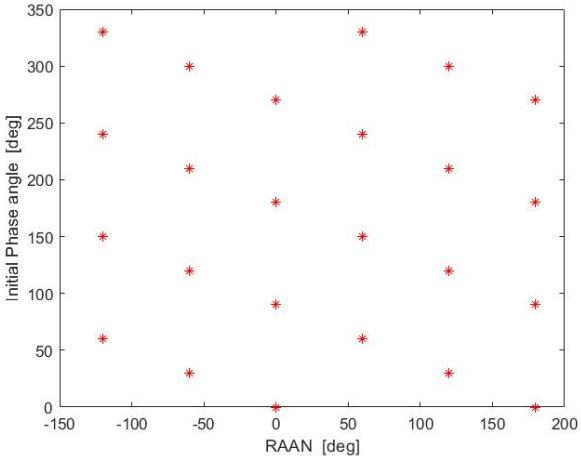

Figure 5.10: GPS Ω versus M.

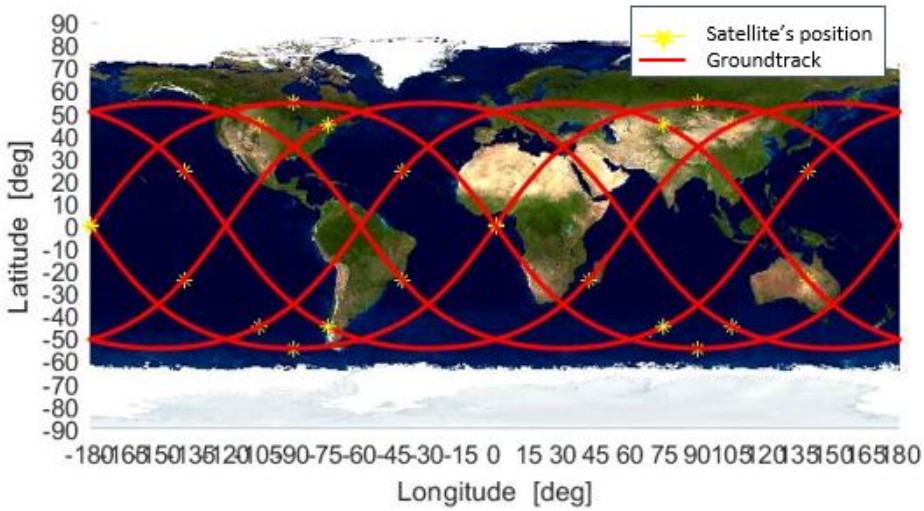

Figure 5.11: GPS groundtrack.

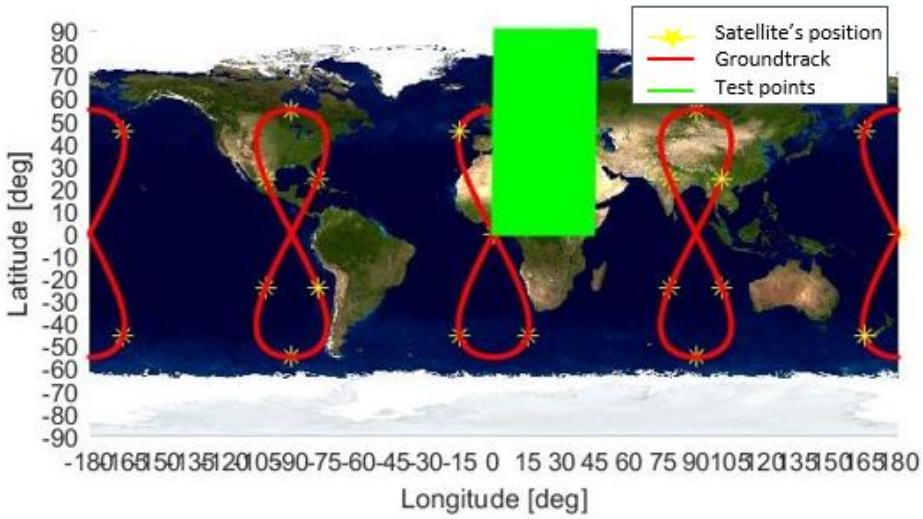

Figure 5.12: GPS "8-shaped" groundtrack.

In both cases, the yellow stars representing the initial positions of the sub-satellite points occupy the same positions: in Figure 5.11 they are the initial positions of all satellites of the constellation, while in Figure 5.12 they represent all the reference positions occupied from the first satellite propagated over one revolution. This is the proof of the consistency on the assumptions made by Lang, described in detail in Section 3.4.

5.1.3 Polar non-symmetric versus inclined symmetric constellations

The Beste [28] and Adams and Rider [24] methods and the Walker [27] and Lang [48] methods are suitable for determining continuous global or zonal coverage of different constellation geometries: polar non-symmetric and inclined symmetric respectively. A direct comparison between these two classes is hereafter reported for continuous global coverage, by analysing the number of satellites T required with varying altitude. The Adams and Rider method and the Lang approach have been used for this analysis, since they have turned out to be more performant and accurate.

Figures 5.13 and 5.14 show the results obtained with h varying in the range between 300 km and 1100 km.

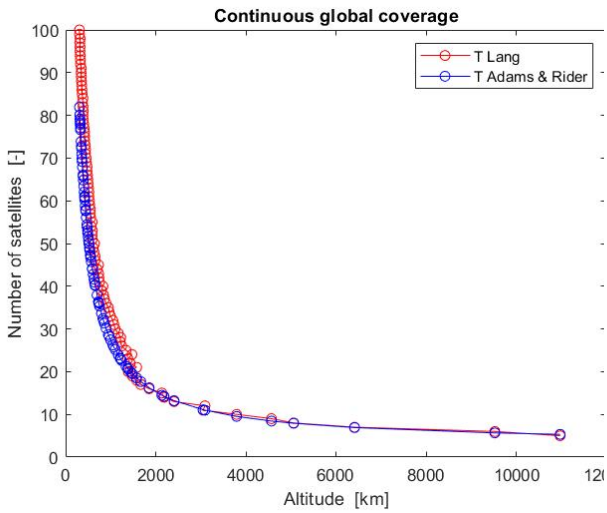

Figure 5.13: Polar non-symmetric versus inclined symmetric constellations.

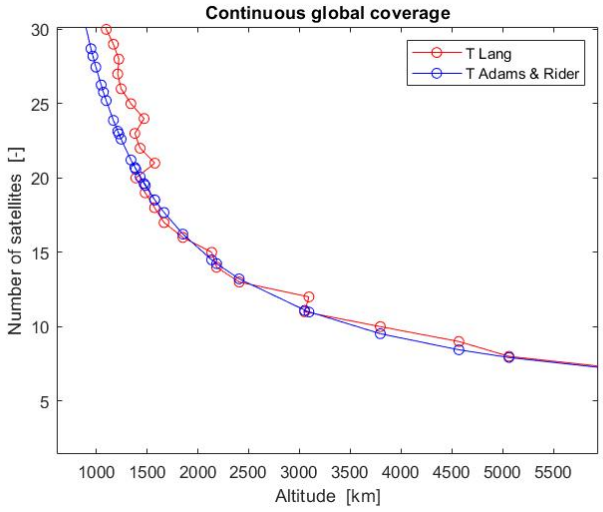

Figure 5.14: Polar non-symmetric versus inclined symmetric constellations zoomed.

The global trend is very similar and in many cases non-polar constellations outperformed similarly sized polar constellations. However, from Figure 5.14 it can be observed that for single continuous global coverage with more than 20 satellites the polar constellations and the Adams and Rider method are likewise more efficient; instead, with 20 or fewer satellites, the non-polar constellations determined throughout the Lang method are equal and sometimes more efficient than an equal number of polar satellites. The list containing the major distinctions that bring to the choice of one between the two configurations is written in Section 2.2.4.

Nevertheless, there are differences between the coverage of the polar and non-polar constellations which are not evident in Figure 5.13: polar constellations always provide the higher coverage in concentric rings about the poles, while non-polar constellations usually offer the higher coverage in the mid to upper latitudes near the inclination of the orbits and often, it is in these highly populated mid latitude regions of the Earth which the greater coverage is desired and so this could be a factor in favor of the non-polar constellations. A second factor, that shall always be kept in mind, is the difficulty to direct launch into polar orbits, that means a higher amount of propellant needed with respect to the quantity needed to populate lower inclination orbits.

5.2 Application and comparison of methods for discontinuous coverage

This section presents the results obtained through application of all the methods suitable for discontinuous local coverage, hence capable of determining revisit time metrics for different satellite orbits and constellations.

5.2.1 Single satellite

As first step in this analysis, the case of one satellite only is considered: the goal is to determine the amount of time this satellite is visible above a specified location and consequently what is the gap time.
In order to perform this study, the geometrical approach developed by Ulybyshev [50] and described in Section 4.2 is used and then compared with the application of the brute force method presented in Section 4.1.

The geometrical approach, which is purely analytical, is valid for satellites in circular orbits and it is assumed that the altitude h, inclination i and minimum elevation angle ε are known. The approach has the attraction of a uniform analytical computation of the revisit times for a single satellite and constellations as the sum of two terms; another attractive property is that the method is very suitable for mass computations, including direct optimisation or parametric study of discontinuous coverage satellite constellations.

A relevant study case is given by the design of satellites in LEO orbits, suitable for communications rather than remote sensing services. The orbit altitude has a great influence on the mission requirements and the satellite performance. Due to this fact, selecting a practical range of altitudes at preliminary stages of the design is important in order to obtain meaningful trade-off studies [53]. The orbits with altitudes below 1000 km are considered as LEO; this upper limit is selected based on the great amount of the Van Allen radiation exposing on the satellite in higher altitudes. On the other hand, at the lower end of the altitude range atmospheric drag is the parameter which plays an important role: for orbital altitudes lower than 500 km the satellite can be affected seriously by atmospheric drag. This drag force results to slow decrement of the satellite altitude and has a negative effect on mission performance. Due to these facts, the range of altitude between 500-1000 km is selected for LEO orbit design. In addition, this range of altitudes is inside the performance margin of the majority of commercial launch vehicles. After selecting an appropriate range of altitudes, the value of inclination i=98 deg is chosen, since it resembles the value of inclination for the Sun-synchronous orbit (SSO), that could be a good practical example (many satellites, especially the ones for Earth observation, are placed in SSO); in addition, the value ε=10 deg is used, as acceptable value for minimum elevation angle.
The reference location on the Earth surface is assumed to be one of the four ground stations of the Estrack core network for tracking satellites or launchers near Earth (Korou in French Guiana, Redu in Belgium, Santa Maria in Portugal and Kiruna in Sweden) [54]. The Redu Ground Station, in Belgium, located at 50 deg North latitude and 5 deg East longitude, is chosen for the present analysis.

The coverage circle of visibility above the ground station for h=1000 km is presented in Figure 5.15 (the central point which is used for λ_c is the station itself); for decreasing altitude, the size of the circle decreases as well but the shape remains the same.

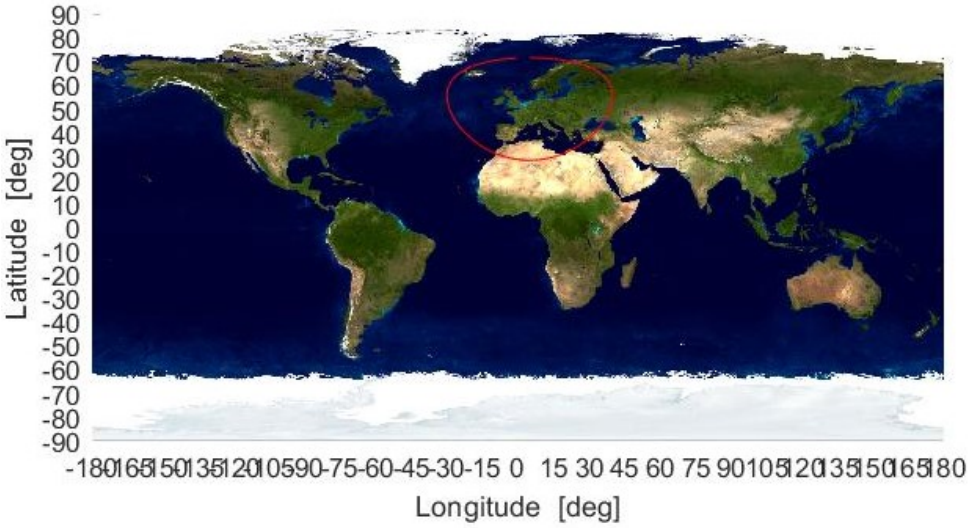

Figure 5.15: Redu coverage circle (ε=10 deg).

For altitude values that vary from h=1000 km to h=500 km, the correspondent revisit times are reported in Table 5.12.

Table 5.12: Revisit times for one satellite in circular orbit with i=98 deg and ε=10 deg (geometrical method).

h [km]	Revisit time [hr]
1000	12.30
900	12.05
800	11.80
700	11.55
600	12.91
500	12.63

The correspondent regions in the two-dimensional space (Ω,t) are double connected, since the latitude of Redu λ_c is less than (i-θ).
The coverage belt for the case at h=1000 km is shown in Figure 5.16, but the plot would have be the same shape even for the other altitude values.

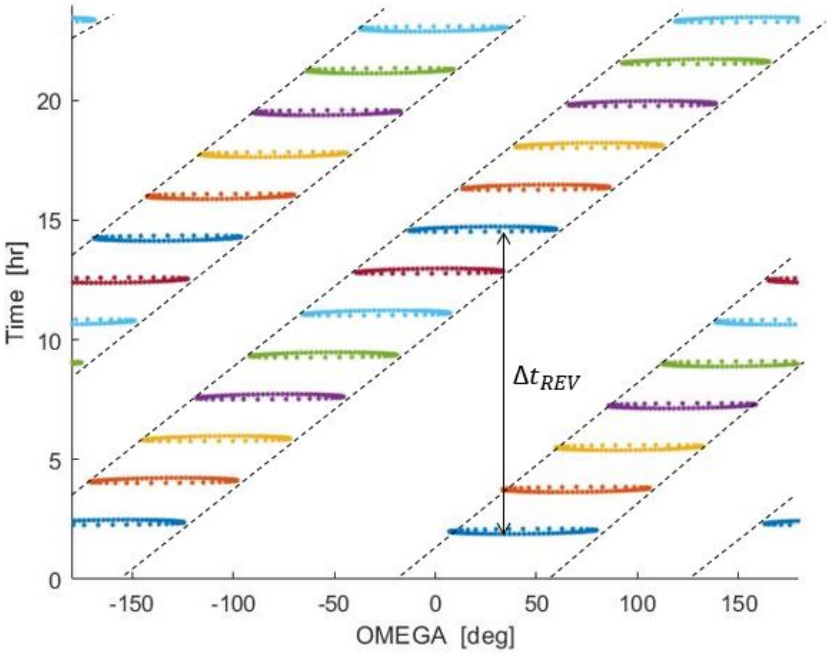

Figure 5.16: Coverage belt for one satellite at h=1000 km.

The same orbital parameters and ground site of interest have been used as inputs for the brute force algorithm, in order to compare the results and check the accuracy. The total propagation time is one day (24 hours), with a 1 second time-step. Table 5.13 shows the results.

Table 5.13: Revisit times for one satellite in circular orbit with i=98 deg and ε=10 deg (brute force).

h [km]	Revisit time [hr]	Visibility interval [hr]
1000	11.54	0.17
900	11.80	0.16
800	12.06	0.15
700	10.67	0.13
600	10.95	0.11
500	11.24	0.09

The brute force method provides also the time spent by the satellite above the minimum elevation angle threshold; the visibility time decreases as altitude decreases, since also the size of the coverage circle diminishes with constant ε.
Instead, the maximum revisit times obtained in both cases are quite similar and they are in agreement with each other; moreover, for the case of one only satellite, the CPU time spent by the Brute Force method is always really low (of the order of 1-2 seconds) and so the time-saving of the analytical method is not relevant for this context.

5.2.2 Satellite constellations for long revisit times

Both the methods developed by Ulybyshev [50], [51] are applicable to satellite constellations; however, the approaches are quite different: the geometrical and purely analytical method presented in section 4.2 is suitable only for constellations with revisit times of more than one orbital period (hence for constellations with a small number of satellites T), while the approach described in section 4.3 is valid for all constellations that have satellites in circular orbits and symmetric arrangement and is capable to analyse both continuous and discontinuous coverage cases.
In addition, this last method takes as inputs the desired performance and gives as outputs the optimal satellite constellation configuration in terms of $(T/P/F)$, exactly the opposite approach faced in the method for long revisit times and in the brute force algorithm.

As first validation example, a three-satellite constellation for discontinuous coverage is used: it is a (3/3/0) constellation with h=1100 km, i=86 deg and ε=10 deg ; the approach for long revisit times can therefore be used. The results for the maximum revisit time are presented in Table 5.14 for different latitudes investigated for both the geometrical and brute force methods.

Table 5.14: Revisit times for (3/3/0) with i=86 deg and ε=10 deg.

Latitude [deg]	Rev time [hr] - geometrical	Rev time [hr] - brute force
0	4.48	3.90
10	4.37	3.90
20	4.26	4.68
30	4.16	3.89
40	4.05	3.32
50	3.93	3.29
60	5.41	5.71

Since the latitudes λ_c are always less than $(i\text{-}\theta)$, the polygons are double. The case (3/3/0), h=1100 km, i=86 deg, λ_c=0 deg is represented in Figure 5.17, where it is possible to see the maximum revisit time occurs between the descending pass of one satellite and the ascending pass of another above the latitude of interest.

The obtained results with the two different methods are quite in agreement, with discrepancies of the order of some minutes probably because of approximations and rounding errors.

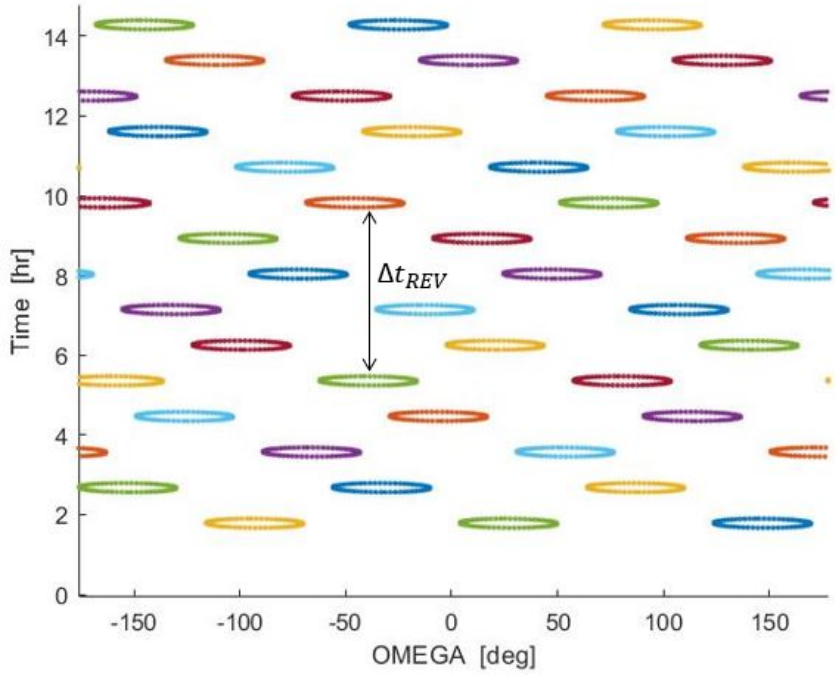

Figure 5.17: Coverage belt for (3/3/0), λ_c=0 deg.

The second example consists in a three satellite constellation for a zonal coverage (3/3/0), h=600 km, i=50 deg and ε=20 deg, with varying latitude λ_c; again, geometrical and brute force approaches are compared and the results are listed in Table 5.15.

Table 5.15: Revisit times for (3/3/0) with i=50 deg and ε=20 deg.

Latitude [deg]	Rev time [hr] - geometrical	Rev time [hr] - brute force
0	5.71	4.77
10	7.20	7.78
20	7.09	7.70
30	8.16	7.51
40	3.63	2.36
50	3.49	2.96
60	8.12	7.99

There are some differences in the revisit times; a possible explanation could be the dependency of the brute force method from the longitude of the site (the reference point on the planet's surface needs to be specified both in latitude and longitude): this implies slightly different results when varying the longitude and leaving the latitude unchanged. On the other hand, the geometrical method is unrelated from longitude and gives the same result independently from the value assumed.

This second study-case deals with double as well as single coverage belts, since both the situations of i-θ<λ_c<i+θ and λ_c<i-θ occur; the transition from double to single coverage

belt for increasing λ_c is shown in Figures 5.18 for λ_c=10 deg, 5.19 for λ_c=20 deg and 5.20 for λ_c=50 deg.

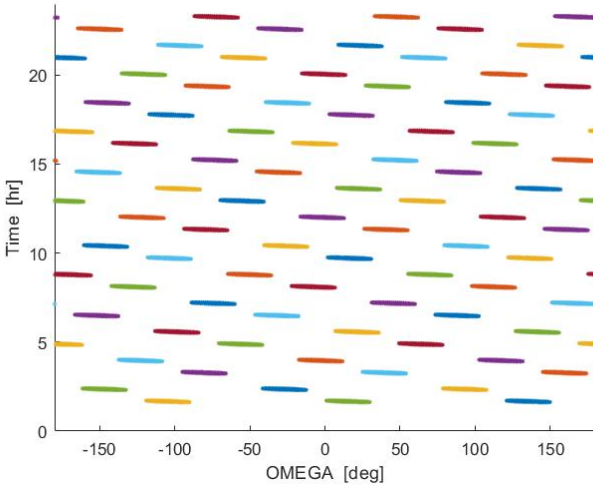

Figure 5.18: Coverage belts for λ_c=10 deg.

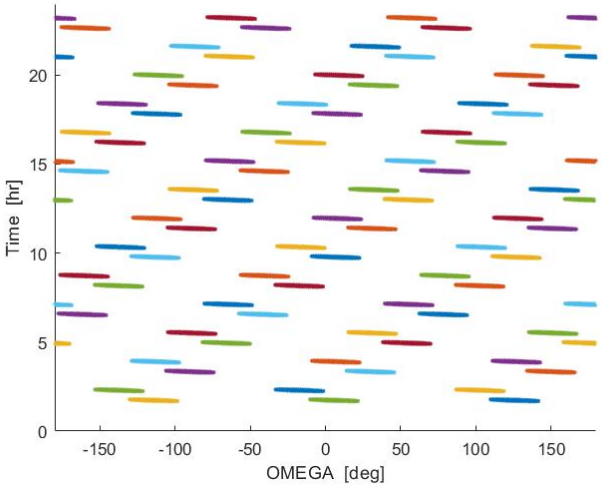

Figure 5.19: Coverage belts for λ_c=20 deg.

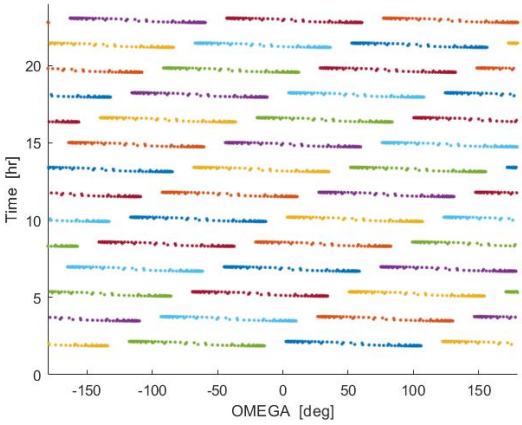

Figure 5.20: Coverage belt for λ_c=50 deg.

Because this method is suitable for revisit times of more than one orbital period only (otherwise the geometrical statements are not valid anymore), the constellations that could be studied involve a small number of satellites T, with maximum 1 or 2 satellites per plane S.

Results for CPU time comparison between the method and the Brute Force approach are presented in Table 5.16 for a (4/4/3), i=73.3 deg constellation at h=500 km. The minimum elevation angle is ε=20 deg and λ_c is set to be 50 deg. Note that the value of inclination is optimised for the minimum revisit time.

Table 5.16: Revisit times for (4/4/3) with i=73.3 deg and ε=20 deg (λ_c=50 deg).

	Rev time [hr]	CPU time [s]
Geometrical	5.08	0.045
Brute force	5.63	2.729

The resulting CPU time is, in both cases, extremely low: this is due to the small number of satellites that must be investigated. However, it can as well be noted how the brute force method is sensible to the increasing number of satellites T: even with only 4 satellites, the computational time is about 60 times higher with respect to the geometrical approach.

To understand why this method is not valid for short revisit times neither continuous view, a (12/3/2) constellation at 1400 km altitude, with 52 deg inclination and a minimum elevation angle of 10 deg is considered, for a latitude λ_c=50 deg. This constellation allows for a revisit time that is quite shorter than its orbital period, which is about 1.9 hours. Figure 5.21 shows the two-dimensional map of visibility.

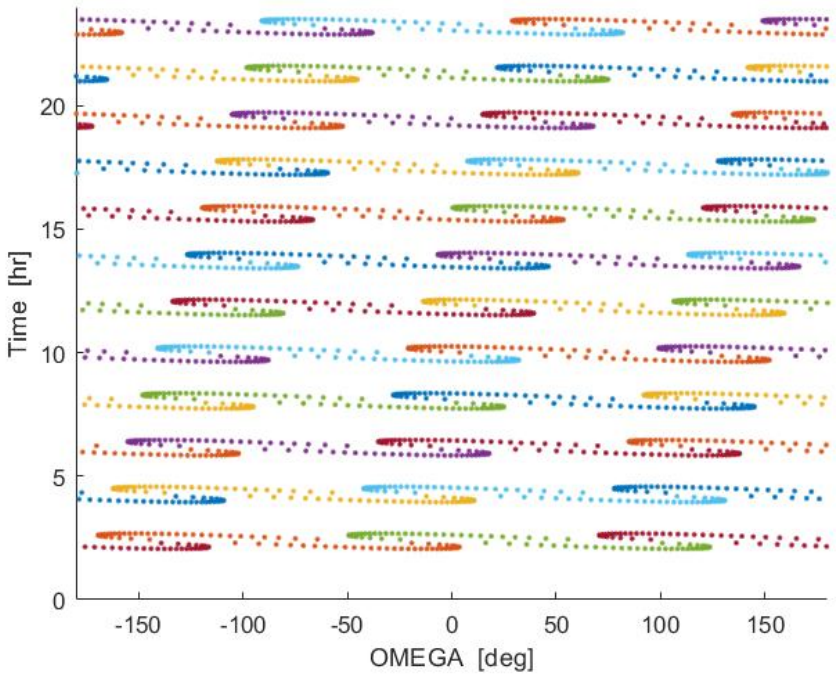

Figure 5.21: Coverage belt for (12/3/2) constellation.

As it can be observed, when the number of satellites increases (or when the altitude increases as well) with respect to the previous cases analysed, the coverage belts are no more distinguishable: they mix each other and a clear geometry does not exist anymore. Moreover, the major property and condition of the coverage belts presented before, namely that for all the points inside the coverage belt the revisit times are near to the orbital

period, is not satisfied anymore. In this case, it is not possible to compute the longitude range $\Delta\Omega$ neither $\Delta\Omega_{REV}$ and so the values for Δt_B or Δt for the revisit time Δt_{REV} computation.

5.2.3 Satellite constellations for short revisit times

The logic of the geometric approach valid for short revisit times is the opposite of both the aforementioned geometrical method and brute force algorithm: it determines the optimal configuration of satellite constellations starting from visibility requirements, both for continuous and discontinuous coverage. Therefore, a direct comparison between the methods is not possible; instead, correspondences in terms of results and requirements are analysed.
The algorithm is well suited for a simple connected convex region; in addition, there are difficulties related with the application of the method for multiple connected regions and it could not be applied to a non-symmetric constellation, as an example, to a near-polar constellation.

In order to explain the principle of work of this method, continuous coverage of a region at a latitude of 50 deg is presented as first application example; the constellation shall be at an altitude of 1400 km, with 52 deg inclination and a minimum elevation angle of 10 deg. The optimal configuration is a (27/3/1) constellation, that lets at any time that at least one grid vertex belongs to the region.
In Figure 5.22, the constellation grid is represented with red stars together with the coverage region: such regions are shown for a few consecutive revolutions, each time shifted to the right by ($\omega_{Earth} \times Period$). As it can be observed, every time at least one satellite is inside the region and so continuous view is guaranteed.

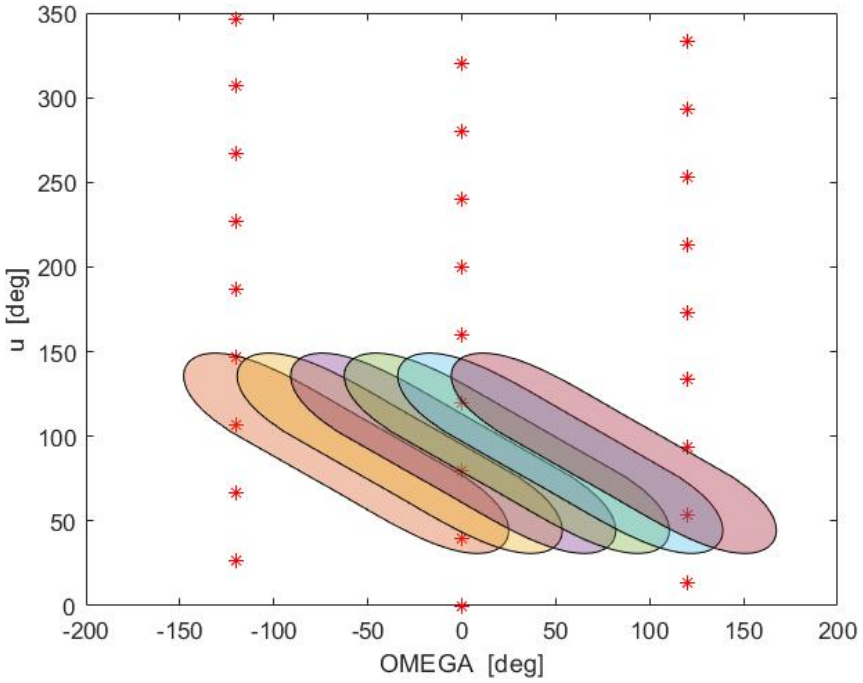

Figure 5.22: Optimum grid for continuous coverage, (27/3/1).

The meaning of this representation would be to show that every time the condition that at least one satellite is inside the region is satisfied: by considering the vertical motion, with satellites on the same plane (represented by stars aligned vertically) that move toward the top, whenever one is leaving the region the following is arriving and enters it while, by considering horizontal motion through the shift of the region to the right, when a satellite moves out the other plane is reached and so another satellite enters the region. In this way, continuous visibility is achieved.

The second example applies the same constraints in terms of altitude, inclination, elevation angle and latitude site investigated, but this time 40 minutes for maximum of revisit time are allowed: this means that for such period there could be zero satellites in view of the location of interest. The optimal resulting configuration has a (12/3/2) configuration. The geometry is represented in Figure 5.23.

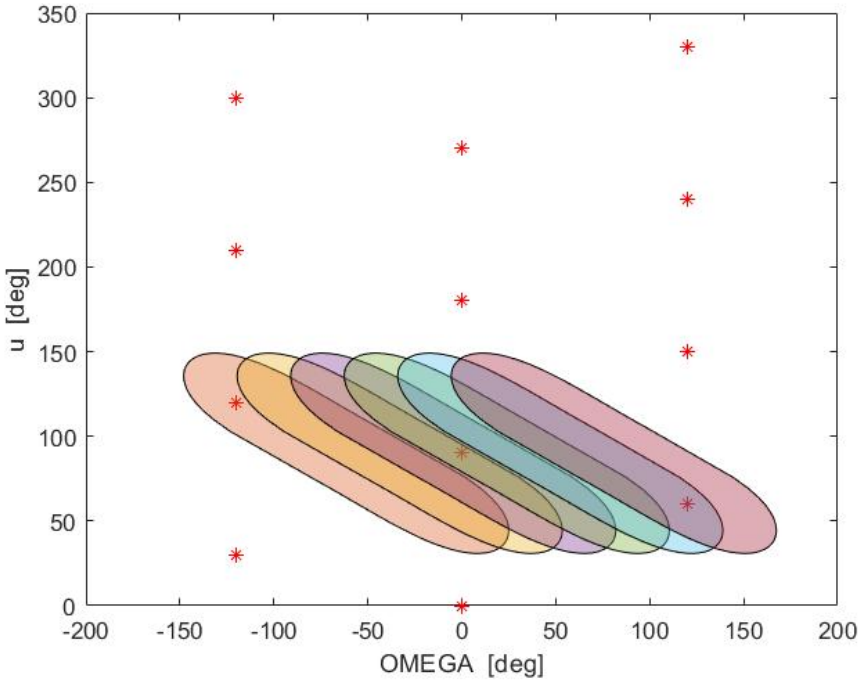

Figure 5.23: Optimum grid for discontinuous coverage, (12/3/2).

Another interesting example considers a communication network using the satellites as relays between two ground stations or users. At any time, the link between these stations is possible if they belong to the access area of a satellite from the constellation; suppose that the stations are located in Belgium and Portugal and are Redu (longitude +5 deg, latitude +50 deg) and Santa Maria (longitude -25 deg, latitude +36 deg) respectively. With a fixed altitude of h=1400 km and elevation angle ε=10 deg, the inclination has been varied in the range [40 deg, 65 deg] in order to find the optimal condition.

The coverage circles for the stations with these numbers are overlapping and their geographical representation is shown in Figure 5.24.

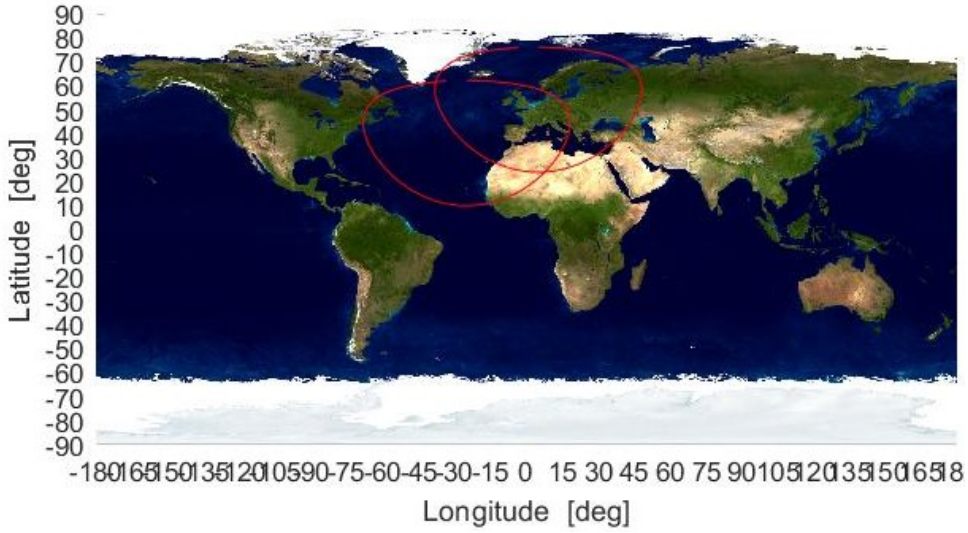

Figure 5.24: Redu and Santa Maria coverage circles.

The trend for varying inclination is shown in Figure 5.25, where it can be noted that the optimal inclination i range is around 60 deg and, in addition, most of the solutions correspond to constellations with 3 orbital planes. With an upper limit for the algorithm of 20 satellites per plane and 10 planes, the optimal configuration is (42/3/1), i=62 deg, found in 30.82 s.

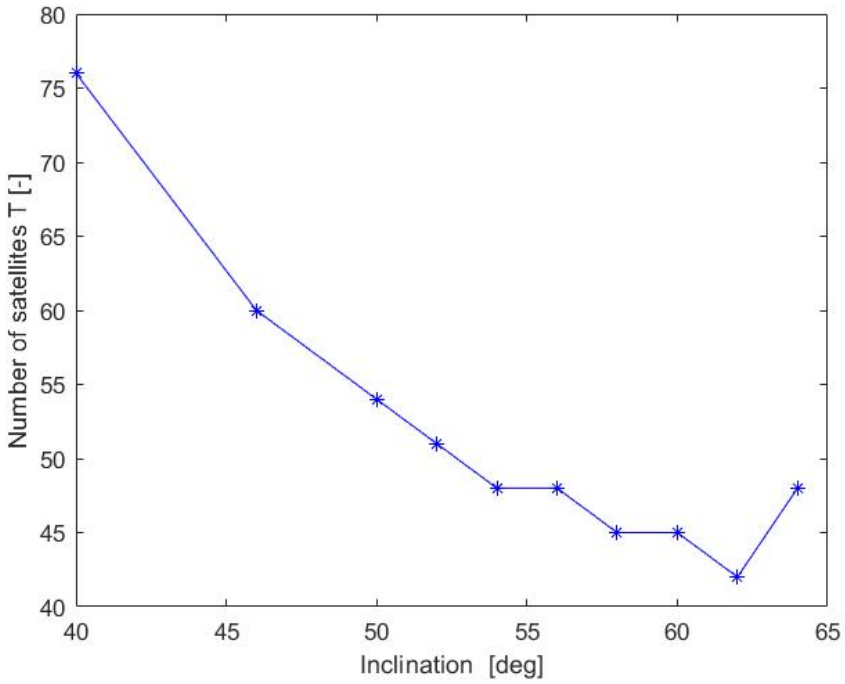

Figure 5.25: Number of satellites versus inclination, at h=1400 km.

As inclination increases, the coverage regions grow in size and the total number of

satellites is decreased; further, there is an optimal inclination and after that the total number of satellites is increased. This is a superposition of two effects: first, it is an extension of the regions (mainly along the x axis) and second, it is the influence of non-convexity: as inclination increases, the regions shrink until the ascending and descending passes separate and eventually the regions are no more single but become double. The correspondent intersection of regions in the two dimensional space (Ω, u) is illustrated in Figures 5.26 and 5.27 for i=52 deg and i=62 deg cases respectively.

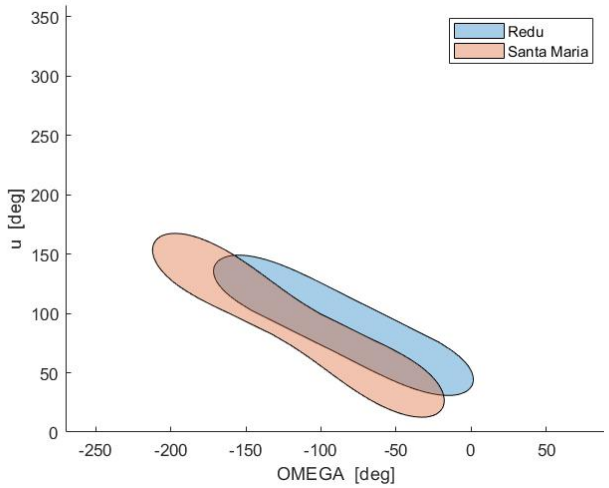

Figure 5.26: Redu and Santa Maria regions, (51/3/1), i=52 deg.

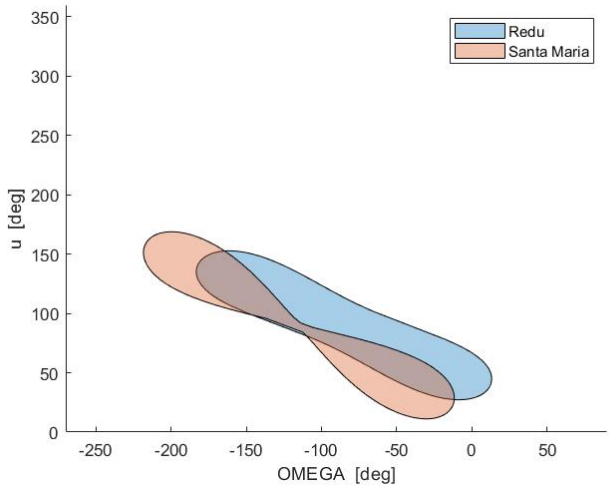

Figure 5.27: Redu and Santa Maria regions, (42/3/1), i=62 deg.

Another case for full region coverage consists in a constellation for continuous coverage of the United States; this implies that, at any time, there is at least one satellite from the constellation with the instantaneous access area involving the full region, or in other words, at any time at least one satellite is visible from all of the points in the United States. A suitable constellation that satisfies such requirements could be the ICO constellation presented in Section 2.4: (12/2/0), h=10390 km, i=45 deg.
Indeed, the coverage function can be computed based on a convex hull for a set of boundary points; the convex hull is the smallest convex set that contains all the points. In order to determine the intersection of the regions that satisfies at continuous coverage and so contains all the United States, three central points in terms of latitude and longitude (i.e. (λ_c, ϕ_c)) have been selected and the correspondent solution, for a minimum elevation angle ε=15 deg, is shown in Figure 5.28, where the darkest section represents the selected boundaries for the determination of the optimal configuration.

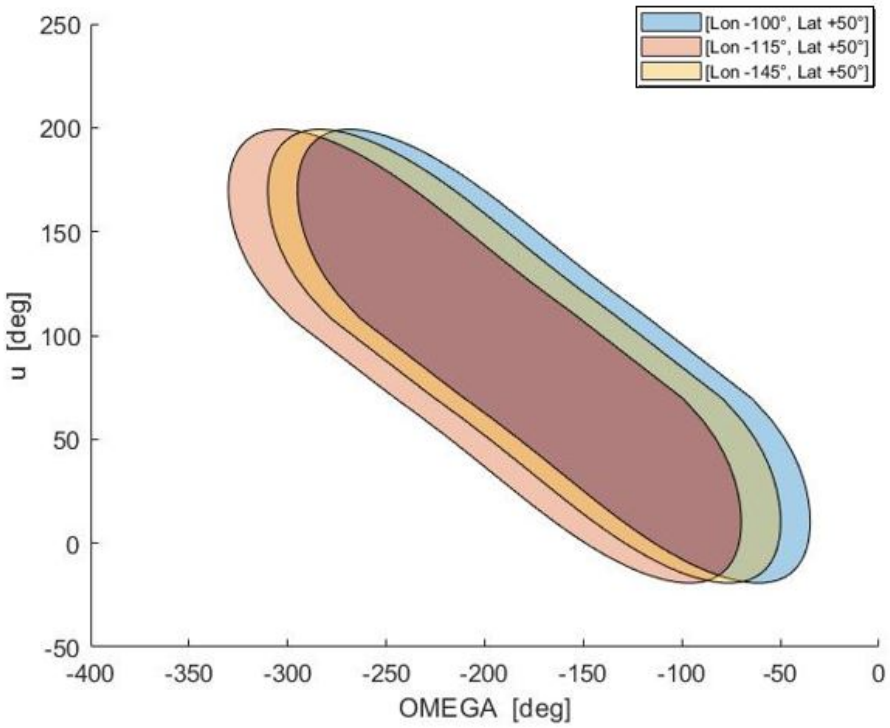

Figure 5.28: Solution region for the United States.

As expected, the optimal solution is (12/2/0), found in 3.73 s since this time the field of investigation have been restricted to $S_{MAX} = 10$ and $P_{MAX} = 5$.

By applying now the brute force method with inputs (12/2/0), h=10390 km, i=45 deg, ε=15 deg, a propagation period of 10 days with 1 s time-step and looking for coverage of the entire United States, the resulting revisit time is always equal to zero, while there are alternations of visibility windows where there are 2 and 4 satellites in view of the region above the horizon. The results are reported in Table 5.17, with a CPU time of 66.74 s.

Table 5.17: Results for ICO constellation.

Multiplicity of coverage	**Average access time [min]**	**Maximum access time [min]**
2	45.82	66.60
4	7.93	28.18

Indeed, the geometrical approach is fast at determining the optimal configuration, but the two methods can not be directly compared, since the numerical brute force requires as inputs the outputs of the Ulybyshev approach [51]. However, by means of the first it is possible to obtain the multiplicity of coverage and the time the satellites spend above the region, while the second is not capable to determine such parameters; hence, a possible way of proceeding in constellation design could be to apply the geometrical method and

then, with the optimal configuration (or a few cases close to the optimal) to apply the brute force method in order to perform a more detailed analysis and obtain all the desired performance parameters.

To illustrate another discontinuous coverage case, a satellite constellation for observation of a region with boundary coordinates in geographic latitudes [+25 deg, +35 deg] and longitudes [0 deg, +20 deg] is considered. Coverage requirements are discontinuous coverage of an arbitrary part for the region with a revisit time no more than 1 hour. Such constellations can be used for remote sensing or weather observations. The satellites are assumed in a circular orbit with i=28 deg, h=1000 km and the minimum elevation angle is equal to 10 deg, with an orbital period equal to about 1.75 hours; the union of visibility circle maps for points of the region is presented in Figure 5.29. This region corresponds to the continuous partial coverage of the region.

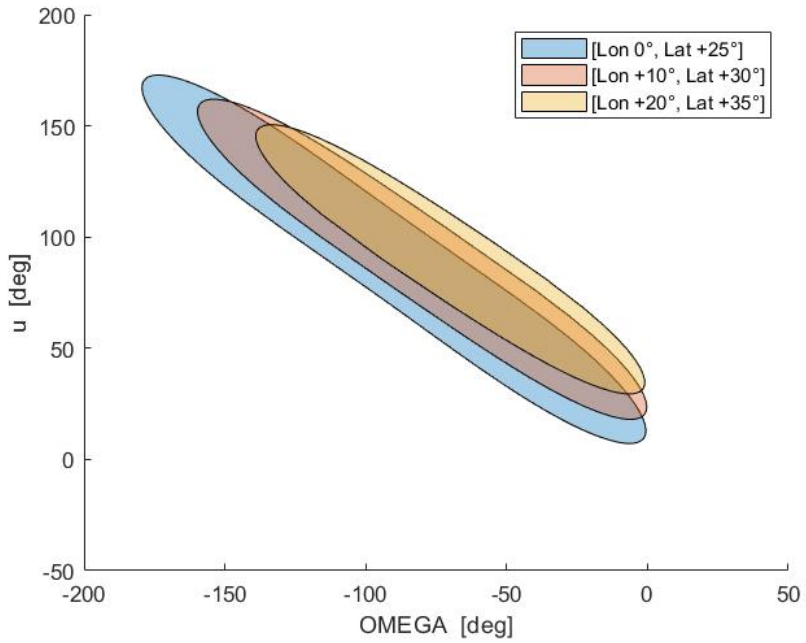

Figure 5.29: Region for partial region coverage.

The extension of the region for discontinuous coverage and a geometrical representation is shown in Figure 5.30. It shall be remarked that these results can be applied to all of the similar regions (i.e. with the same latitude bands in both hemispheres of the Earth and the same range in relative longitude).

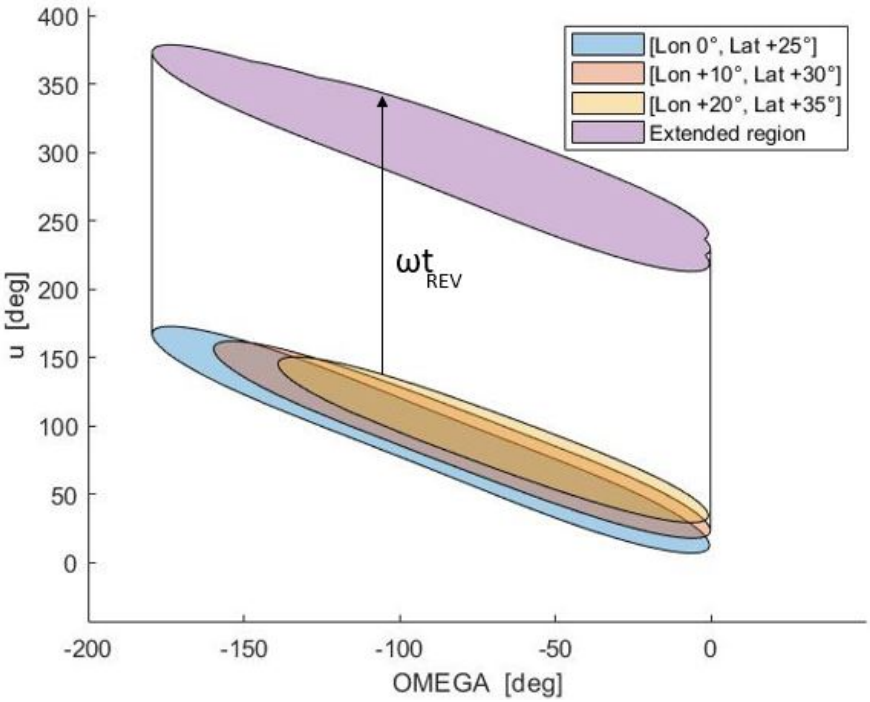

Figure 5.30: Region for discontinuous coverage with maximum $t_{REV} = 60min$.

The optimal solution that satisfies at these requirements is a (9/3/0) constellation, found among a maximum number of planes equal to 5 and of satellites per plane equal to 10. The CPU time is 45.38 s.
However, it must be noted that the computational time increases as the number of boundary points increases, i.e. the maximum acceptable revisit time increases.

In order to check the consistency of the results, this configuration is applied to the brute force method, that in about 4.6 minutes returns what listed in Table 5.18.

Table 5.18: Performance (9/3/0).

Revisit time [min]	**Access time [min]**
37.47	5.92

The maximum revisit time that occurs in 10 days of propagation with a 1 s time-step is approximately 40 minutes, never higher than the requirement of 1 hour.

5.3 Application to generic constellations

This section presents an example of a generic satellite constellation, that is not symmetric and involves elliptical orbits. A suitable case consists in the ELLIPSO concept presented in Section 2.4; the method applied in order to study its performance is the classic numerical brute force algorithm, since the other methods are not directly applicable for such constellations.

The ELLIPSO constellation is a unique constellation that employs both elliptical and circular orbit communications satellites; the use of inclined elliptical orbits permits the biasing of Earth coverage by latitude, longitude and time of day so that satellite coverage can be matched to the market needs for particular geographical regions and their populations daily work schedules. Circular equatorial orbits are used for continuous day and night coverage in the tropics and the Southern Hemisphere down to 55 deg South latitude [3].
The ELLIPSO system is atypical from the classic constellation design methods (Walker, Beste or Ballard), in that it employs sub-constellations of different periods and orbital characteristics (i.e. "hybrid" systems).
The baseline ELLIPSO constellation consists of the BOREALIS and the CONCORDIA sub-constellations (represented in Figures 5.31 and 5.32); the former is made up of two planes of inclined sun-synchronous, fixed line of apsides, repeating groundtrack satellites (five per plane), with ascending nodes at noon and at midnight respectively so that the planes are always nearly edge-on the Sun. The latter is a single plane of eight equally spaced equatorial circular satellites with 4.8 hour periods (5 revolutions per day). The orbital parameters of the constellation are listed in Table 5.19.

Table 5.19: ELLIPSO constellation parameters [3].

Sub-constellation	a [km]	e	i [deg]	ω [deg]	Ω [deg]	TA [deg]
CONCORDIA: 8-sats	14446	0	0	0	0	0
BOREALIS: 5-sats plane 1	10559.271	0.3457	116.565	270	280	72
BOREALIS: 5-sats plane 2	10559.271	0.3457	116.565	270	100	72

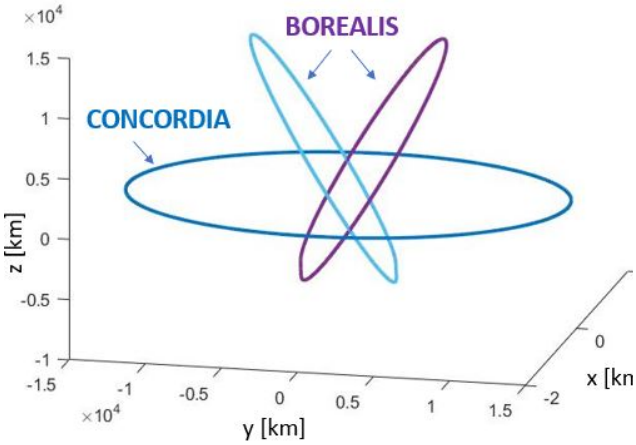

Figure 5.31: ELLIPSO: CONCORDIA + BOREALIS.

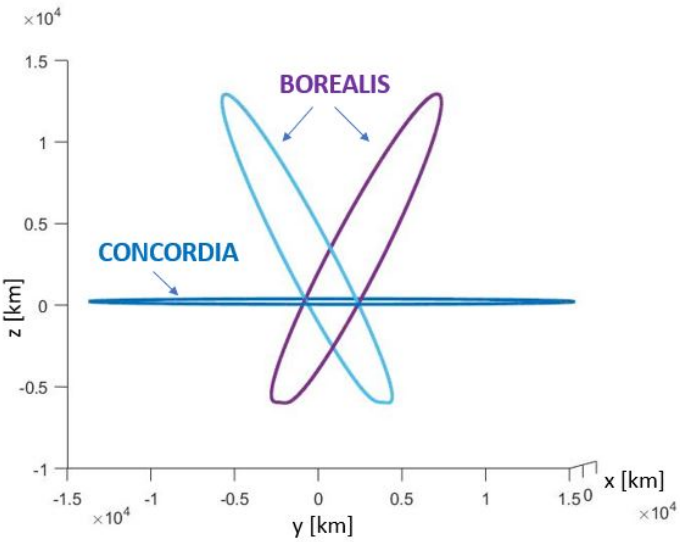

Figure 5.32: ELLIPSO: CONCORDIA + BOREALIS.

Since there are both circular and elliptical orbits, the correspondent central angle radius of Earth coverage is given by the formula:

$$\theta = \cos\left(\frac{R_{Earth}}{r}\cos\varepsilon\right)^{-1} - \varepsilon \tag{5.5}$$

where r is the instantaneous value of the radius of the satellite in its orbit.
By taking the position of all satellites of the constellation at a certain time and determining the correspondent sub-satellite points, Figure 5.33 shows the coverage circles with a minimum elevation angle ε=10 deg, where CONCORDIA circles are red and BOREALIS green.

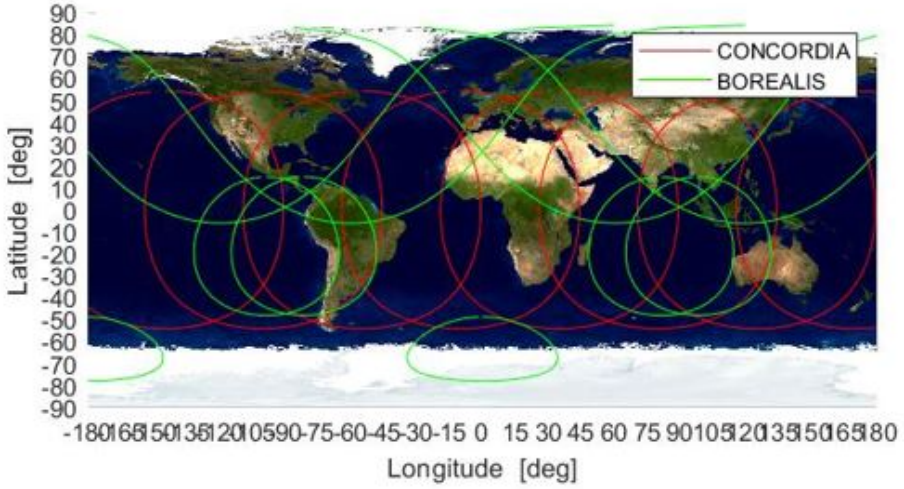

Figure 5.33: Coverage circles ELLIPSO.

The coverage areas have been determined analytically by means of the method described

in section 2.1.1: first, the coverage angle θ is determined by knowing the satellite's position vectors, then the conversion to longitude and latitude angles of the sub-satellite points is performed.
Recalling Equations (2.27) and (2.28), the boundaries of the coverage area are:

$$\lambda_i = \sin\left(\cos\theta \sin\lambda_{sub} + \sin\theta \cos\lambda_{sub} \cos Az\right)^{-1} \tag{5.6}$$

$$\phi_i = \phi_{sub} + \tan\left(\sin\theta \sin Az, \frac{\cos\theta - \sin\lambda_i \sin\lambda_{sub}}{\cos\lambda}\right)^{-1} \tag{5.7}$$

An analysis of the visibility and gap windows over the entire Earth's surface proved a continuous coverage of the central latitudes in the bands [-40 deg, +40 deg], where at least two-fold coverage is always guaranteed and sometimes four-fold coverage occurs, with an average visibility window of 6 minutes. Thanks to the BOREALIS sub-constellation, also the Northern latitudes are covered, with an average revisit time in the [+40 deg, +60 deg] latitude band of about 9 minutes and for higher latitudes of some 15 minutes.
On the other hand, Southern latitudes are less covered: the average revisit time in the band [-40 deg, -60 deg] is about 10 minutes, while it increases at [-60 deg, -80 deg] to approximately 1 hour and 50 minutes until, at -80 deg latitude and on, visibility conditions are never achieved and satellites are never above the horizon. A direct proof of what has just been described is also visible in Figure 5.33.

5.4 Conclusions

The presented analysis was aimed at showing the efficiency and the computational time of each method that assesses coverage performance of satellite constellations. Moreover, every approach has been applied for specific cases depending on the visibility requirements and on the constellation's geometry.

Summarising, the most important distinctions must be made upon polar and non-polar (i.e. inclined) constellations and between constellations for continuous and discontinuous coverage.
To achieve continuous global or zonal coverage with polar non-symmetric constellations, both the Beste's [28] and Adams and Rider's [24] methods can be used. The former could be preferred when the number of satellites per plane S is a constraint or a requirement and single or triple coverage are desired, while the latter should be used for a generic n-fold coverage and if the total number of satellites per plane is not fixed. If continuous global or zonal coverage shall be reached with inclined symmetric constellations, the

Walker circumcircle [27] and Lang [48] methods have been studied. As demonstrated, the Lang approach must be preferred to the Walker method, since it is more performant and less computationally demanding. In addition, Lang can be applied to the design of a constellation for zonal coverage, while Walker developed the method for global coverage only.

It must be highlighted that Beste's and Adams and Rider's methods give as outputs the optimal constellation configuration in terms of T, P and S with selected values for altitude, inclination and minimum elevation angle, while the Lang method needs as inputs the configuration $(T/P/F)$ and i and returns the performance index θ; this is a trial-and-error process, since the value must be compared with the desired visibility requirements and if it is not compliant the process must be repeated with a different configuration.

The same approach of the Beste's and Adams and Rider's analytical methods is followed by the Ulybyshev method [51] for short revisit times: it is suitable for inclined constellations and both if continuous local coverage is desired or discontinuous coverage is allowed. As for the two analytical methods, the inputs for Ulybyshev's are the orbital inclination, the altitude, the minimum elevation angle and visibility properties required, while the output is the optimal satellite configuration $(T/P/F)$ that satisfies such constraints.

On the other hand, the Ulybyshev method [50] for long revisit times can be applied to determine the maximum revisit time above a specific location of small symmetric satellite constellations or even for a single satellite. The method is fast but it should perhaps be used in the first phase of constellation design in order to have rough values for coverage performance.

Lastly, the brute force method is suitable for every constellation geometry and every visibility requirement, but it might be involved to test the coverage performance of a constellation that has been designed yet, since it does not optimise the configuration but it only returns the operating capabilities of the constellation itself.

6. Case studies: applications to real missions

This chapter deals with the application of some of the previously presented methods to missions that are currently under development at the European Space Agency.
The two studies hereafter described are the subjects of two different Concurrent Design Facilities (CDF) in which the author was able to participate; they have been used as test-cases, as real application examples, in order to perform a feasibility study on the developed algorithms and to check the effectiveness of the approach used to determine the coverage performance.

Concurrent design facility

The Concurrent design facility is a state of the art facility equipped with a network of computers, multimedia devices and software tools, which allows a team of experts from several disciplines to apply the concurrent engineering method to the design of future space missions. It facilitates a fast and effective interaction of all disciplines involved, ensuring consistent and high-quality results in a much shorter time [55]. Ideas for new space missions, systems or structures are given a definite blueprint in ESA's state of the art Concurrent Design Facility.
The CDF infrastructure, methodology and processes allow teams of experts from different engineering disciplines to work in close coordination in the same place at the same time to complete the most complex designs imaginable in a matter of a few weeks rather than several months.
The CDF enables concurrent engineering based on teamwork and focused on a common design model that evolves iteratively in real time as the different subsystem experts provide their contributions. Designers and customers agree on requirements and take decisions in real time to allow the best design for the right cost and within the programmatic constraints. The process has been developed and honed so it is now common to produce a costed, risk-assessed conceptual space mission or system design complete with various options and including scheduling, testing and operations in a matter of a weeks [56].

6.1 ELCANO mission

ELCANO, that stands for "European LEO Constellation for Augmentation of Navigation and Other services" is a CDF study on a LEO constellation to provide Positioning, Navigation and Timing (PNT) augmentation services; LEO PNT concepts deal with the possibilities for designing large space infrastructure. ELCANO is a constellation of small satellites to augment resilience, robustness and performances of the Galileo constellation, for rural and urban areas. Figure 6.1 shows the ELCANO constellation compared with the existing Galileo, while Table 6.1 summarises the differences.

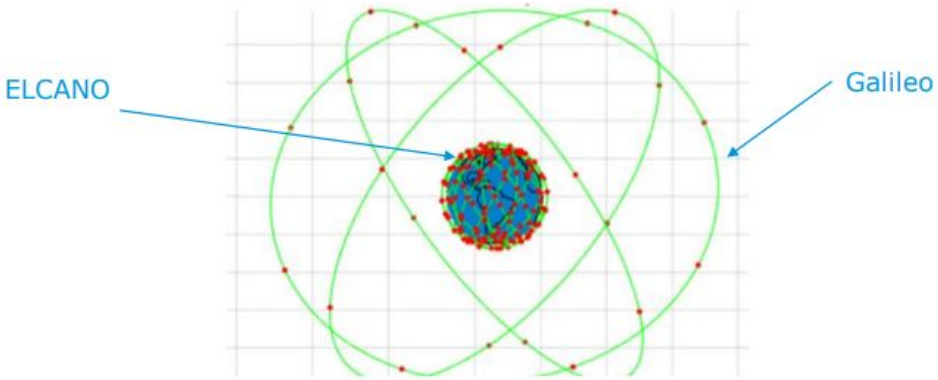

Figure 6.1: ELCANO versus Galileo.

Table 6.1: ELCANO versus Galileo.

		Configuration	Inclination i [deg]	Altitude h [deg]
Galileo		Walker (24/3/1)	56	23222
ELCANO	**Option 1**	Walker (48/4/1)	25	600
		Walker (192/12/1)	55	600
	Option 2	Walker (28/4/1)	30	1200
		Walker (72/8/1)	60	1200
		SOC T=35, P=5	90	1200

It must be specified that there may be three main categories to classify the system concepts involving constellations (typically populated with a few tens to a few hundred nodes in LEO):

- Constellations of small satellites dedicated to PNT; typically New Space nanosatellites/microsatellites;
- Hosted payload on Satcom systems;
- Use of Satcom signals for Signals Of Opportunity (SOOP), e.g. with OneWeb.

The ELCANO study could be identified in the first category.

The constellation design has been performed in order to meet the PNT requirements with minimum number of satellites; the design requirements are:

- Circular orbits with height defined at 600 km and 1200 km;
- Half-cone coverage angle of ≈ 65 deg in order to have, as worst scenario, satellites' Field Of View (FOW) of ≈ 130 deg at 600 km altitude;
- LEO PNT satellites must be able to acquire signals from a multiplicity of GNSS satellites in MEO, with maximum level of aggregate interference as not to degrade effective C/No [(1)] receiver below 27 dbHz;
- With kick off in 2022, Pathfinder A shall be fully operational by 2024 and Pathfinder B by 2025;
- The constellation shall be fully operational by 2028;
- The multi-satellite launch strategy shall be compatible with the required operational availability of the ELCANO constellation.

As stated before, the primary objective of the design process is to find the best configuration with the minimum number of satellites; hence, the two classes considered are: smaller/cheaper satellites in 600 km circular orbits (16U Cubesat class), with passive de-orbiting and larger/more expensive satellites in 1200 km circular orbits (32U Microsat class) with active de-orbiting.
In addition, the constellation might be deployed into three different inclinations, with near-polar planes, mid-inclination planes (≈ 55-60 deg) and tropical planes (≈ 20-25 deg).

After a trade-off among all requirements and subsystems, the ELCANO constellation faces two possible alternative scenario, with two or three separate constellations respectively:

1. Constellation with 240 inclined satellites at 600 km;
   - Walker Delta (48/4/1) with i=25 deg and h=600 km;
   - Walker Delta (192/12/1) with i=55 deg and h=600 km;
2. Constellation with 100 inclined satellites at 1200 km and 35 polar satellites at 1200 km, for a total of 135 satellites;

[(1)] C/No is the ratio of carrier power to the noise power mixed with the signal, in a 1 HZ bandwidth

- Walker Delta (28/4/1) with i=30 deg and h=1200 km;
- Walker Delta (72/8/1) with i=60 deg and h=1200 km;
- Street Of Coverage T=35 in P=5 with i=90 deg and h=1200 km;

These options have been investigated by the author in order to assess performance parameters, coverage properties and to verify the optimal conditions.
Since ELCANO really consists of two (or three) different sub-constellations, each of them has been analysed separately for all the three cases and then the results have been put together in order to determine the global performance.

Option 1

The Lang method [48] was used to analyse separately the two sub-constellations; for the (48/4/1), i=25 deg sub-constellation, the optimal altitude condition of h=600 km, with ε=5 deg, is achieved with continuous coverage in the latitude band [+34.5 deg, -34.5 deg] and the correspondent half-cone coverage angle is θ=19.4 deg.
Instead, the (192/12/1), i=55 deg sub-constellation, results in an optimal altitude h=600 km with minimum elevation angle ε=5 deg if continuous coverage between [+72.4 deg, -72.4 deg] latitudes is desired, with a half-cone angle equal to θ=19.4 deg.

The constellation is represented in Figure 6.2 in ECEF reference frame, while the instantaneous coverage circles of all the 240 satellites are shown in Figure 6.3 and have been determined as described in Section 2.1.1.

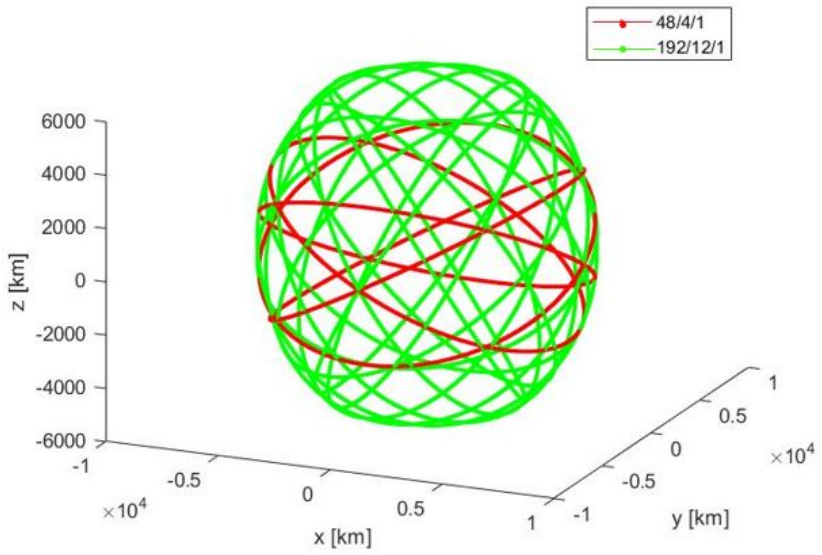

Figure 6.2: ELCANO Option 1.

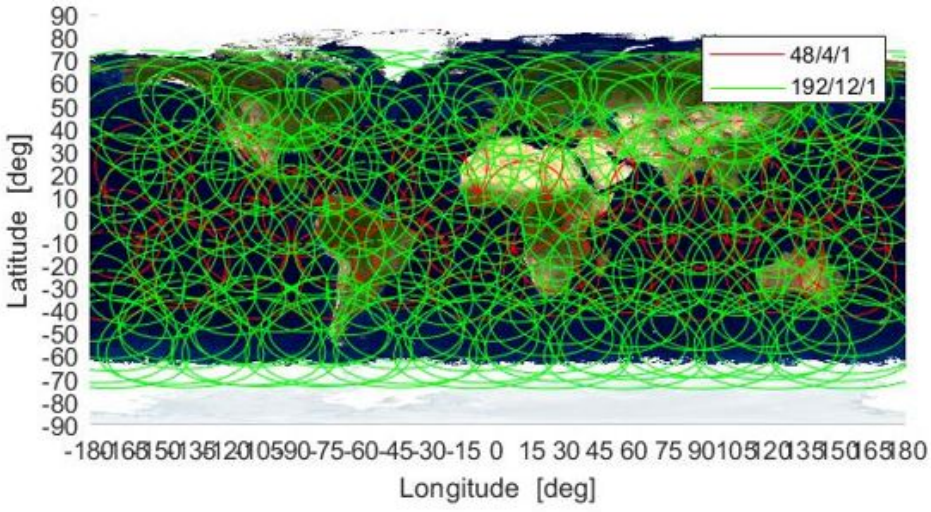

Figure 6.3: ELCANO Option 1 coverage circles.

For the (48/4/1), i=25 deg sub-constellation, the optimal location for a Ground Station is around 10 deg North or South latitude: three satellites are in view at all the times. Instead, for the (192/12/1), i=55 deg sub-constellation, the optimal latitude is around 40 deg North or South, with nine satellites visible while, at 10 deg latitude, a Ground Station would still see four satellites simultaneously. Therefore, a Ground Station located around 10 deg latitude, should see at least seven satellites for Option 1 of the ELCANO constellation.

The choice of altitude equal to 600 km, as well as the value of the inclination, is not only guided by coverage requirements, but many other constraints are involved; for example, the launcher requirements must be taken into account, together with lifetime and station-keeping costs and Δv budgets. Moreover, the importance of respecting space debris mitigation rules must be highlighted. Everything considered, Option 1 configuration is therefore the final result of this trade-off. Indeed, if the altitude would have not be a fixed parameter and if visibility conditions are considered only, in order to achieve full global coverage with both the two sub-constellations separately, keeping the same number of satellites T, inclination i and minimum elevation angle ε, the (48/4/1) sub-constellation should have been deployed at h=12250 km with half cone coverage angle θ=65 deg, while the (192/12/1) sub-constellation at h=1918 km with θ=35 deg.

Option 2

By moving now to the Option 2, with two Walker-type sub-constellations and one Street-Of-Coverage-type sub-constellation, the deployment altitude is h=1200 km. The

Lang method [48] was used to analyse separately the two Walker Delta sub-constellations; for the (28/4/1), i=30 deg sub-constellation, the optimal altitude condition of h=1200 km, with ε=5 deg, is never achieved for continuous coverage in some latitude band, since the number of repeated groundtracks is 7 and so the longitude range to investigate with test points corresponds to $\approx$ 25.7 deg; therefore, even by reducing the value of latitude band for continuous global coverage, the leading parameter that determines the largest θ for coverage performance of the constellation is the longitude range and so the minimum value of altitude that can be reached for continuous global coverage even between [+20 deg, -20 deg] latitude is equal to h=1371 km; the correspondent half-cone coverage angle is θ=29.9 deg.
Instead, the (72/8/1), i=60 deg sub-constellation, results in an optimal altitude h=1200 km with minimum elevation angle ε=5 deg if continuous coverage between [+83.8 deg, -83.8 deg] latitudes is desired, with a half-cone angle equal to θ=28.0 deg.
Lastly, the Beste method [28] was applied for the SOC sub-constellation, with T=35 satellites in P=5 orbital planes and h=1200 km. This configuration, with S=7 satellites per plane and minimum elevation angle ε=5 deg, is capable to achieve 3-fold coverage beyond 66 deg North and South latitude, while single coverage at the same altitude is reached with only T=28 satellites in P=4 orbital planes. Instead, single coverage with 35 satellites divided into 5 planes could be achieved at h=975 km yet.
As for Option 1, even the configuration presented in Option 2 is the result of a trade-off among launcher requirements, mission lifetime, station-keeping costs, Δv budgets and space debris mitigation rules. Indeed, by considering coverage performance only, the application of the methods would have guided toward a different final choice, but this is not the case, since in a real mission there exist many different constraints that must be considered and consequently tuned.

The overall constellation of Option 2 is represented in Figure 6.4 in ECEF reference frame, while the instantaneous coverage circles of all the 135 satellites are shown in Figure 6.5.

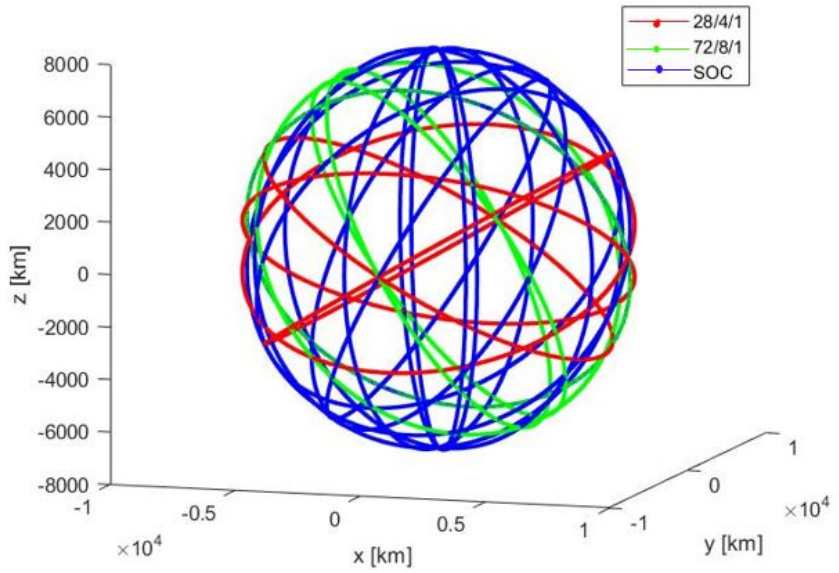

Figure 6.4: ELCANO Option 2.

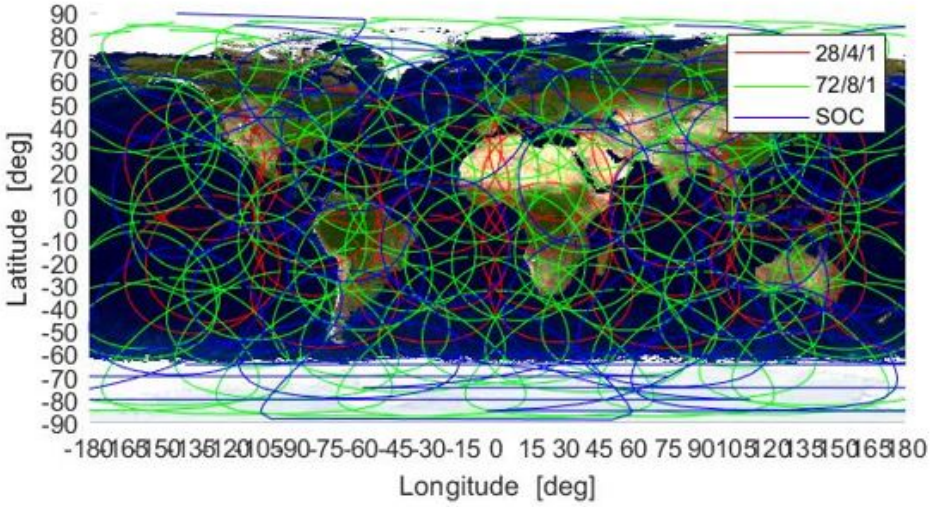

Figure 6.5: ELCANO Option 2 coverage circles.

For Option 2, the optimal locations for the (28/4/1), i=30 deg and (72/8/1), i=60 deg inclined sub-constellations are around 10 deg and 40 deg for North and South latitude as in Option 1, with three or six satellites respectively seen. For the polar sub-constellation, a Ground Station placement as far North or South as possible would be optimal with five simultaneously visible satellites.

6.2 Lunar Communications and Navigation Services mission

The Lunar Communications and Navigation Services (LCNS) is the objective of a CDF, whose aim is to assess three alternative communication and navigation scenarios and then to determine the benefits on the user if these alternatives were in place; in particular, the Lunar Sample Return with LCNS (LUNATIC) mission is studied.
The European Large Logistic Lander (EL3) mission is taken as main user scenario as it contains all the key phases and it's likely to be a good sizing case.

The background for this study is a CDF named Lunar Comms, carried out by an interdisciplinary team from various ESA sites starting with a kick-off on the 20th March 2018 and ending on the 19th April. The goal of the CDF was to perform a preliminary mission design for a constellation of spacecrafts in lunar orbit aiming to provide a data relay and navigation service for lunar missions, including space and ground segment and mission operations.
The Lunar Comms mission was intended to be launched in 2022, with a period of operations of 10 years.
A relay satellites constellation around the Moon provides additional services and redundancy that would be not possible for a direct Earth-Moon link or a single relay satellite. The constellation is able to service the South Pole, the lunar far side and multiple users at the same time; due to the number of satellites in view, long contact times and almost around the clock coverage is possible. Additionally, the communication system requirements can be relaxed for many users. The overall performance increases, since the users are able to communicate at higher data rates more data via the relay constellation. Finally, a constellation around the Moon could as well provide navigation services to asset on cis-lunar space, hence reducing the need for navigation campaigns from Earth. This service will profit for the almost constant view of the relay satellites from the user and the observability in all axis if the constellation is properly designed. Furthermore, the navigation service can be built directly on top of the communications relay service, with very limited impact on the system design both on the relay satellite and on the user.

It must be highlighted that the main landing site considered for the EL3 mission is the Schrödinger Crater, near the South Pole, at the two possible landing sites: [longitude 141.33 deg East, latitude 75.47 deg South] and [longitude 141.89 deg East, latitude 75.30 deg South].

The Lunar South Pole is particularly important from a scientific point of view because of water ice and as potential location of a permanent lunar outpost. The major technical challenge for operating at the South Pole is that the Earth is not usually visible for direct radio communications; therefore, it is necessary to implement early communications capabilities, including telemetry, tracking and control TT&C and mission data transmission to meet early lunar robotic needs. In addition, human missions require almost 24/7 communication coverage which implies more than one relay satellite. Another scientific crucial spot is the far side of the Moon: the lunar far side is inaccessible without a relay satellite, for it is the ultimate radio dead spot, since it never faces the Earth.

Taking all this into account, LCNS represents the implementation of the moonlight initiative, i.e. an European-led delivery of communications and navigation services that will support the next generation of institutional and commercial lunar exploration missions, including enhancing the performance of those missions currently under definition.
The EL3 sample return mission is considered as a good scenario for LCNS and so a reference scenario for EL3, whose launch date is supposed to occur in 2026, has been provided by the customer.

The reference mission phases considered, after launch, are schematically presented in Figure 6.6 and hereafter described.

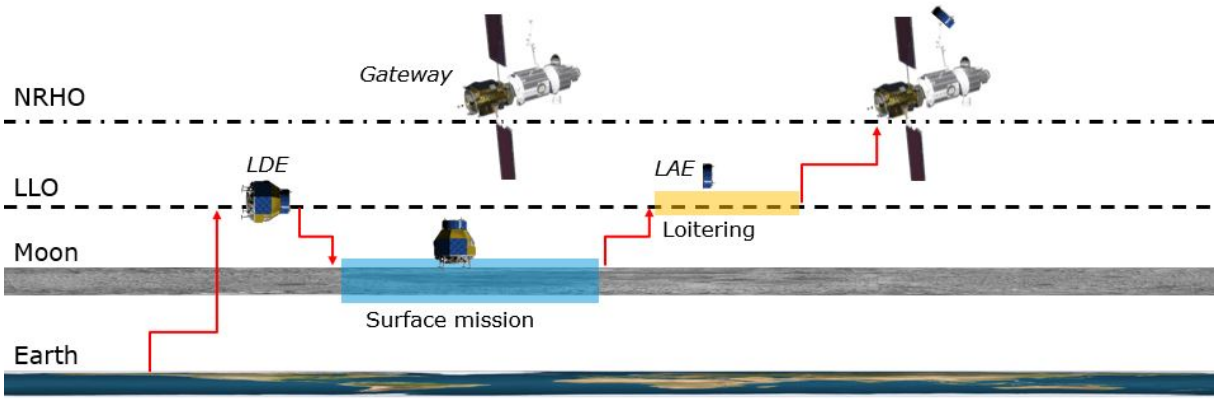

Figure 6.6: EL3 sample return mission profile [57].

1. Transfer Trans-Lunar Injection (TLI) to Low Lunar Orbit (LLO): EL3 is injected into a Moon-bound trajectory

   - by direct injection into a Lunar Transfer Orbit (LTO), with 4-6 days Time of Flight (ToF) and bi-week launch window (Note: this is the current baseline);

- by using a Weak-Stability Boundary Transfer (WSBT), with 3-4 months ToF and daily launch windows (Note: this would imply a $\Delta v \approx 150\frac{m}{s}$ saving).

2. Low Lunar Orbit (LLO), Lunar Orbit Insertion (LOI) and post-LOI loitering: LOI $\approx 700 - 800\frac{m}{s}$ manoeuvre and possible LCNS benefits

   - for pre-LOI precise Orbit Determination (OD) and earlier LOI correction;
   - post-LOI, for precise OD and earlier LOI correction;
   - to fill visibility gaps of ground-based measurements (far side).

3. Descent-Ascent: → LLO loitering → Periselene lowering burn → Coasting Elliptical Lunar Orbit (ELO) arc → Main braking burn → ... → Touchdown / - / Landing site → Main burn ascent → ... → Coasting ELO arc → Circularisation burn → LLO loitering

   - before descent: LCNS could improve OD prior to the periselene lowering burn;
   - after ascent: possible benefit to assist ground-based measurements.

4. Rendezvous: from LLO to NRHO (Near Rectilinear HALO orbit, Gateway orbit) in 1-3 days transfer time

   - possible use of LCNS to assist ground-based measurements;
   - possible improvement of relative Gateway state knowledge;
   - manoeuvre execution errors lead to expensive Trajectory Correction manoeuvres (TCM); it can be mitigated with faster LCNS-aided OD.

5. Surface Operations

It must be noted that realistic schedule and mission costs will impose to have a small constellation; global Moon coverage with multiple satellites is not realistic and not needed due to the limited number of users. Hence, LCNS will provide navigation services in specific time windows and in specific areas of the Moon. As consequence, the user missions will have to adapt the mission planning to ensure that critical operations requiring navigation are performed during the coverage window.

After a trade-off process, the three alternative scenarios for the optimal configuration are:

1. - 1 LCNS satellite for communication,

- Earth GNSS when visibility allows and 1 LCNS satellite with one-way and two-way navigation services for navigation.

2. - 3 LCNS satellites for communication,
   - Earth GNSS when visibility allows and 3 LCNS satellites with one-way and two-way navigation services for navigation.

3. - 3 LCNS satellites + Lunar Pathfinder + Gateway for communication,
   - Earth GNSS when visibility allows + 3 LCNS satellites with one-way and two-way navigation services and 2 LCNS satellites with only one-way navigation + Lunar Beacon in the landing/ascent lovation (Schrödinger basin) for navigation.

The optimised satellites constellation configuration both for navigation and communication performances is made by 5 satellites in highly elliptical orbits around the Moon, all with the same semi-major axis a, eccentricity e, inclination i and argument of perigee ω; the right ascension of the ascending node Ω and true anomalies TA, instead, are different. Table 6.2 summarise all the values for orbital parameters.

Table 6.2: LCNS five-satellite constellation optimised characteristics.

Satellite	a **[km]**	e	i **[deg]**	ω **[deg]**	Ω **[deg]**	**TA [deg]**
1	9750.5	0.7	63.5	90	0	0
2	9750.5	0.7	63.5	90	120	164
3	9750.5	0.7	63.5	90	240	196
4	9750.5	0.7	63.5	90	120	245
5	9750.5	0.7	63.5	90	240	184

The analysis of lunar surface coverage is based on the optimised LCNS constellation; hence, as stated before, the goal of such optimisation phasing presented in Table 6.2 is aimed at improving the surface coverage performance and so the navigation and communication performances of the constellation itself. the optimisation has been performed by changing the satellite's true anomalies TA only, whose values are presented on the last column of the table, while all other orbital parameters have always remain unchanged.
Frozen orbit conditions are used and there are not changes in orbital periods (the semi-major axis is fixed), that remains equal to 24 hours, neither in orbital planes (the right ascension does not change); Figure 6.7 shows the baseline configuration in terms of plane separation, where the three planes are uniformly separated.

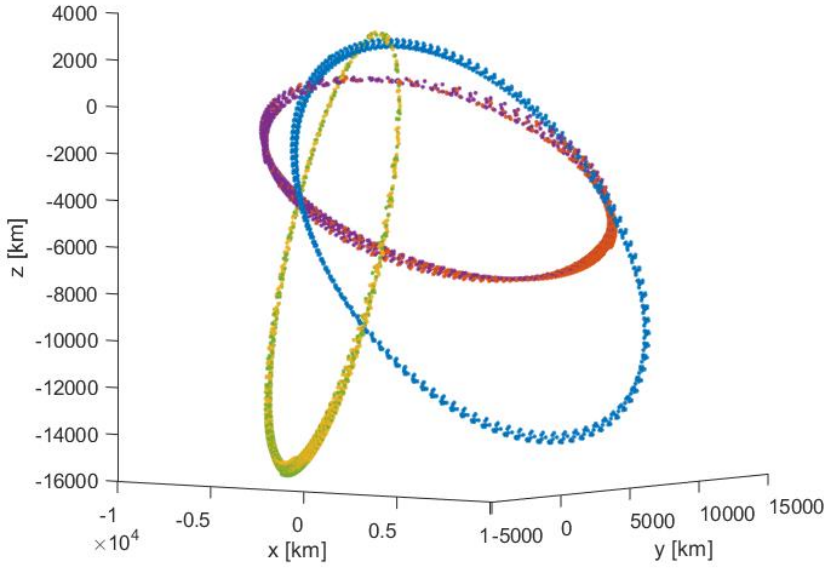

Figure 6.7: LCNS optimal configuration.

Three different cases have been analysed to perform visibility studies: first, 1 satellite only is propagated, then the first 3 on Table 6.2 are considered and lastly all the 5 satellites are involved. In every case study, all the satellites have been considered identical both for navigation and communication interests. The propagation time is always equal to one year, form June 2026 until June 2027 given in MJD2000 reference frame and the position vectors of the satellites as well as the Schrödinger Crater location are determined accordingly to the EME2000 reference frame.
Since the orbits are elliptical and the configuration is not symmetric, the Brute Force method is used to find constellation performances, with a minimum acceptable elevation angle equal to 10^o.
After the propagation, the maximum, minimum and average visibility windows and revisit times have been determined; it must be mentioned that these statistics are based on daily windows.

Table 6.3 shows the numeric results obtained, with consecutive hours of visibility and non visibility windows above the Schrödinger Crater.

Table 6.3: LCNS visibility windows.

		Window duration [hr]	Gap between windows [hr]	Cumulative per day
Option 1	1 sat	19.24	4.67	19.24 hr / 80%
Option 2	1 sat	Inf	-	24 hr / 100%
	2+ sats	20.48	0.48	24 hr[(2)] / 100%
	3 sats	3.07	5.02	9.65 hr / 40%
Option 3	3+ sats	Inf	-	24 hr / 100%
	4+ sats	6.40	2.25	19.10 hr / 80%
	5 sats	2.02	8.80	4.79 hr / 20%

In the first option, with only 1 satellite, the average duration of visibility window is about 19 hours while the gap is less than 5 hours; the last column shows the average percentage of total time of visibility per day and the respective hours: for the first option the value is trivial (that corresponds to an 80% of visibility per day), but this is not the case for the other two. Considering the case of 3 satellites propagated, at least 1 satellite is always visible from the portion of lunar surface of interest; even in the case of at least 2 satellites visible, the total visibility window per day is still of 24 hours, since the frames of one satellite only are very short and so it could be assumed that small station keeping should be capable to remove them. On the other hand, 3 satellites are visible for an average continuous window per day of about 3 hours, while the total time per day corresponds to 9.65 hours. The last case, involving 5 satellites, sees at least 3 of them always visible from the Schrödinger Crater, while the windows start diminishing if the options of 4 or more satellites visible at the same time are considered. Anyway, the average duration of visibility window for 5 satellites is about 2 hours, while the total time per day is about 4.8 hours.

Some examples to clarify the results presented in Table 6.3 are shown in Figures from 6.8 to 6.13 , where the number of satellites visible above the crater is shown in function of time.

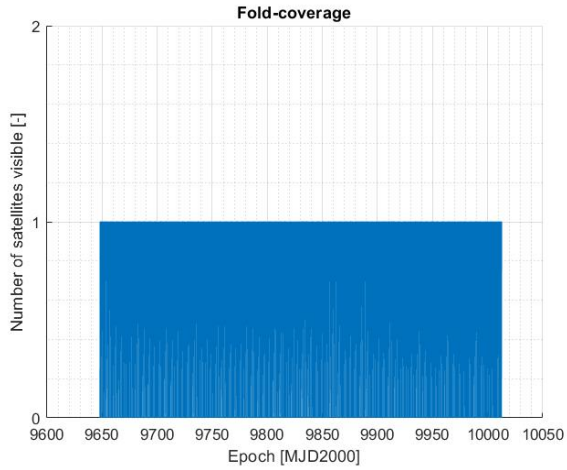

Figure 6.8: Option 1.

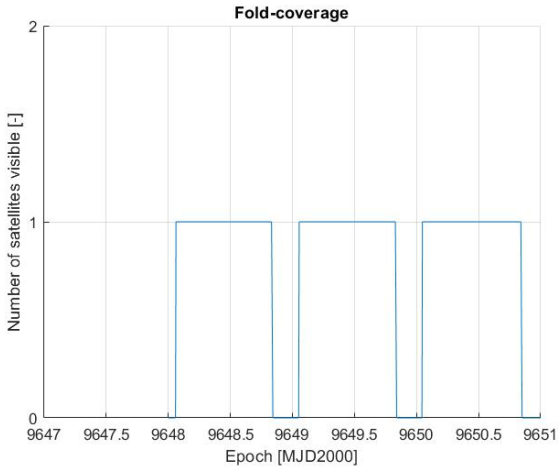

Figure 6.9: Option 1 zoomed.

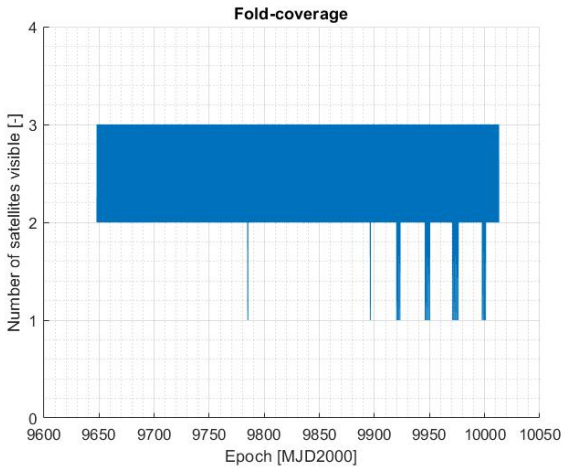

Figure 6.10: Option 2.

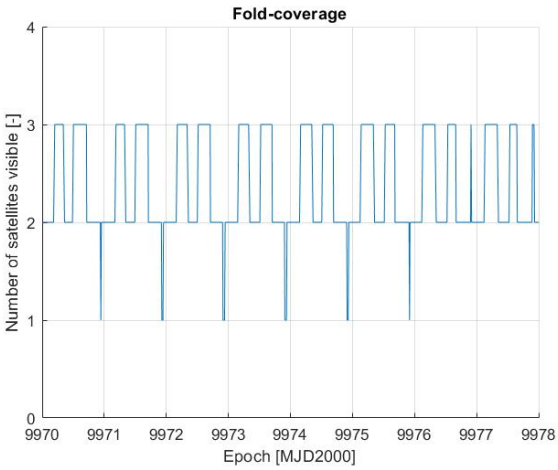

Figure 6.11: Option 2 zoomed.

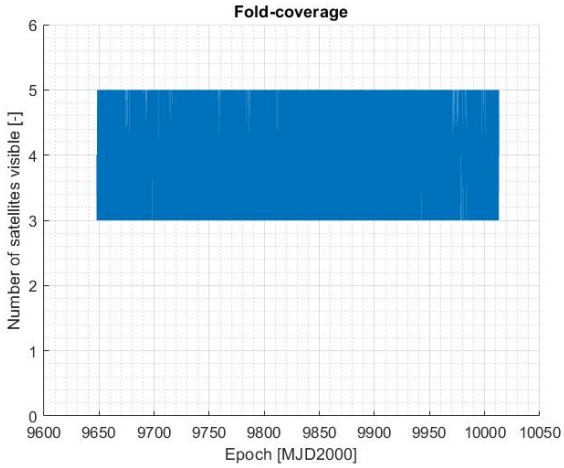

Figure 6.12: Option 3.

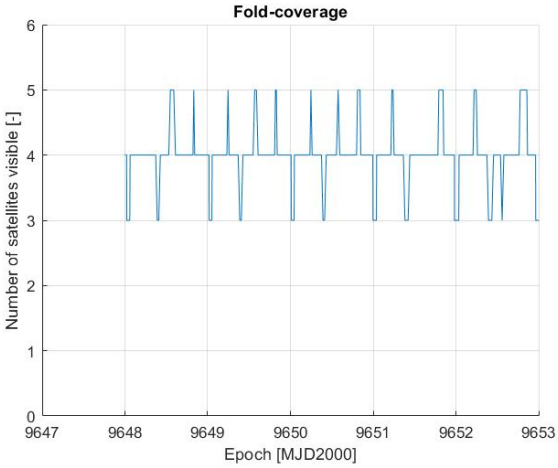

Figure 6.13: Option 3 zoomed.

While for option 1 and 3 the charts are always repeating, Option 2 in Figures 6.10 and 6.11 shows the small windows of 1-fold coverage that occurs and that may be compensated through Station keeping manoeuvres. In option 1 of Figures 6.8 and 6.9, the alternation between visibility and gap windows is clearly distinguishable whereas option 3 on Figures 6.12 and 6.13 reports an alternation of 3, 4 and 5 satellites visible, since at least 3-fold coverage is always guaranteed. This alternation occurs even more times per day and that is why, together with the average visibility windows value, also the cumulative window per day in Table 6.3 has been reported. The same phenomena is visible also in option 2 where, apart from the small frames of 1-fold coverage, 2- or 3-fold coverage alternate.

Summarising, option 1 considers an uniform pattern with a 19 hours visibility window per day and the behaviour is roughly the same in the whole region at latitudes less than 65 deg; in the second option, at least 1 satellite is always visible but with small Station keeping even 2 satellites could be always in view. The small frames in which only one

satellite is visible are due to the equal time-based phasing for uniform distribution along the orbits and it appears after many days of propagation because of the long period adopted. Finally, option 3 brings to at least 3 satellites always visible and used both for communications and navigation purposes.

7. Conclusions

The aim of this thesis was to present and analyse the concept of satellite constellations and the relative design methods, throughout an investigation that allowed an easy and understandable comparison. A study to determine the most efficient and optimal geometries and methods has been carried out, where by optimal what is meant is either minimisation of computational effort or graphical and geometrical representation helping the most to the understanding of the underlying physics, as well as the applicability domain and the accuracy of the results.

The novelty brought by the presented work contributes to the area of satellite constellation design and development: it proposes standardised nomenclature and references and it makes a direct, intuitive and simple comparison of the existing methods. Moreover, the author has developed algorithms that accept as inputs the parameters expressed always in the same form, in such a way it is easier to directly understand the more performant method as well as the more accurate and precise; these algorithms have also been written and organised in order to reduce the computational time as much as possible and to provide results in a clear and well understandable way.
An innovative approach for the determination of the coverage area is also presented; since it is analytical, the computational time is reduced and the accuracy of the results is increased.
Moreover, two real missions have been used as test-cases in order to apply and validate some of the design methods and the approach to determine the coverage area.

The design process for satellite constellations is based on user requirements, which define the figures of merit for certain objectives (e.g. Earth observation, Telecommunications, Navigation and Positioning). Among all figures of merit that characterise a constellation geometry, visibility conditions must always be considered and so the focus of this work has been on coverage requirements [5].
First of all, a distinction between satellites in circular rather than elliptical orbits has been presented: usually, large constellations are deployed in circular orbits, however, several authors investigated even the case of elliptical orbits. Anyway, these geometries involve a small number of satellites and they are applied to coverage of specific locations on the planet's surface rather than on the whole Earth. For this reason, it is difficult to determine a general method, but the geometry should be every time and newly determined depending

on the user needs.

The difference between symmetric and non-symmetric constellations has been considered too: depending on satellite's distribution, the properties of a constellations and the derived design methods are different. A constellation is said to be symmetric when orbital planes are equally spaced, while non-symmetric if they have different spacing; some examples of the first class are given by the Walker [12] and Ballard [26] patterns, while the Street Of Coverage geometry is not symmetric.
Design methods for symmetric constellations are the Walker circumcircle [27] and Lang [48] numerical approaches, as well as the Ulybyshev geometrical methods [50], [51] for long and short revisit times, while for non symmetric constellations the Beste [28] and Adams and Rider [24] analytical methods have been examined.
Another distinction has been made considering the possible requirements for a constellation that could be designed for continuous rather than discontinuous coverage, as well as for global, zonal or local coverage. In addition, if continuous coverage shall be achieved, the condition could be for single, double or in general n-fold coverage.
If continuous global or zonal coverage is desired, the Walker circumcircle, Lang, Beste and Adams and Rider methods can be used, while if discontinuous coverage is allowed the methods for long and short revisit times could be suitable, the first if the revisit time is more that one orbital period, while the second if it is less than one orbital period. Anyway, this last method can also be applied for continuous coverage of a specific location.

Some possible enhancements with respect to what done until now and some future work that could be performed on this topic could be to try to extend the domain of application of the geometrical methods for discontinuous coverage to non-symmetric constellations. Perhaps, a useful way and mathematical expressions to determine the optimal constellation configuration could be found.
Another important step forward could be represented by extending the use of these geometrical methods also for elliptical orbits and to a non spherical Earth, so by taking into account the Earth oblateness. These aspects should only change the expression used to determine the coverage circle (or equivalently the coverage regions in the (Ω, u) space but then the procedure to compute the revisit time should remain the same.
Moreover, a further optimisation of the algorithm implemented for the determination of the optimal configuration of the short revisit times geometrical method could perhaps be useful, for instance by determining the minimum number of boundary points needed to obtain a solution and so by reducing the search field, or even by finding a different way to check if the corner points of the parallelogram are inside the region of visibility.

A. Appendix A

A.1 Counts of time

- JD - Julian Date: number of days since January 1^{st} 4713 BC;
- MJD - Modified Julian Days: number of days since November 16^{th} 1858;
- MJD2000 - Modified Julian Days 2000: number of days since January 1^{st} 2000;

A.2 Reference frames

- ECI - Earth Centered Intertial: intertial, non accelerated, fixed with respect to stars reference frame;
  - J2000 or EME2000: Earth's Mean Equator and Equinox at 12:00 terrestrial time on January 1^{st} 2000; the x axis is aligned with the mean equinox, the z axis is aligned with the Earth's rotation axis or celestial North Pole and the y axis is rotated 90^{o} East about the celestial equator;
  - TEME: True Equator, Mean Equinox, is the frame used for the NORAD two-line elements.
- ECEF - Earth Centered Earth Fixed: not inertial, accelerated, rotating with respect to stars;
  - Positive x axis aligns with the International Earth Rotation and Reference System (IERS) Prime Meridian, positive z axis aligns with the IERS Reference Pole (IRP) that points toward the North Pole and y axis completes the right-handed system.
- Heliocentric Reference Frame: inertial, non accelerated, fixed with the Sun at the origin;
  - HEEQ - Heliocentric Earth Equatorial: the x axis towards the intersection of the solar equator and the solar central meridian as seen from Earth and the z axis is parallel to the Sun's rotation axis;

- HEE - Heliocentric Earth Ecliptic: the x axis towards the Earth and the z axis perpendicular to the plane of Earth's orbit around the Sun (the system is fixed with respect to the Earth-Sun line);
- HAE - Heliocentric Aries Ecliptic: the x axis is towards the First Point of Aries (the direction in space defined by the intersection between the Earth's equatorial plane of its orbit around the Sun, the plane of the ecliptic) and the z axis perpendicular to the plane of Earth's orbit around the Sun. This system is fixed with respect to the distant stars; it is subjected to slow change owing to the various slow motions of the Earth's rotation axis with respect to the fixed stars.

B. Appendix B

B.1 Walker geometry logic code flow

FOR The total number of planes
- $\Omega = W\frac{2\pi}{P}$
- Initial phase $= F\frac{2\pi}{T}$
- FOR The total number of satellites per plane
- $\Omega = \Omega$
- Phase angle $M = \frac{2\pi}{S}$ + initial phase
- END
- END

B.2 Ballard geometry logic code flow

FOR The total number of planes
- $\Omega = W\frac{2\pi}{P}$
- Initial phase $= mS\frac{2\pi}{T}$
- FOR The total number of satellites per plane
- $\Omega = \Omega$
- Phase angle $M = \frac{2\pi}{S}$ + initial phase
- END
- END

B.3 Street Of Coverage geometry logic code flow

FOR The total number of planes -1
- $\Omega = \alpha$
- Initial phase $= \frac{2\pi}{T}$
- FOR The total number of satellites per plane

- $\Omega = \Omega$
- Phase angle $M = \frac{2\pi}{S}$ + initial phase
- END
- END

While

FOR The last (counter-rotating) plane
- $\Omega_{last} = 2\Psi$
- Initial phase $_{last} = \frac{2\pi}{T}$
- FOR The total number of satellites per plane
- $\Omega_{last} = \Omega_{last}$
- Phase angle $M_{last} = \frac{2\pi}{S}$ + initial phase $_{last}$
- END
- END

B.4 Flower constellations geometry logic code flow

Select N_p, N_d, $\mathbf{S}$, F_n, F_d, h_p, i, ω
- Period $T = \frac{N_d}{N_p}\frac{2\pi}{\omega_{Earth}}$
- Semi-major axis $a = \sqrt[3]{(\frac{T}{2\pi})^2\mu}$
- Eccentricity $e = 1 - \frac{R_{Erath}+h_p}{a}$
- Semi-latus rectum $p = a(1-e^2)$
- Const $= 3R_{Erath}^2\frac{J_2}{4p^2}$
- Mean motion $n = \sqrt{\frac{\mu}{a^3}}$

$\dot{\omega} = Const * n(4 - 5\sin(i)^2)$
- $\dot{\Omega} = -2 * Const * n\cos(i)$
- $\dot{M} = -Const * n\sqrt{1-e^2}(3\sin(i)^2 - 2)$

$\Delta\Omega = -2\pi\frac{F_n}{F_d}$
- $\Delta M = 2\pi\frac{F_n}{F_d} * (\frac{n+\dot{M}}{\omega_{Earth}+\dot{\Omega}})$

FOR The total number of satellites per plane -1

- $\Omega(k+1) = \Omega(k) + \Delta\Omega$
- $M(k+1) = M(k) + \Delta M$
- END

C. Appendix C

C.1 Walker circumcircle approach logic code flow

Select: $(T/P/F)$ or equivalently $(T/P/m)$, i and h

- Find Period = orbital period
- Select: total propagation time
- Time-step for the propagation

FOR The whole propagation time

- t = each time step
- FOR i that varies among all T satellites
  - FOR j that varies among all T satellites
    - FOR k that varies among all T satellites
      - $X = \frac{2\pi t}{Period}$
      - $\sin\left(\frac{r_{ij}}{2}\right)^2$
      - $\sin\left(\frac{r_{jk}}{2}\right)^2$
      - $\sin\left(\frac{r_{ki}}{2}\right)^2$
      - θ_{ijk}
      - FOR l that varies among all T excluded the current *(i,j,k)*
        - $X = \frac{2\pi t}{Period}$
        - $\sin\left(\frac{r_{il}}{2}\right)^2$
        - $\sin\left(\frac{r_{jl}}{2}\right)^2$
        - $\sin\left(\frac{r_{kl}}{2}\right)^2$
        - y_1
        - y_2
        - y_3
        - IF $y_{1,2,3} > 0$
          - θ_{ijk} saved
        - END
      - END
    - END
  - END

- END
- END

Among all saved θ_{ijk}, find the maximum value, which represents the worst-case condition, and determine the correspondent altitude h required to satisfy the minimum elevation angle condition (say ε=10 deg). This result must be compared with the actual value of the satellite altitude and see if visibility conditions are satisfied; it is a trial-and-error process, in which initial values shall be varied and tuned until an acceptable solution is found.

C.2 Lang approach logic code flow

Select: $(T/P/F)$ and i

- Find Ω, M through the algorithm of Section 2.2.1
- Find the number of distinct ground traces
- Take the first satellite Ω_1, M_1 as reference for the propagation
- T_{GT} = number of satellites per independent groundtrack
- Longitude band = $\frac{\pi}{T_{GT}}$
- Latitude band = [0 deg - 90 deg] (less for zonal coverage)
- Select the grid step
- Create the grid of test points [longitude,latitude]
- to investigate for visibility conditions (i.e. green area in Figure 3.13)

FOR Each position occupied by the reference satellite

- Build the "8-shaped" groundtrack (Geosynchronous-like)
- Find the correspondent points on the ground [longitude,latitude]
- Find the central angle of coverage θ between each couple
- of test points and satellite points
- END

Among all the θ, find the maximum value, which represents the worst-case condition, and determine the correspondent altitude h required to satisfy the minimum elevation angle condition (say ε=10 deg). This result represents the minimum value of altitude that the constellation must have in order to achieve visibility requirements.

C.3 Brute force approach logic code flow

Select: Total propagation time
- Time-step for the propagation
- Select: ε_{min} = minimum elevation angle acceptable (treshold)

FOR The whole time of propagation
- At each time-step:
- Find position vectors of all satellites
- Find position vectors of all locations of interest on the planet's surface
- Find relative position vectors
- ε = elevation angle reached
- IF $\varepsilon \geq \varepsilon_{min}$
- The satellite is IN VIEW of the current location
- END
- END

To find the n-fold visibility and/or gap time:

FOR The whole time of propagation
- At each time-step:
- IF Satellite IN VIEW = n
- Count time-step IN VIEW
- END
- IF Satellite IN VIEW = 0
- Count time-step GAP
- END
- END

The total time counted is the actual time there are n satellites IN VIEW of the site investigated, while if no satellites are visible, the total time counted is the revisit time. Then, starting from all these values, it is possible to determine the Maximum, Minimum and Average Revisit Time as well as the time n satellites are visible above a surface location.

C.4 Geometrical approach for short revisit times logic code flow

Select: i and h

- Select: central longitude and latitude (ϕ_c,λ_c) of the site of ineterst
- Select: ε elevation angle
- Determine θ coverage angle

Select: spacing between boundary points

In case of revisit time:

- Select: maximum allowed t_{REV}

FOR The whole coverage circle: the central angle varies from 0 to 2π

- γ = each angle
- Find longitudes ϕ
- Find latitudes λ
- END

FOR All the boundary points

- IF $\sin(\lambda) < \sin(i)$
- Find u
- Find Ω
- END
- END

IF Revisit Time

- Expand the region in the y direction
- Find correspondent u, Ω
- END

Select: S_{max} and P_{max}

FOR The total number of planes P_{max}

- FOR The total number of satellites per plane S_{max}
- FOR m that varies from 0 to the current $P \cdot S$

- FOR Each boundary point
- Take x_0,y_0
- $T = P \cdot S$
- $\Delta u = m\frac{2\pi}{T}$
- Find the other three boundaries of the parallelogram
- IF all the vertices of the parallelogram are INSIDE the polygon (*Inpolygon* function of Matlab)
- T, P, m saved
- END
- END
- END
- END
- END

Among all saved acceptable values, find the minimum T and the correspondent P, then determine the phase parameter F as:

FOR All the possible values of the parameter k from *0* to T
- $F = kP - m$
- IF $F > 0$
- F determined
- END
- END

Bibliography

[1] John E. Draim. "Lightsat Constellation Designs". In: *AIAA Satellite Communications Conference* 92-1988-CP (1992), pp. 1361–1368.

[2] James R. Wertz. *Orbit & Constellation Design & Management*. ISBN 978-1-881883-07-8: Space Technology Library, Hawthorne, CA, 2001.

[3] Jozef C. van der Ha. *Mission Design & Implementation of Satellite Constellations*. ISBN 0-7923-5210-6: Kluwer Academic Publishers, Dordrecht, The Netherlands, 1997.

[4] Peter C.E. Roberts Nicholas H. Crisp Sabrina Livadiotti. *A semi-analytical method for calculating Revisit Time for Satellite Constellations with Discontinuous Coverage*. Tech. rep. University of Manchester, 2018.

[5] Simeng Huang Camilla Colombo Franco Bernelli Zazzera. *Comparative assessment of different constellation geometries for space-based application*. Tech. rep. IAC-17, C1, IP, 31, x41252: 68th International Astronautical Congress, 2017.

[6] Mattew Paul Wilkins. *The Flower Constellations - Theory, Design Process and Applications*. Tech. rep. Texas A&M University, 2004.

[7] Paul B. DiDomenico. *A Phase-based approach to Satellite Constellation Analysis and Design*. Tech. rep. Massachusetts Institute of Technology, 1991.

[8] P.R. Escobal. *Methods for orbit determination*. ISBN 978-0882753195: Krieger, London, 1965.

[9] A. Rapiki S. Cakaj B. A. L. Kamo. "The Coverage analysis for Low Earth Orbiting satellites at low elevation". In: *International Journal of Advanced Computer Science and Applications* 5 (2014), pp. 6–10.

[10] J.A. Lawton. "Numerical method for rapidly determining satellite-satellite and satellite-ground station in-view periods". In: *Journal of Guidance, Control and Dynamics* 10 (1987), pp. 32–36.

[11] Charles K. Wilkinson. "Coverage Regions: How they are computed and used". In: *Journal of Astronautical Sciences* 42 (1994), pp. 47–70.

[12] J.G. Walker. *Circular orbit patterns providing continuous whole Earth coverage*. Tech. rep. 70211: Royal Aircraft Establishment, UK, 1970.

[13] W. Hsu D. Ma. "Exact design of partial coverage satellite constellations over oblate Earth". In: *Journal of Spacecraft and Rockets* 34 (1997), pp. 29–35.

[14] Marco Nugnes Camilla Colombo Massimo Tripaldi. *Coverage area determination for conical fields of view considering an oblate Earth*. Tech. rep. DOI: 10.2514/1.G004156: Journal of Guidance, Control and Dynamics, 2019.

[15] Jili Wu Yongjun Li Shanghong Zhao. "A general evaluation criterion for the coverage performance of LEO constellations". In: *Elsevier - Aerospace Science and Technology* 48 (2015), pp. 94–101.

[16] *Iridium Global Network*. URL: https://www.iridium.com/network/globalnetwork/.

[17] *Satellite Technology powered by the Globalstar Satellite Network*. URL: https://www.globalstar.com/en-us/about/our-technology.

[18] *Teledesic*. URL: http://www.astronautix.com/t/teledesic.html.

[19] *The Global Positioning System*. URL: https://www.gps.gov/systems/gps/.

[20] *Glonass System Documents*. URL: https://www.glonass-iac.ru/en/GLONASS/.

[21] *What is Galileo?* URL: https://www.esa.int/Applications/Navigation/Galileo/What_is_Galileo.

[22] Leslie D. Westbrook Madhavendra Richharia. *Satellite Systems for personal applications*. ISBN 9780470714287: John Wiley & Sons, LTD, DOI:10.1002/9780470665619, 2010.

[23] Yury Razoumny. "New research methodology for Earth periodic coverage and regularities in parametric localization of optimal LEO satellite constellations". In: *Advanced in the Astronautical Sciences* 13 (2014), pp. 3117–3136.

[24] Y. Fun Hu Ray E. Sheriff. *Mobile Satellite Communication Networks*. ISBN 0-471-72047-X: John Wiley & Sons, LTD, Baffins Lane, Chichester, West Sussex, PO19 1UD, England, 2001.

[25] Roger L. Freeman. *Satellite Communications*. DOI 10.1002/0471208051: John Wiley & Sons, LTD, Baffins Lane, Chichester, West Sussex, PO19 1UD, England, 2002.

[26] A.H. Ballard. "Rosette Constellations of Earth Satellites". In: *IEEE TRW Defense and Space Systems Group* AES 16, NO. 5 (1980), pp. 656–673.

[27] J.G. Walker. *Continuous whole Earth coverage by circular-orbit satellite patterns*. Tech. rep. 77044: Royal Aircraft Establishment, UK, 1977.

[28] D.C. Beste. "Design of Satellite Constellations for Optimal Continuous Coverage". In: *IEEE General Research Corporation* AES 14, NO. 3 (1978), pp. 466–473.

[29] John E. Draim. "A Common Period four-Satellite Continuous Global Coverage Constellation". In: *AIAA Satellite Communications Conference* 86-2066 (1986), pp. 112–120.

[30] David Castiel John E. Draim Paul J. Cefola. "Elliptical Orbit Constellations - A new paradigm for higher efficiency in Space Systems". In: *IEEE Aerospace Conference Proceedings* DOI 10.1109 (2000), pp. 27–36.

[31] Christian Bruccoleri Daniele Mortari Matthew P. Wilkins. *The Flower Constellations*. Tech. rep. Texas A&M University, 2004.

[32] Jean-Luc Palmade Erick Lansard Eric Frayssinhes. "Global Design of Satellite Constellations: a multi-criteria performance comparison of classical Walker patterns and new design patterns". In: *Acta Astronautica* 42 (1998), pp. 555–564.

[33] *Galileo Space Segment*. URL: https://gssc.esa.int/navipedia/index.php/Galileo_Space_Segment.

[34] *Glonass Space Segment*. URL: https://gssc.esa.int/navipedia/index.php/GLONASS_Space_Segment.

[35] *Globalstar Satellite Network*. URL: https://satellitephonestore.com/globalstar-satellite-network.

[36] *SaVi Constellations*. URL: http://www.geom.uiuc.edu/~worfolk/SaVi/constellations.html.

[37] *Iridium Network Overview*. URL: https://www.roadpost.com/iridium-satellite-network.

[38] *Iridium Where*. URL: https://iridiumwhere.com/about/.

[39] *O3b Satellite Overview*. URL: https://spaceflight101.com/spacecraft/o3b/.

[40] David Castiel John E. Draim. "Optimisation of the Borealis and Concordia sub-constellations of the Ellipso personal communications system". In: *Acta Astronautica* 40 (1997), pp. 183–193.

[41] *Satellite Networks: Constellations*. URL: https://savi.sourceforge.io/about/lloyd-wood-iwssc-08-tutorial.pdf.

[42] *ICO F1, ..., F15*. URL: https://space.skyrocket.de/doc_sdat/ico.htm.

[43] *OneWeb slashes size of future satellite constellation*. URL: https://spacenews.com/oneweb-slashes-size-of-future-satellite-constellation/.

[44] *OneWeb Mini-satellite Constellation for Global Internet Service*. URL: https://directory.eoportal.org/web/eoportal/satellite-missions/o/oneweb.

[45] Crawley Portillo Cameron. "A technical comparison of three LEO satellite constellation systems to provide global broadband". In: *Acta Astronautica* 159 (2019), pp. 1–16.

[46] *Starlink Satellite Constellation of SpaceX*. URL: https://directory.eoportal.org/web/eoportal/satellite-missions/s/starlink.

[47] *SpaceX Gives More Details on how their Starlink Internet Service Will Work*. URL: https://www.universetoday.com/140539/spacex-gives-more-details-on-how-their-starlink-internet-service-will-work-less-satellites-lower-orbit-shorter-transmission-times-shorter-lifespans/.

[48] Thomas J. Lang. "Optimal Low Earth Orbit Constellations for Continuous Global Coverage". In: *Advances in the Astronautical Sciences* 93-597 (1993), pp. 1199–1216.

[49] J.G. Walker. *Coverage predictions and selection criteria for satellite constellations*. Tech. rep. 82116: Royal Aircraft Establishment, UK, 1982.

[50] Yuri Ulybyshev. "Geometric Analysis and Design Method for Discontinuous Coverage Satellite Constellations". In: *Journal of Guidance, Control and Dynamics* 37 (2014), pp. 549–557.

[51] Yuri Ulybyshev. "Satelite Constellation Design for Complex Coverage". In: *Journal of Spacecraft and Rockets* 45 (2008), pp. 843–849.

[52] *Inpolygon function*. URL: https://it.mathworks.com/help/matlab/ref/inpolygon.html.

[53] Sebastian Franchini Ali Ravanbakhsh. "System Engineering Approach to initial design of LEO Remote Sensing missions". In: *IEEE International Conference* 978-1-4673-6396-9/13 (2013), pp. 659–664.

[54] *Estrack Ground Stations*. URL: https://www.esa.int/Enabling_Support/Operations/ESA_Ground_Stations/Estrack_ground_stations.

[55] *What is the CDF?* URL: http://www.esa.int/Enabling_Support/Space_Engineering_Technology/CDF/What_is_the_CDF.

[56] *Concurrent Design Facility*. URL: https://www.esa.int/Enabling_Support/Space_Engineering_Technology/Concurrent_Design_Facility.

[57] *EL3 sample return mission profile*. URL: http://vcdf.